General Disclaimer

One or more of the Following Statements may affect this Document

- This document has been reproduced from the best copy furnished by the organizational source. It is being released in the interest of making available as much information as possible.

- This document may contain data, which exceeds the sheet parameters. It was furnished in this condition by the organizational source and is the best copy available.

- This document may contain tone-on-tone or color graphs, charts and/or pictures, which have been reproduced in black and white.

- This document is paginated as submitted by the original source.

- Portions of this document are not fully legible due to the historical nature of some of the material. However, it is the best reproduction available from the original submission.

Produced by the NASA Center for Aerospace Information (CASI)

NASA CR-

(NASA-CR-144686) A 2C GHz DEPOLARIZATION EXPERIMENT USING THE ATS-6 SATELLITE Final Report, 1 Jan. 1974 - 31 Aug. 1975 (Virginia Polytechnic Inst. and State Univ.) 105 p HC $5.50 CSCL 17E G3/17

N76-12112

Unclas 04407

Virginia Polytechnic Institute and State University

Electrical Engineering

BLACKSBURG, VIRGINIA 24061

Final Report

by

A 20 GHz DEPOLARIZATION EXPERIMENT USING THE ATS-6 SATELLITE

C. W. Bostian

E. A. Manus

R. E. Marshall

H. N. Pendrak

W. L. Stutzman

P. H. Wiley

S. R. Kauffman

Prepared for

NASA/Goddard Space Flight Center
Greenbelt, Maryland 20771

Contract NAS5-21984

September 10, 1975

1. Report No.	2. Government Accession No.	3. Recipient's Catalog No.
4. Title and Subtitle The VPI&SU ATS-6 20 GHz Depolarization Experiment		5. Report Date September, 1975 6. Performing Organization Code
7. Author(s) C. W. Bostian, W.L. Stutzman, R.E. Marshall, E.A. Manus, P.H. Wiley, H.N. Pendrak, S.R. Kauffman		8. Performing Organization Report No.
9. Performing Organization Name and Address Electrical Engineering Department Virginia Polytechnic Institute & State Univ. Blacksburg, Virginia 24061		10. Work Unit No. 11. Contract or Grant No. NAS5-21984
12. Sponsoring Agency Name and Address NASA Goddard Space Flight Center Greenbelt, Md. 20711 E. Hirschmann, Code 951, Technical Officer		13. Type of Report and Period Covered Final Report: 1 Jan. '74-31 Aug. '75 14. Sponsoring Agency Code

15. Supplementary Notes

16. Abstract

This report describes a depolarization experiment using the 20 GHz downlink from the satellite ATS-6. Its contents include (1) an operational summary of the experiment, (2) a description of the equipment used with emphasis on improvements made in the ATS-5 signal processing receiver, (3) data on depolarization and attenuation in one snow storm and two rain storms at 45° elevation, (4) data on low angle propagation, (5) conclusions about depolarization on satellite paths, and (6) recommendations for the depolarization portion of the CTS experiment.

17. Key Words (Selected by Author(s))	18. Distribution Statement
polarization, depolarization, millimeter wave propagation, attenuation, ATS-6, communications satellites	

19. Security Classif. (of this report)	20. Security Classif. (of this page)	21. No. of Pages	22. Price*
U	U	105	

* For sale by the National Technical Information Service, Springfield, Virginia 22151.

TABLE OF CONTENTS

Page

1. Introduction 1
   1.1 Purpose of the Experiment 1
   1.2 Organization of this Report 1
   1.3 Narrative History 2
   1.4 Operational Summary 6

2. Experiment Description 8
   2.1 Overall Setup and Block Diagram 8
   2.2 Antenna Characteristics and Performance 8
      2.2.1 Specifications 8
      2.2.2 Performance 11
      2.2.3 The Effects of Water on the Antenna 11
   2.3 Antenna Pointing and Tracking 21
   2.4 The Receiver 25
      2.4.1 R.F. Front End 25
      2.4.2 IF Section 28
         2.4.2.1 Limitations of ATS-5 IF Receiver 28
         2.4.2.2 Final Receiver Modifications 32
         2.4.2.3 Results of Modification 35
      2.4.3 Calibration 36
   2.5 Radars 38
      2.5.1 Introduction 38
      2.5.2 Search Radar Construction 39
      2.5.3 RD-110 Radar Modifications and Repairs 41
      2.5.4 Doppler Radars 44
      2.5.5 X-Band Weather Radar 44
      2.5.6 Use of the RD-110 Weather Radar 45
   2.6 Weather Instruments 45
   2.7 Data Collection System 45

3. Results 48
   3.1 Introduction 48
   3.2 Clear-Weather Changes in the Received Polarization Angle . . 48
      3.2.1 Introduction 48
      3.2.2 Data 50
      3.2.3 Discussion of Possible Mechanisms 50
         3.2.3.1 Introduction 50
         3.2.3.2 Validity of the Measurement Technique 53
            3.2.3.2.1 Introduction 53
            3.2.3.2.2 Antenna Pattern Assymetry 53
         3.2.3.3 Off-axis Reception 55
            3.2.3.3.1 Introduction 55
         3.2.3.4 Mechanical Drift in the Ground Antenna Positioning System . . . 64
         3.2.3.5 Satellite Yaw Variations 64
         3.2.3.6 Variations in the Satellite Antenna Pointing 64
         3.2.3.7 An Overlooked Propagation Effect 66
            3.2.3.7.1 Experimental Data 66

Page

3.2.3.7.2 Faraday Rotation 66
3.2.3.7.3 Scattering by Stratified Layers . 68
3.2.4 Conclusions 69
3.3 Depolarization by Snow 69
3.3.1 Introduction 69
3.3.2 Data and Analysis 71
3.3.3 Conclusions 79
3.4 Data Collected During Rain 80
3.5 Measurements at Low Elevation Angles 85
3.5.1 Introduction 85
3.5.2 Narrative Discussion of the Data 87
3.5.3 Antenna Pattern Broadening 88
3.5.4 Clear Weather Attenuation at Low Angles 89
3.5.5 Rain Attenuation at Low Angles 89
3.5.6 Polarization Effects at Low Angles 93
3.5.6.1 Pattern Broadening 93
3.5.6.2 Clear Weather Polarization Angle Variations 93
3.5.6.3 Depolarization 93

4. Conclusions 100

5. References 102

6. Appendix 104
6.1 Plans and Recommendation for CTS 104
6.1.1 Introduction 104
6.1.2 Antenna 104
6.1.3 Tracking 105
6.1.4 Receiver Recommendations for CTS 105
6.1.5 Radar 105
6.1.6 Weather Instruments for CTS 106
6.1.7 Data System for CTS 106
6.2 Project Personnel 106

1. Introduction

1.1 Purpose of the Experiment

The Virginia Polytechnic Institute and State University (VPI&SU) ATS-6 experiment was primarily concerned with the depolarizing effects of precipitation at millimeter wavelengths. Depolarization occurs when electromagnetic waves are scattered by bodies which lack spherical symmetry and whose dimensions are a significant fraction of a wavelength. Because depolarization will produce crosstalk in planned dual-polarized dual-channel millimeter wave communications systems, it has been studied extensively on terrestrial radio systems and several mutually consistent theoretical models have been developed. (Bostian et al.,1974) (Wiley, Stutzman, and Bostian, 1974) (Watson and Arbabi, 1973) The predictions of these models agree well with experimental data taken on linearly polarized ground systems; this experiment addressed the question of whether the terrestrial models must be modified to describe satellite path depolarization.

1.2 Organization of this Report

This report has three objectives. First, it provides NASA with a complete record of our activities and conclusions during the ATS Millimeter Wave Experiment. Second, it discusses our experiment problems and their solution in considerable detail. These are primarily of interest to experimenters who have NASA ATS-5 millimeter wave receivers and Ku band radars and who will be using them in the CTS program. It also may benefit those groups now designing or operating earth stations to make depolarization measurements with ATS-6 (in Europe), CTS, OTS, the AT&T-Comsat Domsat, etc. Third, the report presents what we at VPI&SU have learned from the ATS Experiment about 20 GHz propagation in the atmosphere.

Those readers with primary interest in propagation may wish to proceed immediately to Chapters 3 and 4. Those interested strictly in the equipment may want to begin with Chapter 2. For the general reader the rest of this chapter is devoted to an administrative and operational history of the project.

1.3 Narrative History

Construction of the VPI&SU 20 GHz propagation research earth terminal began on February 1, 1974. Our initial projections indicated that June 15, 1974 would be the earliest day that the earth station could perform depolarization data acquisition with the satellite. The tasks involved were divided into six areas with each area being under the leadership of one of the investigators. The Project Engineer was responsible for coordinating all of the individual tasks.

The first of the six construction areas was the design and assembly of a digital system to control the experiment and store the data. This system included a digital controller to interface a time-worn Raytheon PB-440 computer and all data acquisition systems. PB-440 software writing was part of the digital system design. The data and telemetry area included weather instruments, telemetry lines from weather instruments and other data points to the digital controller, and the FORTRAN data processing program. The receiving system consisted of a tracking antenna pedestal, a dual linearly polarized antenna, an ATS-5 intermediate-frequency receiver and a NASA-designed RF front end. A 15.6 GHz weather surveillance radar and six military surplus AN/PPS-18 doppler radars were included in the storm sensing area. The communications area encompassed TWX communications to and from ATSOCC and the link between the PB-440 and the IBM 370 in the VPI&SU Computing

Center. The last area consisted of constructing a 20' x 20' building to house the earth terminal electronics and pouring a concrete pad for the antenna pedestal.

In February of 1974 all the RF hardware and test equipment described in the original research proposal were ordered. A site for the earth terminal was chosen about one (1) mile west of the main campus. (Lat., 37°13'46"; Long., 80°26'16"; Alt., 2119 ft.) It became apparent as work began on the ATS-E receiver that it would require an unexpected amount of technical attention before it would be a dependable part of the receiving system.

By March 15, 1974 most of the critical RF hardware had been delivered and the construction phase of the project was on schedule. The digital system was 37% completed although most of this percentage represented design and software. The receiving system was 74% complete, but the ATS-E receiver continued to devour valuable man hours for troubleshooting and repairs. This effort was greatly aided by many telephone conversations with Terry Duffield of Martin Marietta. The data, telemetry, and communications areas were very nearly complete by this time; however, there was still two wind gauges to be placed along the satellite-earth path. The storm sensing Ku band radar was 90% completed by Spring. However, the unexpected work load imposed by the ATS-E receiver forced us to abandon efforts on the doppler radar units until personnel were available. The tracking station was now 70% completed.

Two weeks before the June 15th target date for data acquisition, project personnel decided to concentrate all efforts on those areas essential to establish an operational earth terminal. On June 19, 1974 at 1625 GMT, the VPI&SU earth terminal locked on to the 20 GHz CW beacon. The signal

level was marginal and the problem was traced to a faulty RF amplifier. After the RF front end was repaired and brought within specifications, the antenna positioning system was tested. The initial polarization angle was -19.5° and a +0.56° elevation offset and a +1.52° azimuth offset from SLAP predictions were noted.

From The Project Engineer's point of view, July, 1974 was the beginning of a chain of events that were most detrimental to the experiment. Both RDL 18.95 GHz local oscillators failed and we managed to produce one serviceable unit from the two defective units. There were five (5) local oscillator (L.O.) failures throughout the entire project; not only did these failures rob the experimental team of time needed elsewhere, it rendered the earth terminal useless and data could not be collected. Other RF front end failures during the experiment included one (1) mixer, one (1) amplifier, and two (2) waveguide switches. By the end of July, the VPI&SU earth terminal was capable of acquiring data on a 24-hour basis in the manner prescribed by the contract objective.

By the end of the Summer of 1974 the experimental apparatus was essentially complete. By this time data acquisition was the main objective; however, this required considerable manpower in order to maintain the RF front end. In October, data acquisition was hampered by two of the L.O. failures, one of the waveguide switch failures, and a mixer failure.

Operations during the month of November resulted in the first recorded 20 GHz snow depolarization. A preliminary analysis indicated a maximum 4 dB change in the system cross-polarization due to snow.

Project personnel were inappropriately rewarded by another local oscillator failure in December of 1974. The bad receiver L.O. was exchanged with the good test L.O. and the system was again operational.

After overcoming another L.O. failure in January of 1975 personnel began testing the NASA furnished RDL 20 GHz Gunn source for use in calibrating the RF front end. Tests indicated a frequency stability of 1 MHz/°C and this was found to be incompatible with the receiver sweep speed of 4.0 KHz/second. Repeated attempts to lock onto the Gunn source with the earth terminal receiver all resulted in failure.

By the end of February all data acquisition systems were operational. The PB-440 computer was receiving tracking data (AZ & EL) from the IBM 370 in the University Computing Center and propagation data could be delivered to the 370 for analysis. It was during this lull that we compiled a record of the received clear weather polarization angle and noticed as much as a 2.2° change over the last six months. At this time we attached a level to out antenna pedestal in order to rule out the possibility of receive antenna pedestal motion. To this writing we have observed no motion of the antenna pedestal.

The Blacksburg spring rains brought ample opportunities for data acquisition along with more hardware failures and tighter spacecraft scheduling. The ATS-E receiver began demanding daily alignment of the VCXO control circuitry. This problem was solved by the design and implementation of a new circuit described in Section 2.4.2. The fifth and last local oscillator failure occurred in April; however, replacing it with our last spare was no problem for the now well experience L.O. replacement team. A two (2) degree change in the polarization angle was observed in April.

May provided us with ample rain for data acquisition; however, the precipitous abandonment of the priority system at ATSOCC resulted in the loss of scientifically exploitable data. On May 6, 1975 we made extensive

attenuation and depolarization measurements with the 20 GHz CW in clear weather while spraying water on and near the receiving antenna. Results of and comments on this test are included in Section 2.2. Spacecraft movement began in mid May and preparations were made for obtaining important low elevation angle data. On June 7, 1975, during a scheduled polarization angle check, the antenna positioner failed and destroyed all RF and control cables. The damage was repaired by June 9, 1975, and low elevation angle data acquisition resumed. Loss of sight (LOS) of the 20 GHz CW occurred at VPI&SU on June 13 (Friday), 1975, at 2100 GMT.

1.4 Operational Summary

Table 1.1 lists chronologically the data acquisition events which produced orientative results. The first ten (10) events represent data taken at nominal synchronous pointing. The events beginning on June 10, 1975, represent low elevation angle data (<15.0°). A thorough discussion of these events can be found in Chapters 3 and 4.

Table 1.1. Operational Summary

Date	Maximum Attenuation (dB)	3 dB Period of Greatest Fade (Minutes)	Maximum Rain Rate (mm/hr.)	Minimum CPR Detectable (dB)	Ground Antenna Polarization Angle (Degrees)	Measured CPR (dB)	Lowest Measured CPR (dB)
31 Dec. 1974	5.4	5.68	12.70	**	-19.5°	---	---
25 Jan. 1975	3.6	***	10.00	**	-19.5°	---	---
31 Jan. 1975(1)	0.8	---	< 0.36	-35.0	-19.5°	-28.0	-29.4
31 Jan. 1975(2)	0.8	---	3.33	-35.0	-19.5°	-27.9	-30.4
14 Mar. 1975	4.0	***	6.08	-40.0	-21.5°	-36.0	-38.0
18 Mar. 1975	1.5	---	5.46	-40.0	-19.5°	-40.0	-40.0
30 Mar. 1975	7.7	57.75	15.24	-40.0	-21.2°	-25.0	-40.0
28 April 1975	1.0	---	3.56	-40.0	-21.0°	-34.8	-40.0
1 May 1975	8.3	***	11.94	-40.0	-21.0°	-31.2	-40.0
27 May 1975	14.0	8.00	95.30	-32.0	+ 6.0°	≤ -34.0	≤ -32.0
12 June 1975	17.0	8.00	30.00	-20.0	+49.0°	≤ -20.0	≤ -20.0
12 June 1975	22.0	16.00	34.20	-20.0	+52.0°	≤ -12.0	≤ -20.0
12 June 1975	20.0	5.00	15.00	-20.0	+46.0°	≤ -20.0	≤ -20.0

** Receiver operation was marginal and CPR could not be measured. Attenuation data only were collected.

*** The 3 dB period extended beyond the time for which we were able to use the satellite.

2. Experiment Description

2.1 Overall Setup and Block Diagram

Figure 2.1 presents a block diagram of the VPI&SU 20 GHz earth terminal. The 20 GHz depolarization data acquisition system was controlled by a Raytheon PB 440 computer. A digital controller handled all commands to the earth terminal hardware and controlled the introduction of all propagation and meteorological data into PB 440 storage. A link between the PB 440 and the VPI&SU IBM 370/158 system was established to transfer antenna pointing data to the PB 440 and to send all depolarization data back to the 370 system for processing. Meteorological data sources included six (6) tipping bucket rain gauges, two (2) wind velocity sensors, and a 30 mile 15 GHz weather surveillance radar. Propagation data was obtained by switching the receiver input between the co-polarized and cross-polarized feeds of the four (4) foot dual linearly polarized antenna at 0.5 Hz. Antenna pointing commands to the Scientific Atlanta elevation-over-azimuth pedestal originated in the Satellite Look Angle Program (SLAP) on disk in the IBM 370/158 system.

2.2 Antenna Characteristics and Performance

2.2.1 Specifications

The antenna was made by Control Data Corporation, Boston Space and Defense Division. It is a four-foot diameter, front-fed parabolic reflector antenna with dual linear polarizations. The purchasing specifications were:

Frequency: 20.0 GHz

Reflector: 4 feet in diameter

Feed: Scalar (Corrugated horn)

Spars: Symmetrical four spar support system aligned with polarization planes.

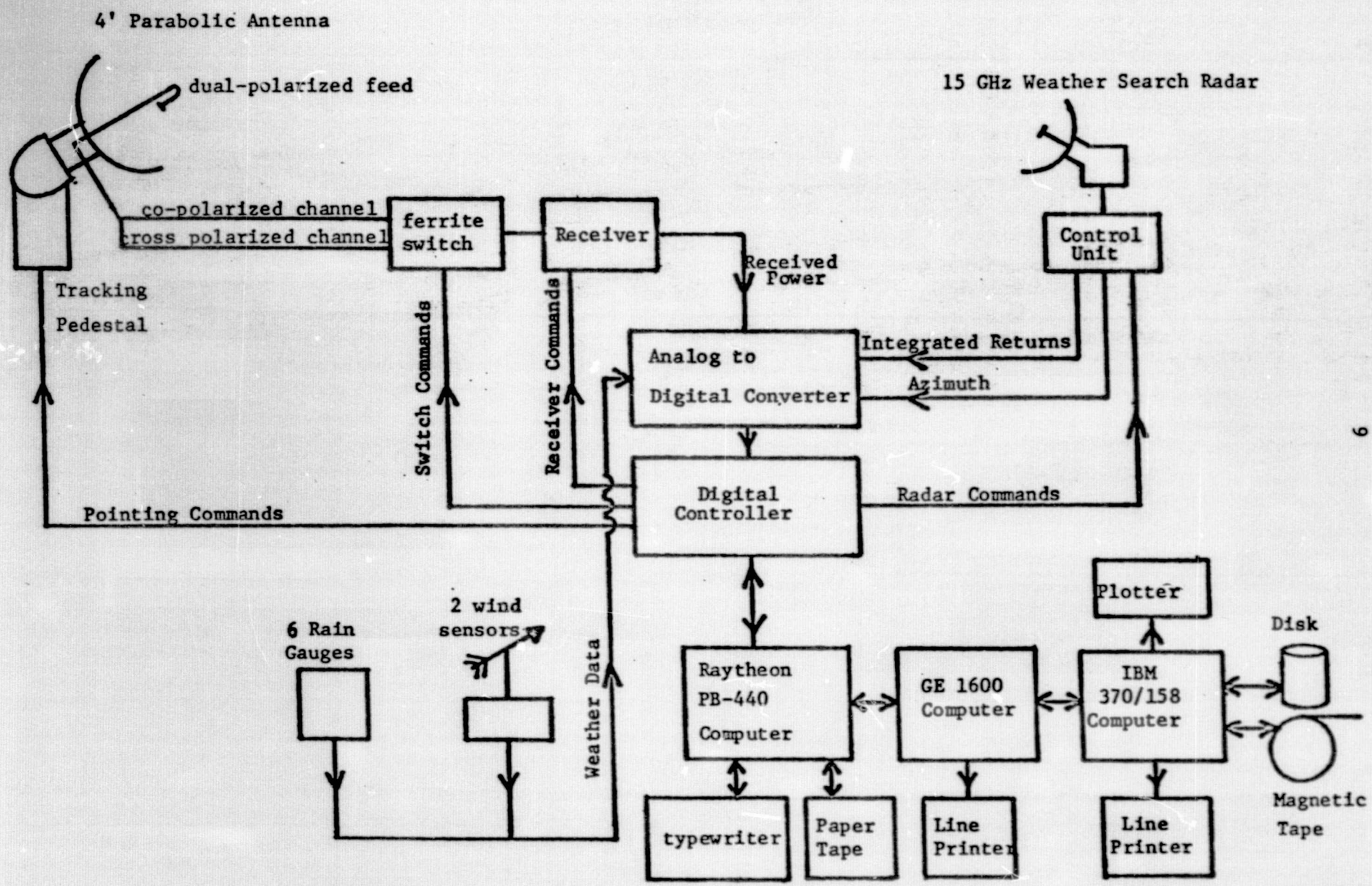

Figure 2.1 Experimental Setup

Waveguide inputs: WR42

Orthomode transducer: Maximum possible isolation and orthogonality

Cross polarization: Minimum possible over the main beam, at least -40 dB on axis.

Antenna pattern plots: To be supplied with delivery of antenna. Principal plane and 45° plane patterns are to be measured. Patterns with and without mylar window are to be made. Co and cross polarization patterns for each of the above also required.

The antenna met all of the above specifications with two exceptions. First, the spars were not aligned with the polarization planes as specified. This deviation appeared to have no significant effect on the antenna patterns as supplied by Control Data Corp. Also the cross polarization sensitivity of our system is receiver-limited and not antenna-limited. The second deviation was that no 45° plane patterns were supplied by Control Data Corp.

Antenna performance was measured by the vendor as follows. The port-to-port isolation is 48.0 dB. The thru-arm was chosen as the cross-polarization channel to obtain lowest noise. From the several antenna patterns, the typical pattern parameters are:

Beam width (3 dB)	0.9 degree
First side lobe	-22. dB
Cross polarization level (on-axis)	-40. dB or better
Cross polarization level (peak)	-34. dB

The gain was computed to be 45.8 dB.

A mounting structure to adapt the antenna to the polarization positioner was built and installed. It is essentially two parallel 3/4-inch thick aluminum plated with standoff rods separating them. One plate is mounted to the positioner and the antenna is attached to the other plate. Large holes

in the plates accomodate the waveguides. Twist-flex waveguide sections allow the whole antenna assembly to rotate without using waveguide rotary joints.

2.2.2 Performance

Antenna performance over the duration of the experiment was very good. (See Section 2.3 for a discussion of pointing and tracking and Section 3.2 for polarization level angle effects.) Since the clear weather residual cross polarization level was not measurable we cannot place a precise quantitative value on RF cross polarization level. From our measurements we conclude that system isolation was at least -40 dB. Evidently the spacecraft (20 GHz parabola) antenna as well as our receiving antenna had very good cross polarization response. Since no pre-flight cross polarization patterns were avaiable for the spacecraft (20 GHz parabola) antenna, the above comments are important for inferring spacecraft antenna performance.

2.2.3 The Effects of Water on the Antenna

The receiving antenna is entirely exposed to weather, and thus it is important to understand the effects of water on and around the antenna structure. During a real rain it is impossible to separate the attenuating and cross polarization effects due to rain along the path and effects due to water on the antenna. Thus a comprehensive series of tests were run to determine effects of water on and around the antenna. This was accomplished by spraying water with a hose. A discussion of the tests and results are given below.

On 6 May 1974 from 1830 to 2100 Z the satellite was transmitting on 20 GHz (parabola) in the CW mode. Throughout the transmission the z-axis intercept was longitude 80.4° and latitude 36.9° (Blacksburg location is longitude 80.4° and latitude 37.2°). The weather was clear, temperature 80°F, and a wind of 10 to 15 mph from the west.

The IF receiver (gain control = 6.0) was calibrated first. The curve is shown in Figure 2.2. The number of decibels of attenuation inserted between the 1.05 GHz calibration source (12 dBm) is shown (an additional 47 dB of fixed attenuation is present also). Thus, for example, the first chart division in from the top (marked 49 dB) corresponds to 12 dBm - 49 dB - 47 dB = -84 dBm. This is the co-polarized power level received from the satellite during the test.

The sequence of tests and the results are numbered and discussed below.

1. The co-polarized output was peaked by scanning the antenna in elevation and azimuth about the predicted SLAP pointing angles. There was no offset.
2. The cross polarized output was nulled by rotating the polarization positioner. Figure 2.3 shows the chart recorder output. The RF channels were switched once every two seconds between the co-polarized channel (upper curve) and the cross polarized channel (lower curve). Note that -21.5° on the positioner gives a null response, i.e., the incoming wave polarization and the cross polarized mode of the antenna are 90° with respect to each other. Referring to Figure 2.2 the co-polarized level corresponds to a calibration setting of 49 dB while the cross polarization level is below 61 dB. This is a 12 dB fixed attenuator in the co-polarized channel, the residual (or clear weather) system channel isolation (at -21.5°) is better than 32 dB.
3. Water was sprayed from a hose up into the satellite path without wetting the dish or feed. The results are shown in Figure 2.4. It is obvious that the water did not affect the system outputs. In other words, small volumes of water along the path are not detected

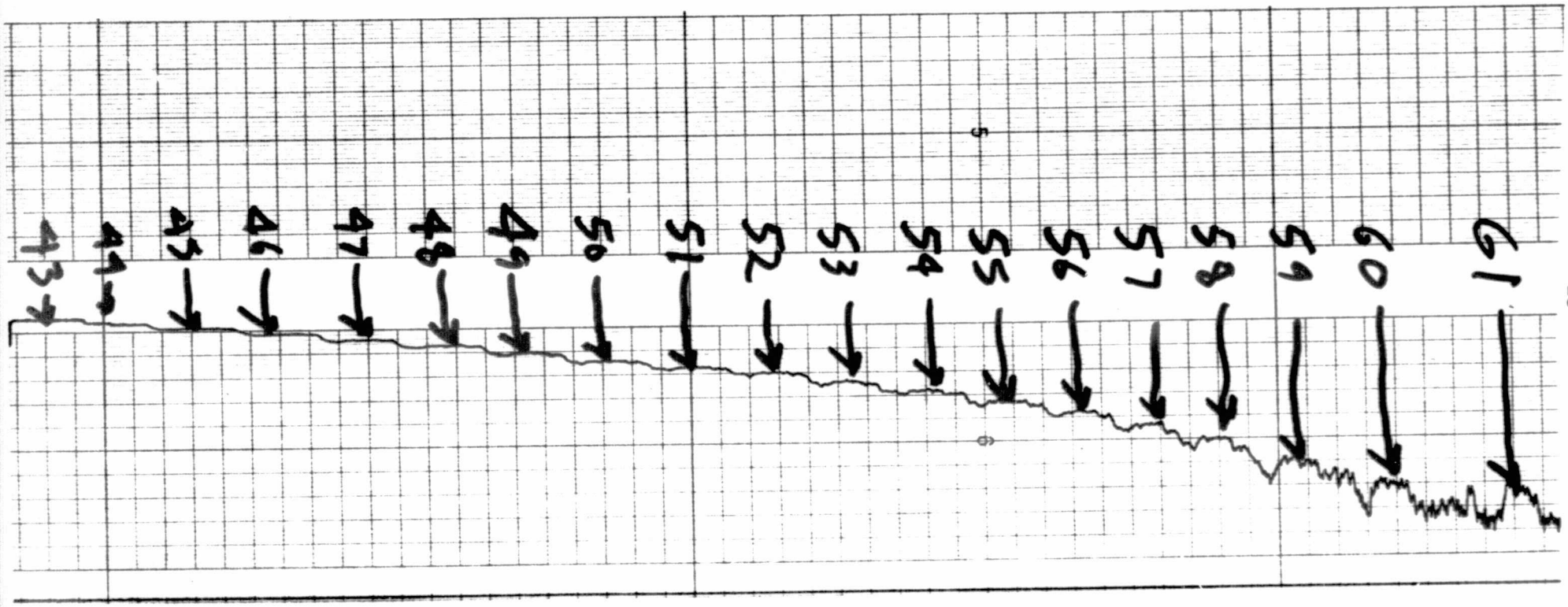

Figure 2.2 IF receiver calibration for 6 May 1975. Sweep rate 0.4 KHz/second. Gain control = 6.0.

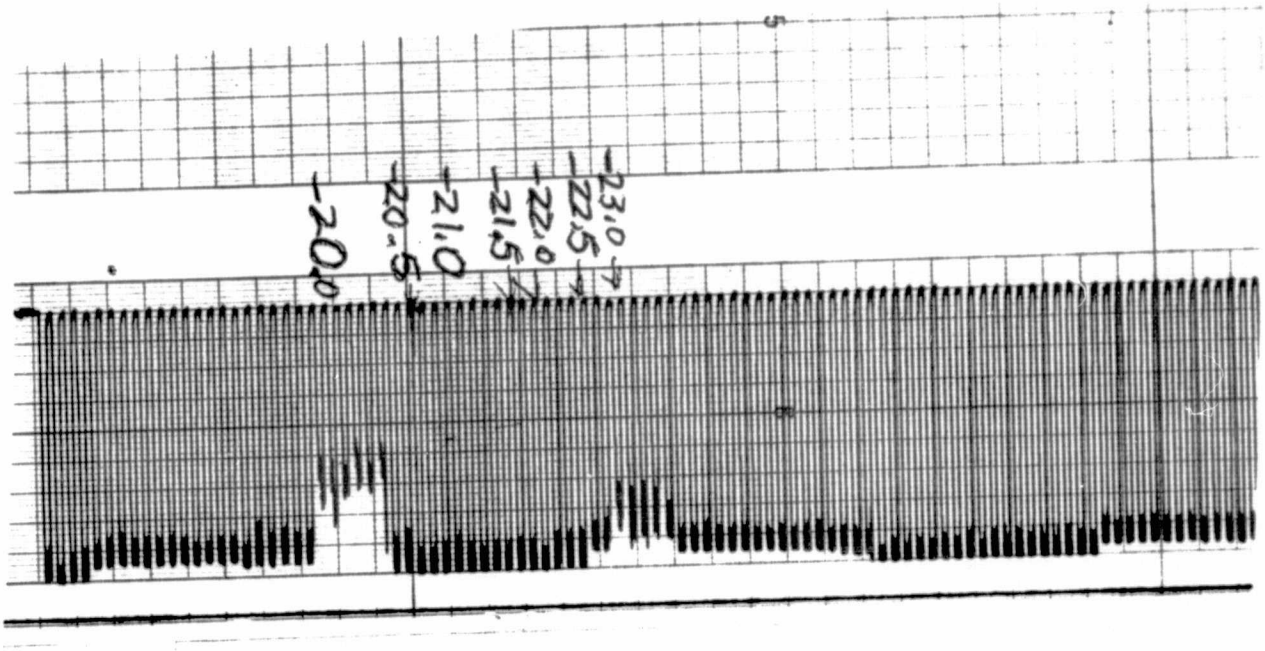

Figure 2.3 Cross-polarization nulling for changes in polarization positioner angle. Null angle = 21.50°.

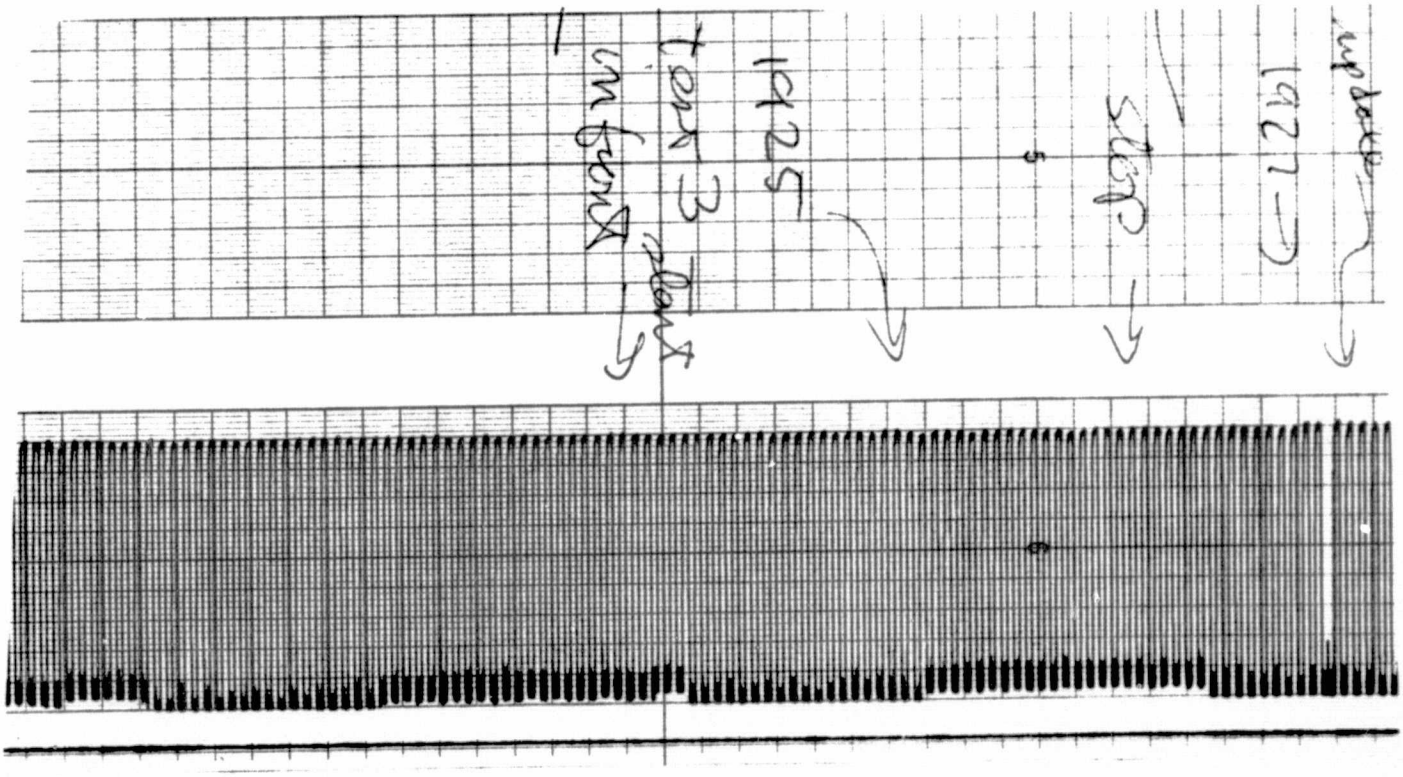

Figure 2.4 Test 3 - Water sprayed in front of antenna into path.

even when near the antenna.

4. In this test water was sprayed onto the dish with minimum wetting of the feed. The dish was thoroughly saturated several times. The results are shown in Figure 2.5. Note that the cross polarized output was unaffected and the co-polarized output changed only a fraction of a dB (about 0.3 dB maximum).

5. For this test water was sprayed between the dish and feed without significant wetting of either. The results shown in Figure 2.6 indicate no effect whatsoever.

6. The final test was more dramatic. Water was sprayed directly onto the feed from several angles. As shown in Figure 2.7, initially there was no effect. Then the cross polarized level came up and the copolarized level came down and crossed over. The channels were switched manually to identify the outputs; the channels to which the chart reader trace corresponds are identified. The cross-polarization level at maximum was 50 - 52 + 20 = 18 dB. The hypothesis at the time this happened was that water had splashed (from the struts) into the feed horn corrugations and/or throat. The antenna was pointed to zenith hoping that the water would run out (remember that this is a front-fed dish). Upon repointing and reacquiring the satellite signal the performance was unchanged. Next the antenna was lowered and water was removed from the corrugations and the antenna was shaken to free water droplets. Again, upon repointing and reacquiring the response was still poor. It was decided that water must be in the horn throat, thus the antenna was again lowered and water was located and removed from the throat. Evidently some water was against the mylar window which is about two

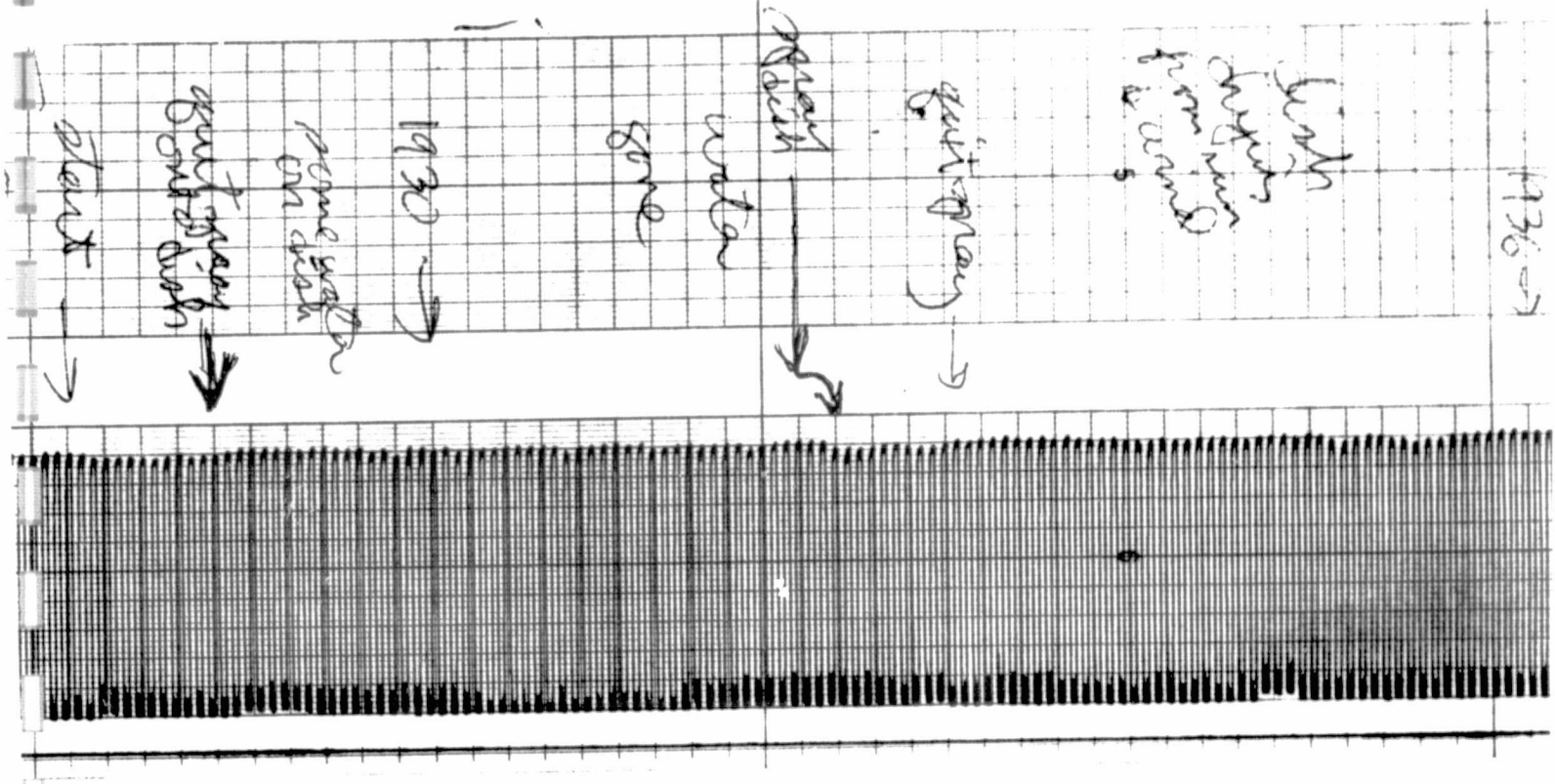

Figure 2.5 Test 4 - Water sprayed onto dish.

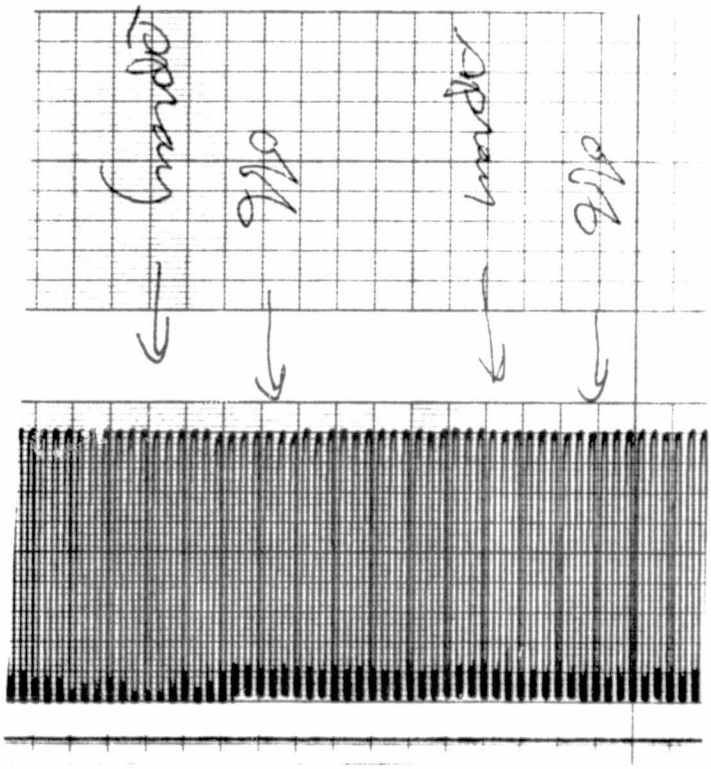

Figure 2.6 Test 5 - Water sprayed between feed and dish.

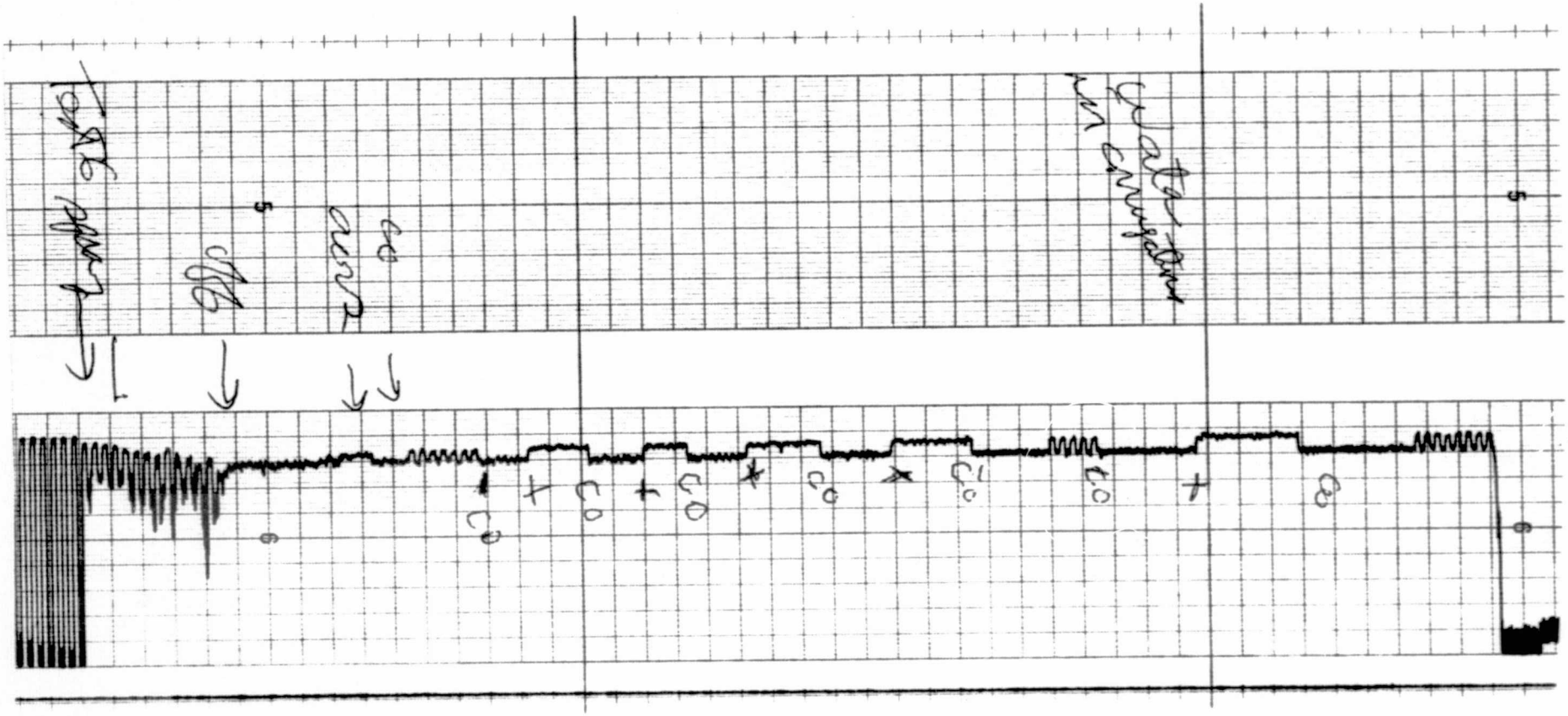

Figure 2.7a Test 6 - Water sprayed onto feed.

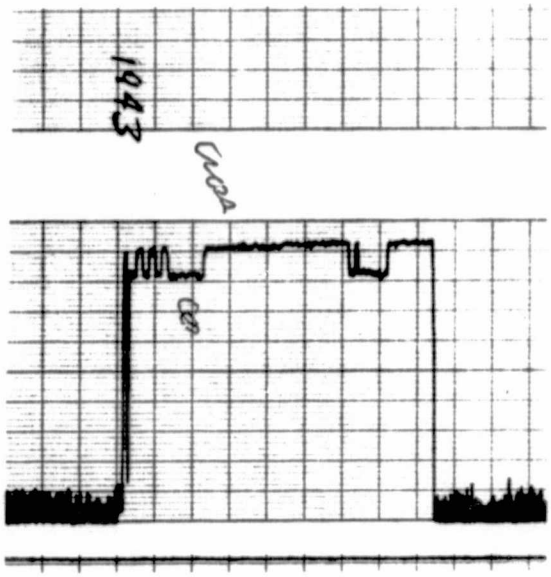

Figure 2.7b Test 6 - Response after moving antenna to zenith and back.

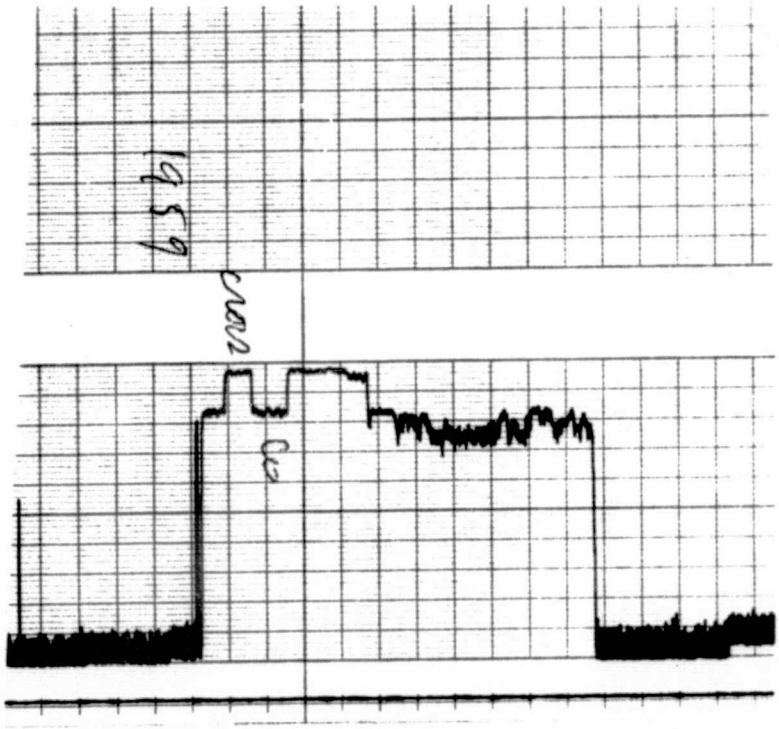

Figure 2.7c Test 6 - Response after removing water from feed horn corrugations.

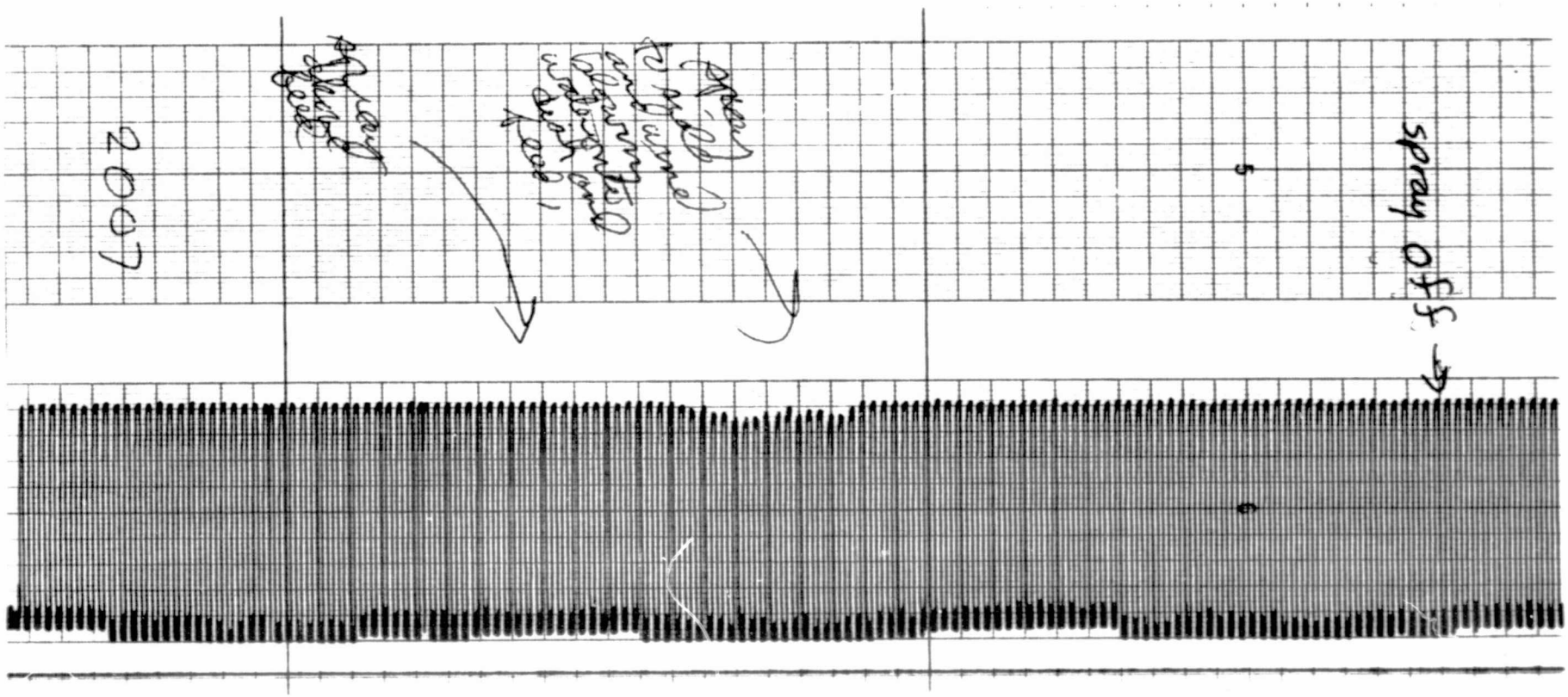

Figure 2.7d Test 6 - Response after removing water from feed horn throat followed by more water sprayed onto feed.

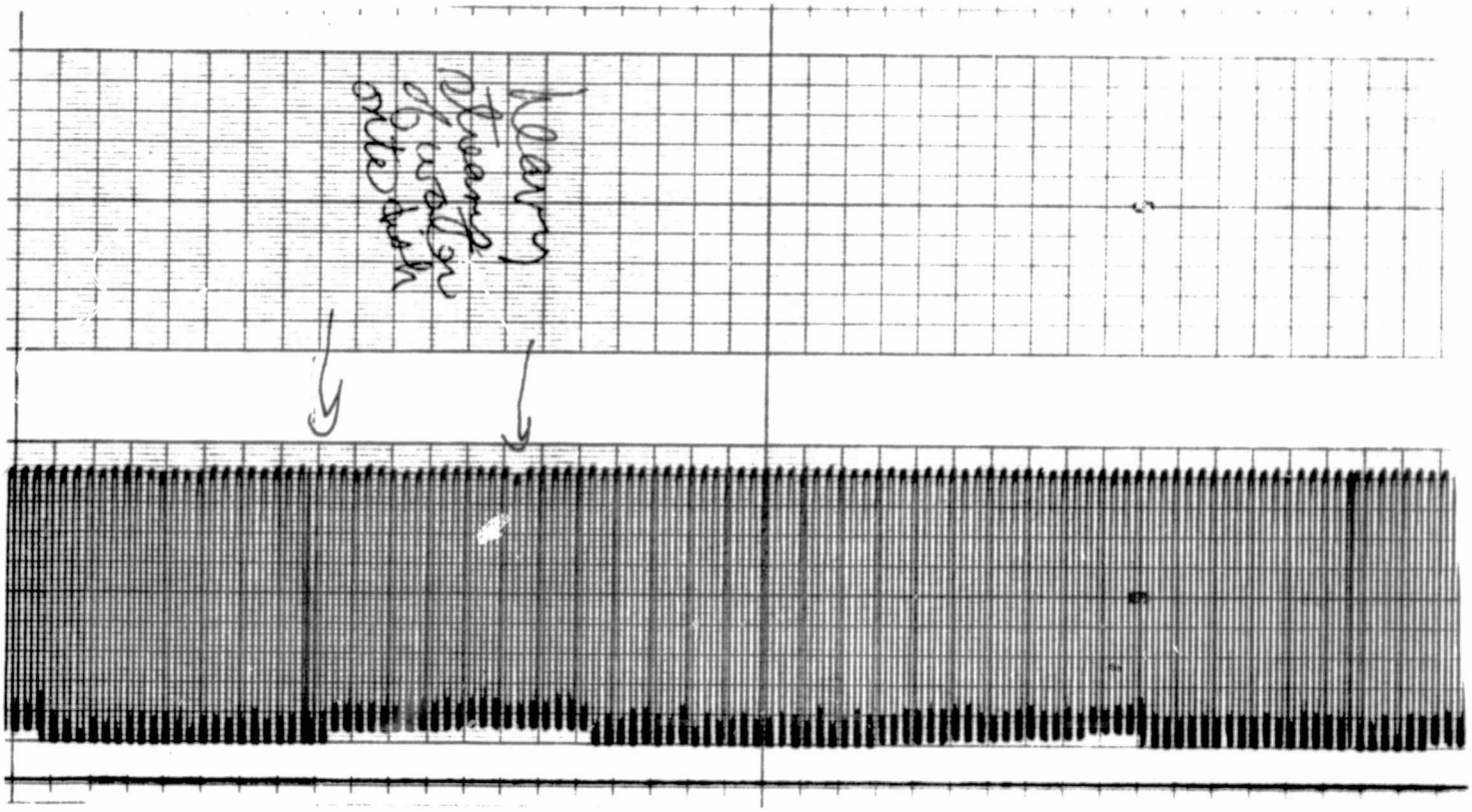

Figure 2.7e Test 6 - Water sprayed onto dish following feed test.

inches in from the horn aperture. After this was done the antenna returned to its normal clear weather performance.

This series of tests may be summarized rather simply. Water on the entire antenna structure has no effect on cross polarization and at most 0.3 dB loss in copolarized signal with one exception. When water enters the throat of the feed horn a significant increase in cross-polarized output occurs and noticeable attenuation appears. This is a castastrophic effect and is difficult to correct. In the unlikely event that this would happen during a real rain (it has never happened to us) the effect would remain even after the rain has stopped. Thus, for all practical purposes, water on the antenna has no effect.

2.3 Antenna Pointing and Tracking

Tracking data were obtained in two ways. The primary source was in-house generated data using the SLAP (Satellite Look Angle Program) program developed at Ohio State University (Hodge, 1973). Osculating orbital elements provided by NASA every two weeks were required for input to the program. A printout of elevation and azimuth angles at ten-minute intervals was obtained from the SLAPDATA program for the two-week period. Simultaneously, these data were compressed and stored in on-line disk files at the main IBM 370 computing center. The antenna could be pointed manually using the printout or a program track mode could be selected. The computer at the Tracking Station (PB 440) stored two days of tracking data and sent pointing commands to the pedestal console of ten-minute intervals. Data transfer to the PB 440 was as shown in Figure 2.8. By flipping a switch on the PB 440 console a short steam of JCL (Job Control Language) was sent over telephone lines from the tracking station through the GE 1600 computer in the Computer Engineering

Flow Diagram for Tracking Data Generation and Transfer

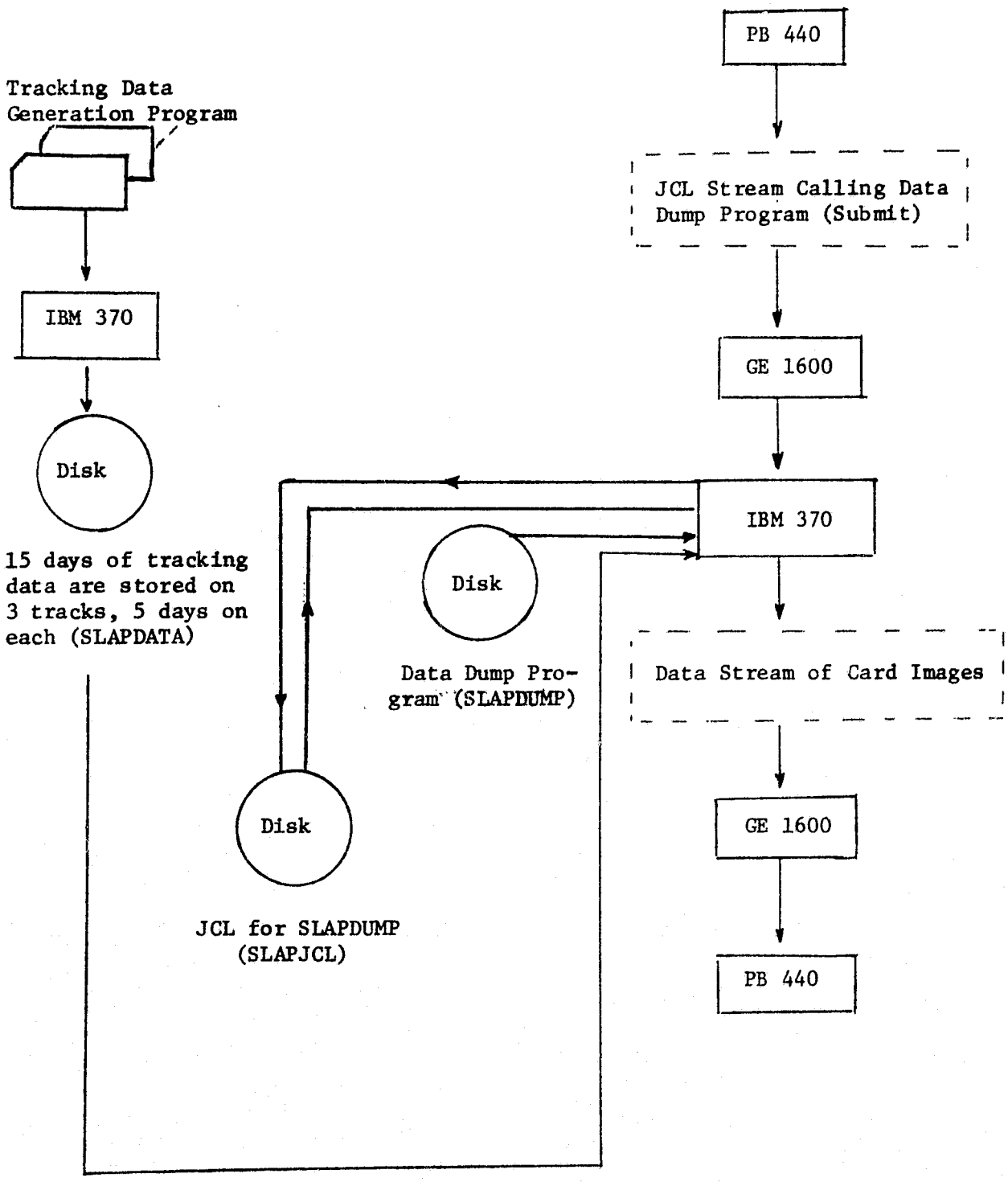

Figure 2.8

Laboratory in Whittemore Hall and on to the main IBM 370 Computer in Burruss Hall. This JCL stream initiated the SLAPDUMP program which dumped tracking data in a stream of card images back to the PB 440 over the same route. The SLAPDUMP program looked up the current day and time. It then searched through the data stored on disk which was generated by the SLAPDATA program. Upon locating the current (Universal Time) day it pulled that day and next day's data and sent it to the PB 440.

The second source of tracking data was that supplied by NASA for our station. It was a printout of elevation and azimuth angles in half-hour intervals. These data were mailed to us every two weeks.

A comparison of SLAP and NASA tracking data with actual look angles of the satellite (as obtained by peaking the receiver response) was made over the duration of the experiment. The deviation between SLAP predictions and the actual values was less than 0.1° in elevation and 0.2° in azimuth for all but a few instances. The deviations between NASA predictions and actual values was less than 0.1° in elevation and 0.3° in azimuth in most cases. Occasionally the deviation in azimuth for NASA predicts would be over 0.5°. We conclude that SLAP is slightly more accurate. It is valuable, however, to have an independent check on tracking data.

The pointing accuracy of our pedestal appears to be very good. However, a few unusual things did occur. In June of 1974 when we first acquired the satellite, elevation and azimuth offsets were established as 359.44 (or -0.56) and 358.48 (or -1.52) degrees, respectively. These offsets are due to several factors. First, the pedestal may not have been exactly aligned with true north. Second, the mechanical additions to the pedestal (polarization positioner and mounting adapter) may have caused misalignments.

Around the end of 1974 and beginning of 1975, rather large deviations

from predicted and actual pointing directions began to occur (about 0.5° in azimuth). To compensate for this the azimuth offset was changed to 357.88 on January 19, 1975 and to 357.48 on February 4: a total change of one degree from the original offset. In order to check the mechanical stability of our pedestal a level was attached to the pedestal and checked regularly. No changes in the level of the pedestal has ever been detected. Since February 4, the offsets have not been changed and tracking prediction has been very good. The reasons for changes in azimuth tracking offset during December and January remains a mystery.

A pointing and polarization angle calibration system was attempted. This consisted of an RDL Gunn diode, cavity-tuned, 20 GHz oscillator; a Scientific-Atlanta standard gain horn antenna; two 40 dB Lab-X fixed attenuators; and the 80 dB Flann programmable attenuator. All components except the programmable attenuator were supplied by NASA. These components were connected to form a transmitter. This unit was placed on top of a tall campus building and the antenna at the tracking station was aligned with the calibration unit antenna. This first test (in March, 1975) resulted in no received signal at the tracking station. After more discussions with the engineer at RDL, who had responsibility for construction of the Gunn oscillator, we found out that the frequency stability is 1 MHz per degree Centigrade. The passband of our receiver at IF is about 1.5 MHz and post detection bandwidth is about 50 Hz. Thus frequency stability is very important and the Gunn oscillator is really not an appropriate source. In fact, the engineer at RDL stated that he had no knowledge of the required stability and speculated that the Gunn oscillator would not work in our application. Therefore a series of frequency stability tests were run using a probe antenna and frequency counter. Under laboratory conditions the frequency would very as much as 0.5 MHz in a few seconds and

as much as 50 MHz over 24 hours. A second attempt to receive the signal with the transmitter on the roof of a tall building was made on 13 May, 1975. This time the frequency counter was used to monitor the frequency and the source was mechanically tuned by hand in hopes of keeping the transmitter on 20.0 GHz. Exposed to the air currents outside, the source drifted several hundred MHz during a minute. A few times the receiver indicated a strong amplitude pulse as the transmitter sweep through in frequency, however, the stability was not enough to obtain phase lock. Perhaps a very sophisticated temperature stabilization scheme would have stabilized the frequency, but only one month remained in the project and no further work was done on the calibration unit.

A properly designed calibration system would have been of great value to our project. Assuming a stable frequency source (such as used in the L.O.'s) and a mechanically stable mount, we would have had a continuously available calibration source. This would have provided an absolute power level signal (since the transmitter and path parameters are well known) from which receiver tests could have been made. The programmable attenuator could have been stepped in series of one dB steps to give complete dynamic range calibration of the receiver. Also, the calibration unit could have been used to monitor changes (if any) in pointing angles and polarization angle. A negative result would have ruled out any receiving system variations.

2.4 The Receiver

2.4.1 R.F. Front End

Figure 2.9 represents the RF front end in block diagram form. With the exception of the attenuator in the copolarized channel and the ferrite switch, this is a standard NASA supplied ATS-6 front end. A design theorist would be

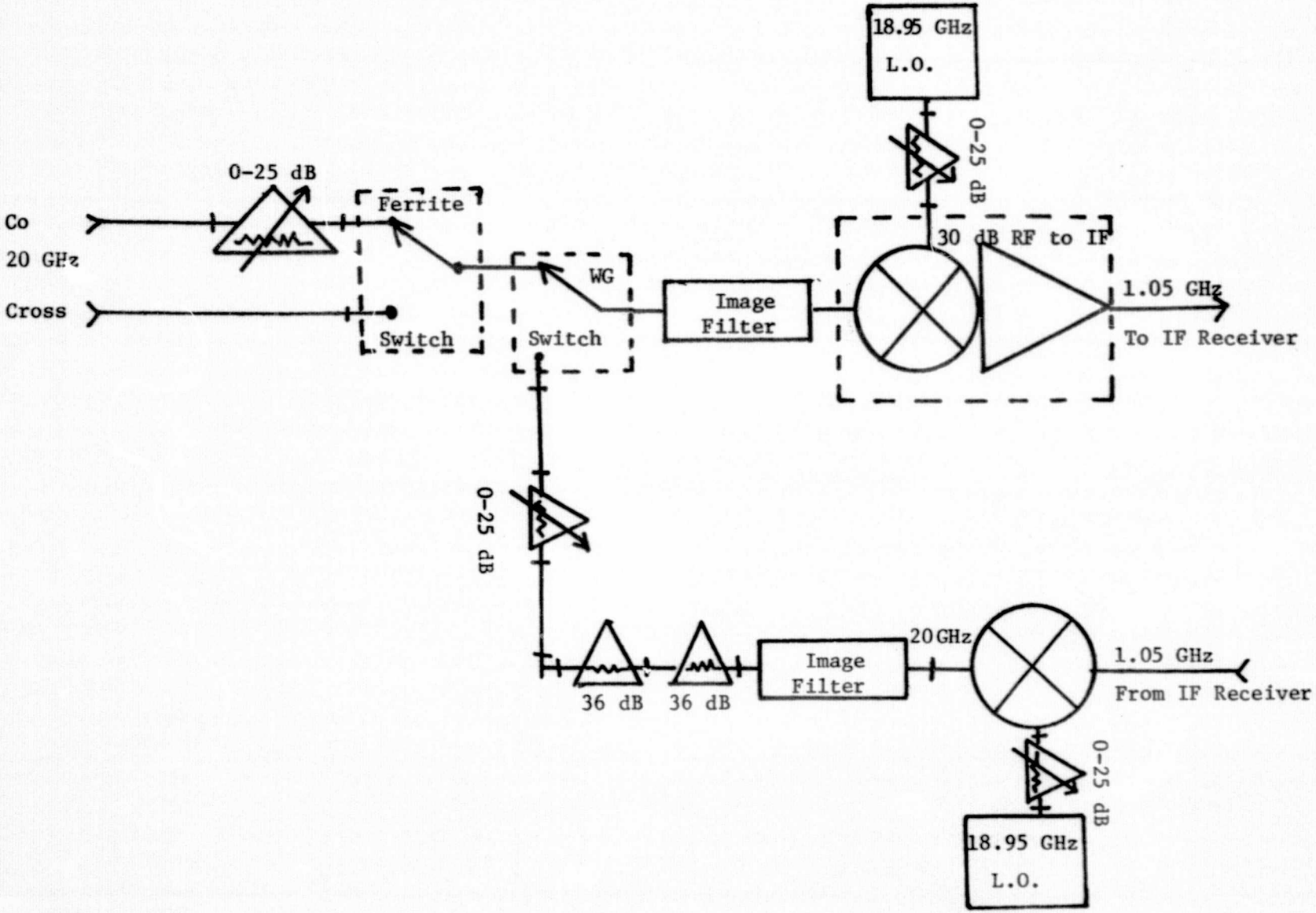

Figure 2.9 VPI&SU 20 GHz ATS-6 RF Front End

offended by the 12 dB attenuator in the co-polarized channel ahead of any amplification; however, this was necessary because the low level cross polarized component could not tolerate further attenuation. Below are the hot sky noise (N_{TO}) calculations for both channels.

Co-Polarized Channel

NF ≈ 24.3 dB, F = 269.15

N_{TO} = -114.7 dBm

Cross-Polarized Channel

NF ≈ 12.3 dB, F = 16.98

N_{TO} = -114.7 dBm

The sensitivity of the ATS-E IF receiver is -115.0 dBm which means that with the front end attenuation that we used and without any additional attenuation between the RF and IF sections the output signal to noise ratio is 0 dB at the low end of the receiver dynamic range. The downlink power budgets for all experimenters concerned with co-polarized signal were generous enough to avoid this problem by placing the attenuation between the RF and IF receivers rather than ahead of the first mixer. But for experimenters concerned with acquiring the cross-polarized signal, this attenuation would be intolerable. All this discussion emphasizes that it is very difficult to transform an attenuation measuring receiver into a depolarization measuring receiver without including a low noise amplifier in the cross-polarized channel.

As mentioned in the narrative history section we experience five (5) local oscillator failures, two (2) waveguide switch failures, one (1) amplifier failure in the twelve months the RF front end operated. It seems necessary to place more emphasis on component reliability at the terrestrial end of the propagation path.

2.4.2 IF Section

2.4.2.1 Limitations of ATS-5 IF Receiver

The major problems encountered with the ATS-5 IF receiver resulted from instabilities in the phase lock loop (PLL) circuits. A block diagram of the major circuit components in the PLL is shown in Figure 2.10. The PLL is built around a 16.5 MHz variable frequency crystal oscillator (VCXO). The output of the VCXO is multiplied by 60 in frequency and supplied to the first mixer. The mixer output at 60 MHz is filtered and reduced by the second mixer to 10 MHz where phase detection is performed. The phase detector (actually a mixer) produces an output voltage proportional to the phase error between the 10 MHz IF signal and the 10 MHz reference oscillator. The error voltage is processed by the VCXO filter, sweep and bandwidth control circuits before being applied to the VCXO. It is these processing circuits which determine the characteristics of the entire PLL signal processor. When the receiver was first examined on arrival, we observed several wires, a potentiometer, and a battery hanging from the chassis box containing these processing circuits (a sure indication of trouble to come).

A schematic diagram of the VCXO filter, Sweep and Bandwidth Control circuits is shown in Figure 2.11. There were three distinct problems in these circuits which affected the PLL operation and eventually led to a redesign of this entire section of the receiver. The problems were (1) sweeping backwards on the slow sweep range, (2) lack of sensitivity, and (3) inadequate sweep range. In Figure 2.10 operational amplifier A1 is operated as an integrator and generates a voltage ramp which is summed with other voltages by A3 and used to control the frequency of the VCXO. Operational amplifier A2 is also operated as an integrator and integrates the error signal from the phase detector (mixer). The integrated error signal is also

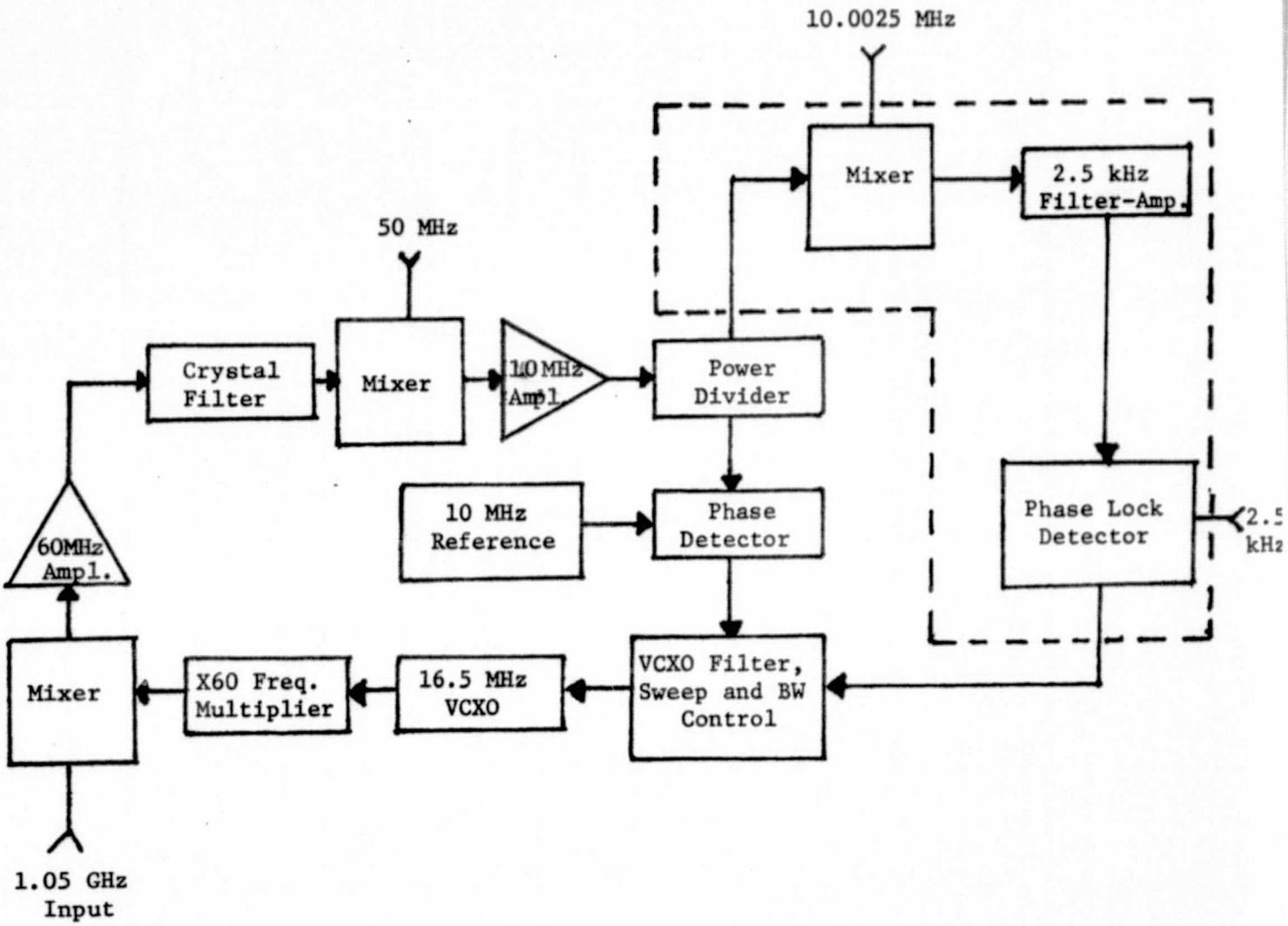

Figure 2.10 Block Diagram of Major Circuit Components in PLL

ORIGINAL PAGE IS
OF POOR QUALITY

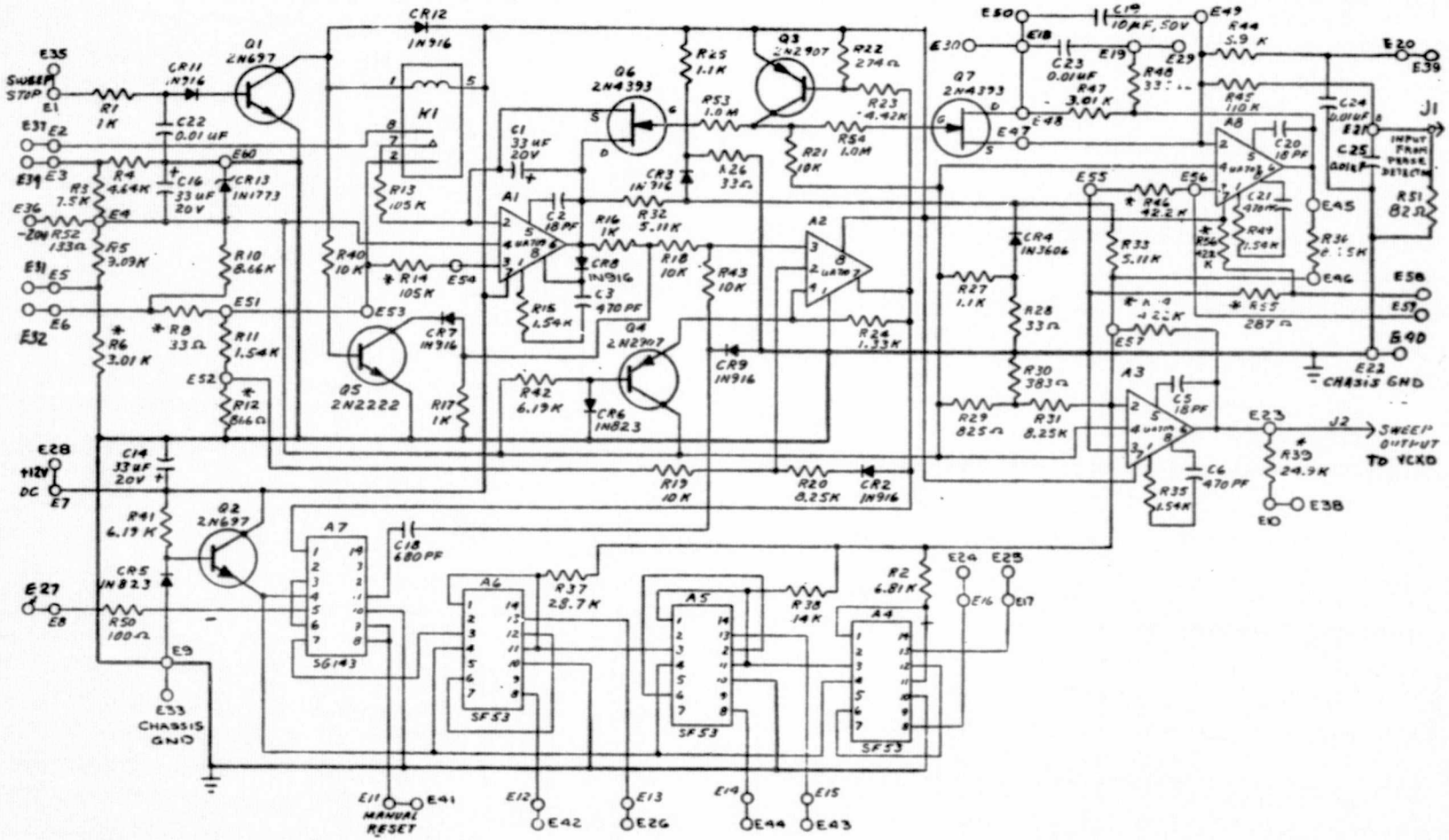

Figure 2.11 VCXO Filter, Sweep and Bandwidth Control Circuit Schematic

summed by A3 and forms part of the VCXO control voltage. Flip-flops A4, A5, and A6 supply fixed voltages to A3 (and hence to the VCXO) which determine the sector of operation.

During normal operation, and before signal acquisition, the output of A8 should be zero since the mixer output contains only noise (the integral of which is zero). Relay K1 is energized applying a small voltage to integrator A1 which is integrated to produce the sweep ramp. When a phase lock is detected relay K1 is deenergized and the sweep stops. Lock is maintained by the integrated error signal supplied by A8.

The first problem encountered was incorrect sweep speed on the slow range and even sweeping backwards. This was caused by a gross unbalance of op amp A8 causing the bias current to be integrated and producing a voltage output with no signal (only noise) input. The output of A8 was then a ramp which was added to the sweep ramp by A3. Depending on the relative magnitudes of the two ramps, the sweep could be increased, decreased, stopped, or reversed. Even after the signal is acquired and the sweep of A1 is stopped, the tendency of A8 to continue sweeping on its own would tend to pull the circuit out of lock and therefore reduce the sensitivity. Two methods were tried to correct this problem in the original circuit. One was to connect a MOSFET (2N4351) across capacitor C19 which would short out this capacitor when the receiver was not phase locked. Then only A3 could contribute to the sweep. The second correction was an attempt to reduce the unbalance of op amp A8 using a potentiometer type balance circuit. This proved to be a very critical adjustment. When properly balanced the sensitivity was acceptable, but 30 minutes later the circuit would be unbalanced again due to temperature variations in the bias current of A8. Also the balance potentiometer was connected to both the +12 and -12 volt power supplies in order to

derive the correct bias voltage, and this led to unbalance of A8 due to power supply variations.

The second problem which caused a reduction in the sensitivity was inherent in the design of the circuit. When the receiver is sweeping, capacitor C1 (associated with A1) charges in order to produce the voltage ramp, and the voltage across C1 is part of the voltage applied to the VCXO. When phase lock occurs and the sweep is stopped, C1 begins to discharge. In order to stay at the same VCXO frequency, the voltage output of A3 must be constant. Hence the circuit must move slightly out of phase lock until the integrated error voltage of A8 can compensate for the decrease in voltage across C1. This causes a significant increase in the minimum signal input required to acquire and maintain a phase lock.

The third problem we encountered was insufficient sweep range. Although the VCXO was intended to operate with control voltages between -5 and +5 volts, the original circuit only produced voltages in the range -2.5 to +2.5 volts. Our first solution was to provide a 3 position range switch which would offset the voltage applied to the VCXO and provide overlapping sweep ranges of -5 to 0 volts, -2.5 to +2.5 volts, and 0 to +5 volts. We could then utilize the full range of the VCXO.

2.4.2.2 Final Receiver Modifications

After making the preliminary modifications described in the previous section, we found that we still had a receiver which required very frequent adjustment and which lacked sensitivity. After careful consideration we concluded that the entire VCXO Filter, Sweep and Bandwidth Control circuit should be redesigned with a goal of eliminating the problems we had observed. The first step was to perform a detailed analysis of an operational amplifier

used as an integrator to see what factors were important in the design of a stable and balanced (free from drift) integrator. The results are shown in Figure 2.12. The output voltage v_o is the sum of three terms. The third term determines the amplifier offset and is independent of the integrating capacitor, C, and the input voltage v_i. It is competition between the other two terms which determines the stability and drift characteristics of the integrator. The second term represents the integral of the input voltage and is the desired output of the integrator. The magnitude of this term depends on the produce R_- and C which is the integrator time constant. The first term represents drift and instability and can produce an output voltage with no input voltage. However, this term depends only on the size of the integrating capacitor and the offset current imbalance, I. The integrator stability will be optimized if the second term is made as large as possible with respect to the first term. There are two ways to do this. First, the current imbalance I can be made as small as possible. This is accomplished by choosing an op amp with input bias currents i_+ and i_- as nearly equal as possible. Since R_- is determined by the required time constant, i_+ must be smaller than i_- in order to guarantee that R_+ is positive. If this is done the variations in I with temperature will also be minimized. The second way to minimize the first term is to make the capacitor as large as practical while maintaining the product of R_- and C constant. Both of these methods to minimize the integrator drift were used in the redesigned circuit.

The second problem to be overcome was the discharge of capacitor C1 in Figure 2.12 after phase lock was obtained. This can be corrected by combining the functions of A1 and A8 so that the same capacitor which is used to generate the sweep is also used to integrate the error signal. Therefore only one op amp needs to be balanced or stabilized. This was also done in

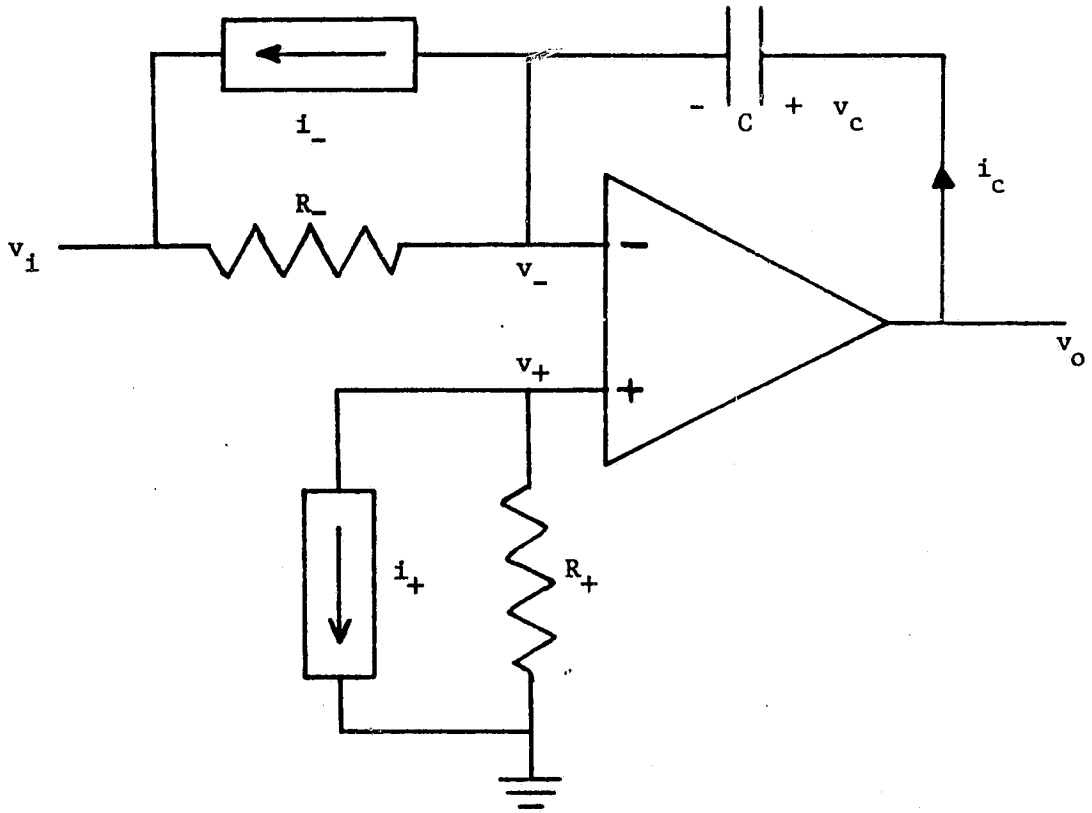

$$v_+ = -i_+R_+ \quad \text{and} \quad v_- = v_i + (i_c - i_-)R_-$$

Since $v_+ = v_-$, $-i_+R_+ = v_i + i_cR_- - i_-R_-$

$$i_c = \frac{i_-R_- - i_+R_+ - v_i}{R_-} = i_- - \frac{R_+}{R_-} i_+ - \frac{v_i}{R_-}$$

$$v_o = v_c + v_- = v_c + v_+ = \frac{1}{C}\int (i_- - \frac{R_+}{R_-} i_+ - \frac{v_i}{R_-})dt - i_+R_+$$

Let $I = i_- - \frac{R_+}{R_-} i_+$

$$v_o = \frac{1}{C}\int Idt - \frac{1}{C}\int \frac{v_i}{R_-} dt - i_+R_+$$

$$= \frac{IT}{C} - \frac{v_i t}{R_-C} - i_+R_+$$

Figure 2.12 Block diagram of the receiver modification.

the new design.

The final problem of obtaining the desired sweep range was accomplished by designing the new circuit to provide sweep voltages to the VCXO in the range -5 to +5 volts without the necessity of a range switch.

The final circuit which was incorporated into the receiver in place of the original VCXO Filter, Sweep and Bandwidth Control circuit is shown in Figure 2.13. Operational amplifier A1 performs both functions of sweep and phase lock. It is selected to satisfy the requirements previously described. Switch S1 selects the sweep speed of either 4 KHz/sec. or 0.4 KHz/sec. MOSFET Q1 allows sweep to occur when it is on and stops the sweep when it is off. The sweep stop signal is produced by the phase lock detection circuit. The filter characteristics of A1 are the same as those of the original circuit. The capacitors have been increased by a factor of 80 and the resistors decreased by the same factor. This alone increases the stability by 80 times. Operational amplifier 2 serves as a comparator to detect the end of the desired sweep cycle. A3 is a one-shot multivibrator which generates a reset pulse at the end of each sweep cycle. A6 is used as a 3 bit binary counter to determine one of eight sectors in the automatic mode. The count in A6 is advanced by each reset pulse so that all eight sectors are swept sequentially. In the manual mode, sector switch S2 determines the sector to be swept. Op amp A5 sums the sector voltage to the control and sweep voltages from A1 and produces the output to the VCXO. A4 produces a regulated +5 volts for the logic.

2.4.2.3 Results of Modification

The problems encountered in the original VCXO Filter, Sweep and Bandwidth Control circuit were eliminated in the new design. The circuit as shown

in Figure 2.13 was optimized for the 0.4 KHz/sec. sweep speed since this speed realizes the greatest sensitivity and is normally used. As a result of excessive loading on the mixer by the 68 ohm resistor at the 4 KHz/sec. sweep speed, the circuit sometimes fails to lock on a weak signal at this speed. This has been no problem for us. If desired, however, an additional pole on switch S1 could be used to switch in a smaller integrating capacitor at the 4 KHz/sec. speed. Then a larger resistor could be used (in place of the 68 Ω resistor) to reduce the loading on the mixer while maintaining the same time constant.

The operation of the new circuit at the 0.4 KHz/sec. sweep speed is very good. With the old circuit (and with everything adjusted as well as we could) the lower limit of signal into the IF receiver at 1.05 GHz at which we could maintain a phase lock was -118 dBm. Most of the time we could not do nearly this well. Now we can maintain lock down to -134 dBm. In addition the circuit will sweep up to and lock onto a signal of -134 dBm. Previously the signal had to be at least -100 dBm to acquire lock. The potentiometers connected to pin 3 of A1 in Figure 2.13 were adjusted when the circuit was installed and have not required readjustment. The sensitivity has remained the same.

2.4.3 Calibration

The original ATS-E receiver included calibration circuits at both input and IF frequencies. Leakage problem made the 20 GHz calibration system very difficult to use and for most of the experiment no local oscillator was available to drive it. For these reasons most of our calibration was done at IF.

The IF system used a Frequency Sources 1.05 GHz oscillator as a calibration source. The oscillator output remained constant at 12 dBm. Fixed

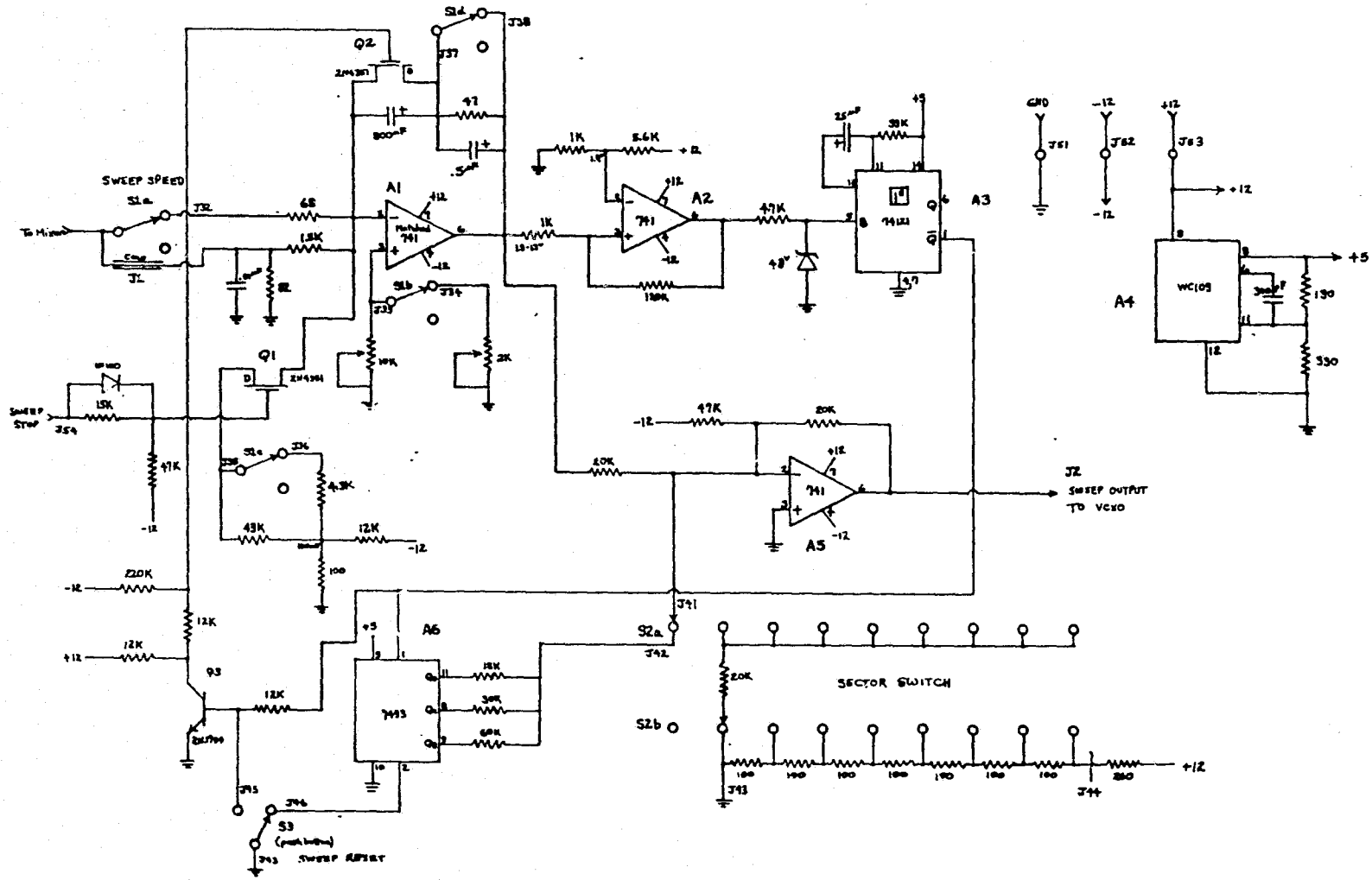

Figure 2.13 Redesigned VCXO Filter, Sweep and Bandwidth Control Circuit

attenuation of 50 dB and a 10 to 90 dB variable attenuator were used between the source and IF receiver. The fixed attenuation consisted of four attenuators in series. These were calibrated separately by using the calibration source, the calibrated variable attenuator and the IF receiver.

Initially the calibration source and the attenuators were mounted inside the IF receiver cabinet. Signal leakage from the N type connectors in the attenuator chain made this arrangement unsatisfactory. Calibration readings at low signal levels would change if the spacing between the attenuator chain and chassis changed. Also, the operator could not get near the fixed attenuator while calibration was in progress.

To solve the problem the source, the 15 VDC supply, and the attenuators were removed from the IF receiver cabinet. These were mounted in a 10" x 11" x 24" metal housing with carrying handle. The source, the variable attenuator, and the four fixed attenuators were connected with 7 mm semi-rigid coax. Each unit and its connectors were shielded with an aluminium housing. All housing-to-chassis joints of these shields were sealed with conducting tape. An AC rectifier was installed to power the 15 VDC regulator. Thus the only connecting cable to the IF receiver was a coax carrying the attenuated 1.05 GHz calibration signal. Accurately repeatable calibration charts were obtained with the calibration unit.

The coax line from calibrator to receiver added 9 dB of fixed attenuation. Therefore the absolute signal level could be determined from the attenuator setting by

$$\text{dBm} = +12 - 59 - \text{variable attenuator setting.}$$

2.5 Radars

2.5.1 Introduction

A NASA supplied RD-110 Bendix aircraft weather avoidance radar was converted

to a weather search unit with the addition of a pedestal which allowed a 360° horizontal rotation of the antenna. Pertinent radar specifications are shown in Table 2.1. We intended to construct a radar-to-computer interface which would provide (a) computer tracking of storms (b) early warning to operators' homes that rain was approaching (c) computer analysis of rain rate from tipping buckets versus radar backscatter. The electronic interface was completed, but due to the unforeseen large number of man days required for maintenance on the PB-440 computer, the computer software was not completed. Two other radars were tested briefly, but time did not permit their full implementation

2.5.2 Search Radar Construction

A description of the construction of the search radar follows. A housing of wood contains the transmitter, the 28 VDC to 400 Hz, 115V converter, a 64 increment electronic azimuth pulse generator, a 10 circuit slip ring unit donated by Polyscientific Corporation, a K-band WR-62 rotary joint from NASA, a 15 cu. ft./min. ventilator fan, and an intercom connection jack. A Scientific Atlanta polarization positioner (model 5601-1-51) with a 1:1 synchro is mounted on top of the housing. The housing is located on a platform on the roof of the Tracking Station. The antenna unit is attached to the positioner in a manner that allows the radar beam to be pointed from zero to ninety degrees in the vertical plane by use of a scan control. Therefore the radar beam can be directed along the satellite path, if desired.

Mounted in the Scientific Atlanta antenna position control console is a Sorensen DCR-40-10A power supply, the radar indicator unit, a servo driven azimuth indicator, and an A-scan oscilloscope. The indicator has a 90° PPI presentation. This was used in the vertical plane to give a visual indication of altitude and intensity of weather for any azimuth pointing.

Table 2.1.

RD-110 Weather Radar Specifications

RADAR CHARACTERISTICS	
Radar Range	9, 15 and 30 miles, selectable
Peak Power Output	8 kW (nominal)
Transmitting Frequency	15.5 ± 0.1 GHz (Ku-Band)
Klystron Operating Frequency	15.43 to 16.63 GHz
Pulse:	
Amplitude	4.85 to 5.15 kV
Width	1.5 μs nominal
Repetition Rate	800 p/s
Duty Cycle	0.0012

RECEIVER CHARACTERISTICS	
Intermediate Frequency	30 MHz
Gain	100 dB
Noise Figure	12 dB
Sensitivity Time Control	Effective to 3 miles (sq. law)

Figure 2.14 shows the radar-computer interface block diagram. The circuit was designed to provide the computer with an integrated backscatter signal for 0 to 5 mile, 5 to 10 mile and 10 to 15 mile range from one burst of radar transmission. The integrated video is collected 64 times in 360 degrees of azimuth rotation of the antenna.

The positive going range gate activates a one-shot multivibrator with Schmitt trigger (74121). The four resets (R) are triggered and the system is ready to integrate backscatter. The azimuth indicator is a disk with 64 holes on an 8-inch diameter. The disk rotates with the antenna. An LED activates a photo transistor each time a hole passes between them. The azimuth mark and the first succeeding system trigger causes the J-K flip-flop to have Q_1 and $\overline{Q}_2$ as positive outputs. Then the AND gate denoted X provides an output which (1) calls the computer multiplexer (2) zero sets the integrator through a one-shot multivibrator and two transistors (3) saturates the FET integrator gate through the 741 amplifier. Any backscatter is integrated and collected by the computer. The five-mile range marked causes the J-K flip-flop to go to the $\overline{Q}_1$, Q_2 state. This action opens the FET gate on the 0-5 mile integrator and activates an identical integrator circuit connected to the AND gate output Y. The ten-mile range marker provides a similar action for an integrator circuit connected to AND gate output Z. At the end of the range gate the system is reset.

A 64 counter provides azimuth BCD information to the computer. An LED, photo transistor pulse generator resets the counter once each 360 degrees rotation of the antenna.

2.5.3 RD-110 Radar Modifications and Repairs

The range gate, range marker and trigger signals were brought from indicator board TB 201 (Bendix Manual I.B. 2110A) to the interface circuit with

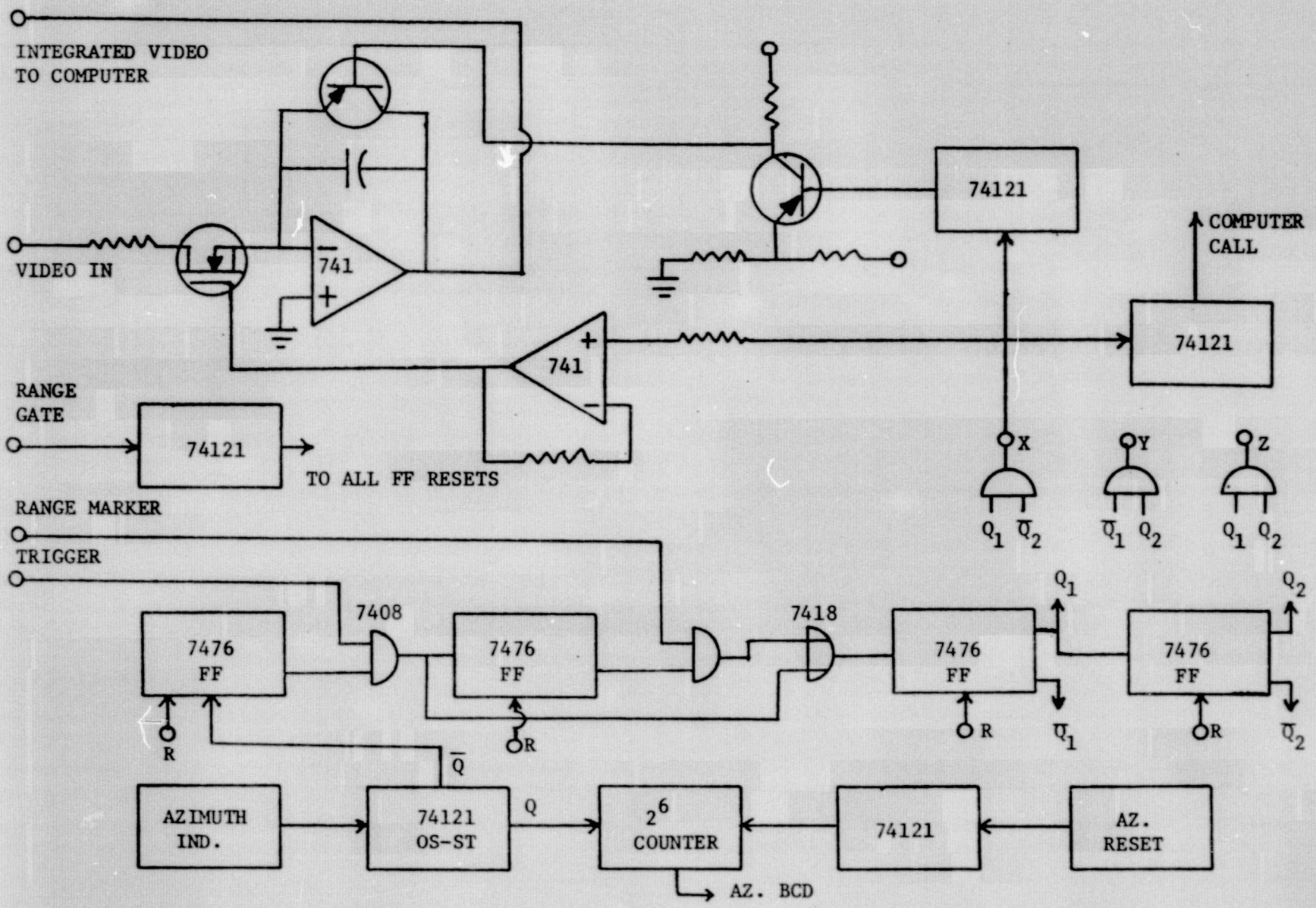

Figure 2.14 Radar-Computer interface block diagram.

RG 122 coax. The radar 90 mile range was converted to a 15-mile range. On indicator board TB 201, R230 was changed to 33K ohms, R231 to 10K ohms and capacitor C209 was changed to 600 pF. The 15 mile range was desirable because the antenna required approximately an 8 degree elevation to avoid backscatter from mountains. At the 15 mile range the beam axis is at an elevation of about 10,000 ft. Most severe storm fronts do not exceed this elevation. Therefore the 15 mile range was selected and the 90 mile range was changed because it was of least use at this geographical location.

The range gate generator in the indicator (TB 201) failed several times. Transients would fire UJT Q207 which would cause destruction of Q206. A 150 ohm resistor was placed between CR208 and R246. A diode was connected from base to emitter of Q206. A 1000 pF capacitor was placed across R241 for speed-up action. The circuit operated without failure after the changes.

The source of transients was traced to the 8.5 KV supply, PS1. Two of the supplies failed after only a few hours operation. Tests showed that the CRT current was 5 μA to 75 μA from low to high intensity. The CRT maximum current rating is listed as 100 μA. Apparently the high voltage package had a design flaw. It was replaced with a Spellman 8.5 KV supply, model UH 15P10 X 156, located external to the indicator unit. The supply operates from a 10 VDC, 300 mA source. No failures have occurred in the indicator for seven months of operation.

The transmitter kylstron became gassy after a few hours of operation. The TK 113 Klystronics unit was replaced with a NASA spare unit. The klystron was peaked on the main mode by observing backscatter from a fixed target and by adjusting for maximum AFC flutter as described in the manual.

Output of the Avionics inverter dropped to 103 volts which reduced the radar power. The ventilator fan was inoperative. The unit was replaced with

a NASA spare and its output has remained at 115 volts. The fan still does not run. Whether the fans are faulty or both are disconnected will be determined before the CTS experiment begins.

Creepage and corrosion between the 300 VDC pin and the 28 VDC pin destroyed Bendix Connector SP07E-20-39P on the radar interconnect cable. The 300 VDC pin was transported completely and the rubber mold was desintegrated. The cable assembly was replaced with a NASA spare unit on loan for the remainder of the project.

2.5.4 Doppler Radars

The Department of Navy transferred six AN/PPS-18 homodyne doppler units, to NASA/Goddard. Characteristics are:

Frequency	9.3 GHz
PRF	8 KHz
Peak power	2.5 W
Range	3000 M
Input power	12 VDC at 1A.

Some investigation of the operation of these units was conducted by interested students. The radars are extremely sensitive and frequency changes were noted for targets moving at different angles with respect to the receiving dipole array. Perhaps rain drop velocity and direction could be established with these radars. However, considerable carefully controlled testing would be required to establish the usefulness of these doppler units in weather research.

2.5.5 X-Band Weather Radar

The NASA supplied 9.4 GHz AVQ/46 weather radar was bench tested. The transmitter has a faulty modulation transformer. Evidence of previous arcing

was noted at the transformer output terminals. Apparently, the transformers are available from RCA and replacement does not appear to be a difficulty.

2.5.6 Use of the RD-110 Weather Radar

As stated previously, the RD-110 radar was not interfaced to the computer. The radar proved extremely useful, however. Station operators quickly learned to interpret the PPI and A-scan presentations. The storm intensity, velocity and direction could be estimated. Valuable lead time was provided to acquire the satellite. Also the passing of the storm could be accurately predicted and the satellite released without undue delay.

2.6 Weather Instruments

The weather instruments employed were five tipping bucket rain gauges and two wind velocity sensors. Three of the rain gauges were along the nominal satellite path (200° azimuth), and the remaining two were at right angles to the path. Figure 2.15 sketches the location of all instruments. The weight of 0.01 mm of rain would trip each bucket generating a pulse. The time of each pulse occurrence was recorded and stored in the PB-440. The two wind velocity sensors were distributed along the satellite path and provided wind direction and wind speed information to the PB-440. The maximum wind loading allowable with the four (4) foot dish was 60 mph. Anytime the PB-440 detected a wind speed of 60 mph or higher, it would slew the antenna to zenith.

2.7 Data Collection System

A Digital Controller controlled the basic timing of the experiment. The received satellite signal was sampled at a one second rate and every two seconds, just after the sample, the receiver was switched between the co-polarized cross-polarized input channels. The wind sensors were also sampled at a two second

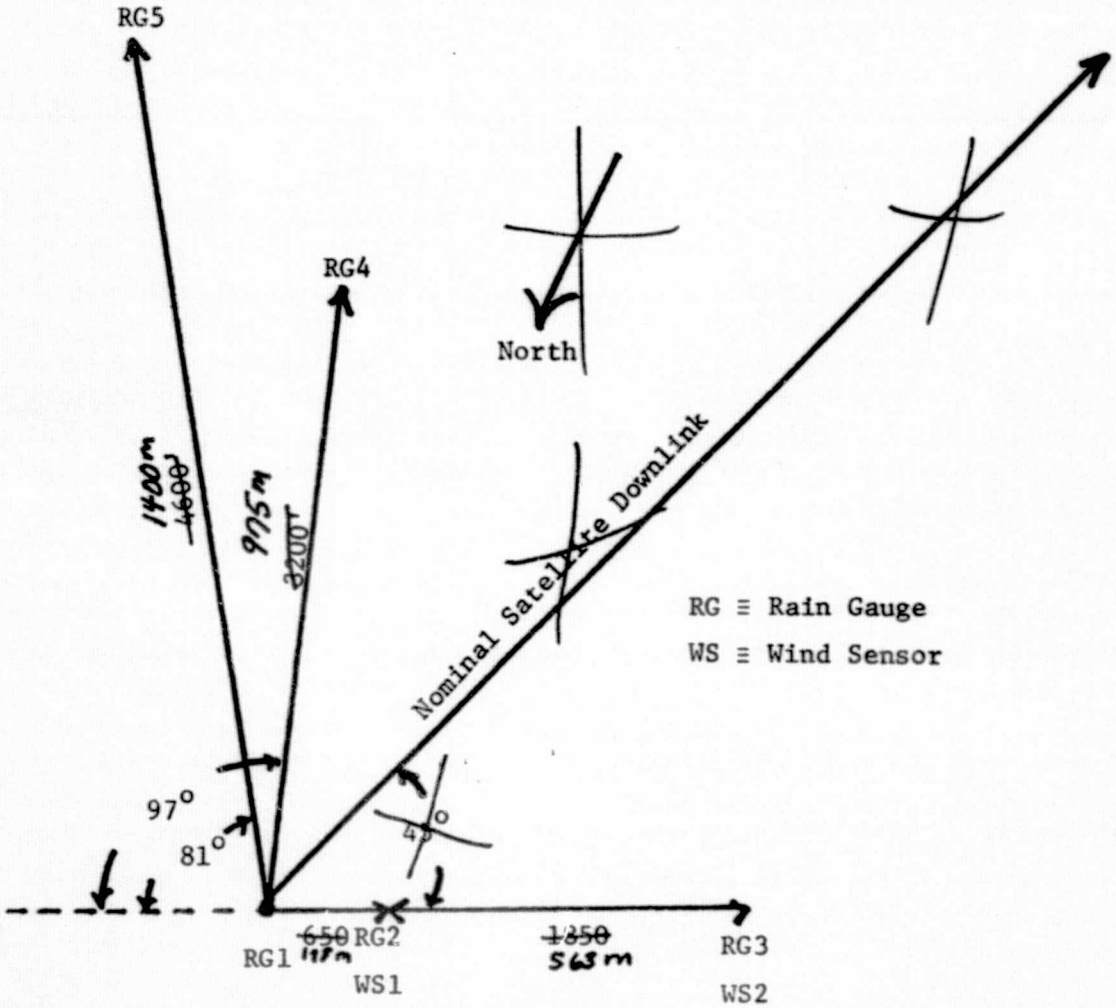

Figure 2.15 Map of Meteorological Instruments with Respect To the Satellite Path. RG1 is Located at the Tracking Station.

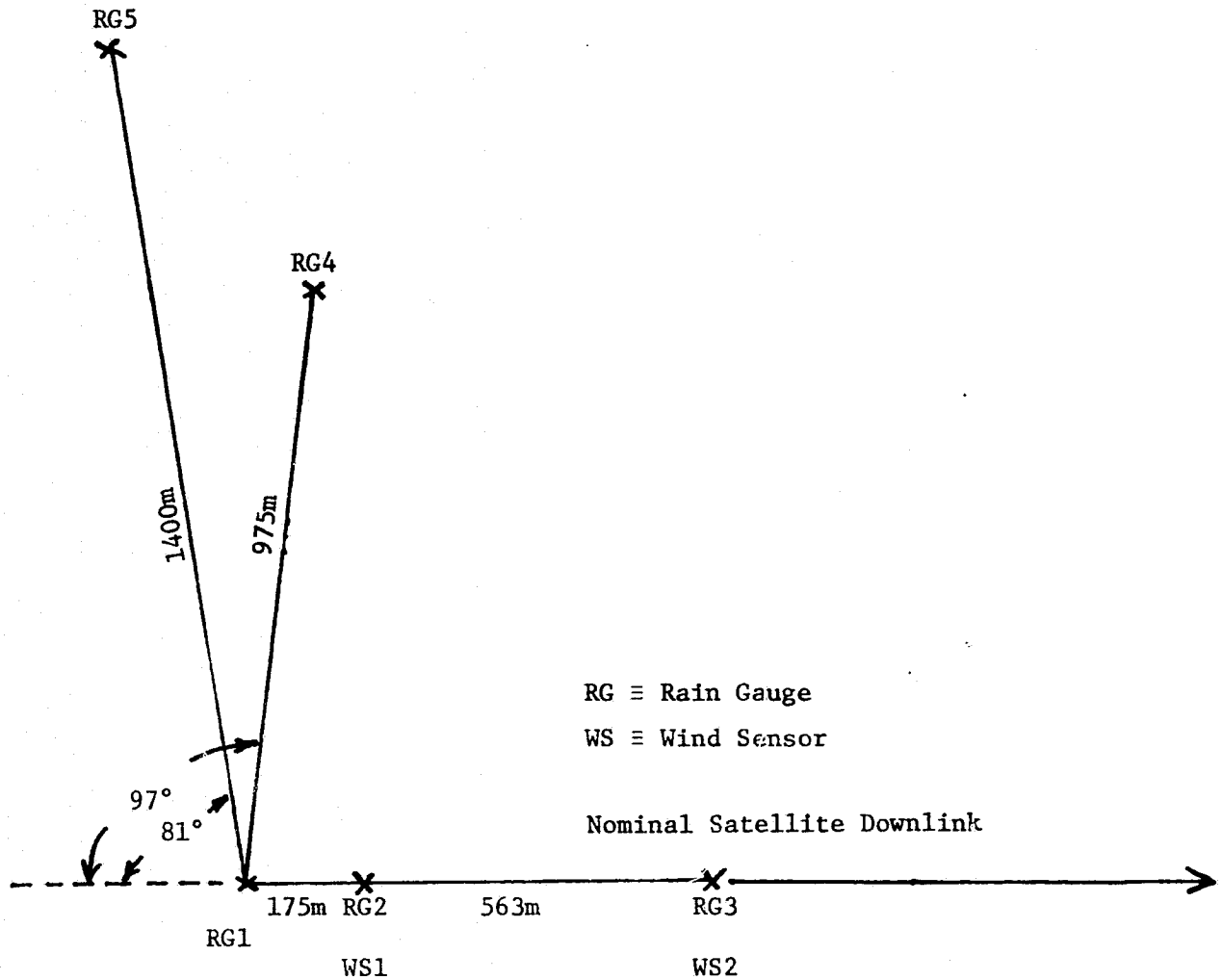
RG5
RG4
1400m
975m
97°
81°
RG ≡ Rain Gauge
WS ≡ Wind Sensor
Nominal Satellite Downlink
175m
RG2
563m
RG3
RG1
WS1
WS2

rate. Rain data were stored asynchronously whenever a rain gauge tripped.

All data passed through the Digital Controller where the analog signals were digitized and all of the signals were tagged with an identifying "what number" and a binary time accurate to two tenths of a second. At this point an interrupt was generated to make the data available to the computer.

Once in the computer all data was handled in the same manner. Each piece of data was compared to the previous piece of data with the same "what number." If the value was significantly different from the preceding value the data, along with the "what number" and the time of that value was stored in core. To be retained the difference between two successive pieces of data must be greater than four parts out of two hundred fifty six. This procedure was decided on to prevent filling core with redundant data since we only had 8K of core.

Two sections of core, each consisting of 2K were allocated for data storage. When one section was filled the program would then store in the other section while punching the data in the section that had just been filled on paper tape. This temporary storage of data was necessary because the 370 is shut down during storms which is when we normally took data. Stored data were later transmitted to the 370.

3. Results

3.1 Introduction

This chapter presents the results of our investigation. For most of the experiment, the spacecraft was positioned near 95° W. longitude and our nominal look angles were 45° elevation and 200° azimuth. As the spacecraft began its drift toward India, it moved across the sky and set in the west. While it was setting, we collected considerable data on rain and clear weather propagation at low elevation angles. Since low angle effects may differ from those encountered under normal high angle propagation conditions, we will discuss data taken above 15° elevation first and end this chapter with a discussion of our findings at angles below 15°.

3.2 Clear-Weather Changes in the Received Polarization Angle

3.2.1 Introduction

Before one can measure precipitation depolarization or design a dual polarized receiving system for a communications satellite, the clear weather polarization state of the received signal must be determined. On a linearly polarized terrestrial radio system the normal received polarization is fixed by the physical orientation of the transmitting antenna. In the absence of refractive effects this means that, if dual-polarized transmitting and receiving antennas are properly aligned and securely mounted, the clear-weather cross polarization isolation of the system will not change with time. As Watson and his associates have shown, refractive effects leading to off-axis reception will produce clear weather changes in the observed cross polarized signal level, but these could be corrected by properly repointing the receiving antenna (without changing its polarization) and do not represent a true depolarization of the propagating wave.

When we began this experiment we expected the satellite link to behave the same way. The ATS-6 spacecraft maintained a north-south linear polarization on the transmitted signal to within an accuracy of ±0.1°. (In the spacecraft coordinate system, the angular rotation of the transmitted polarization away from the north-south axis corresponds to the satellite yaw, and this was controlled very tightly.) The apparent polarization of the spacecraft signal at our location depends upon the satellite attitude, the ground and spacecraft antenna pointings, and the spacecraft location (i.e. the latitude and longitude of the subsatellite point); as long as these remain fixed the clear weather polarization of the satellite signal should not vary. Hence, we should have been able to point our antenna at the satellite, rotate our polarization to minimize the received CPR (thus, aligning the transmitting and receiving antennas), and find the same clear weather CPR whenever the satellite had the same pointing and the ground antenna was properly pointed toward the satellite. Put another way, the ground antenna polarization angle giving minimum CPR in clear weather should have been the same for the same pointing of the satellite so long as the satellite remained on station. For compact notation, we will call this angle, ω_o.

Our initial observations in July and October 1974 indicated an angle of -19.5°; since the accuracy of this measurement depends upon how well our antenna pedestal is aligned with vertical, this value agrees reasonable well with the theoretical prediction of -17.6° for the nominal satellite location. In fact, it is closer to the theoretical value than measurements reported by the other millimeter wave receiving sites (who used single-polarized antenna systems).

Not expecting ω_o to change, we did not recheck it on a regular basis until February, 1975. The reason for starting then was that in December, 1974,

and January, 1975, we had a series of receiver malfunctions. In looking for the cause of one case of reduced receiver sensitivity, we disassembled and cleaned the antenna feed. The feed is positioned by a set of alignment pins designed to prevent changes in the feed position during disassembly or reassembly, but after putting the feed back together, we rechecked ω_o and found that it had changed to about -21.5°. While it can never be established that our working on the feed did not change the apparent value of ω_o, we were startled by the change and began a program of checking ω_o every time the spacecraft was pointed at VPI&SU. To our surprise, we noted a day-to-day variation in ω_o.

3.2.2 Data

The raw data are difficult to present graphically since each point is based on a plot of CPR versus the antenna polarization angle ω_o. A sample measurement appears in Figure 3.1. One determines ω_o by estimating the position of the null. To minimize the error in doing this, the null was found by finding the center point between the two halves of the "V" at three or four locations and averaging these. Table 3.1 presents the results of this measurement procedure for the times that the spacecraft was available in clear weather and pointed at VPI&SU.

3.2.3 A Discussion of Possible Mechanisms

3.2.3.1 Introduction

Possible mechanisms for the observed ω_o variations include:

a. Improper measurement techniques

b. Off-axis reception

c. Mechanical drift in the ground antenna positioning system

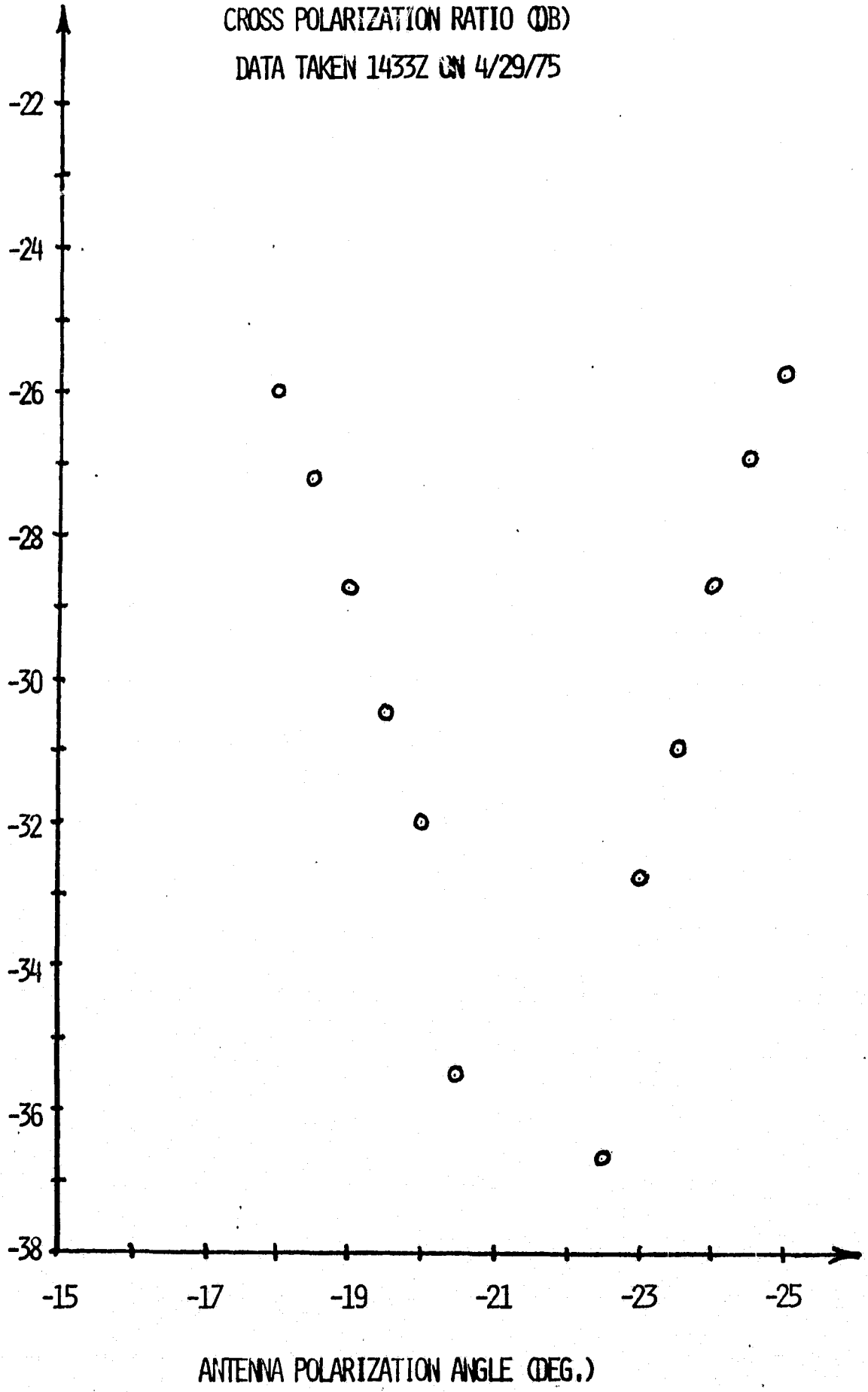

Figure 3.1. Variation of CPR with antenna polarization angle.

Table 3.1. Polarization Angle Measurement With VPI&SU Pointing

Date(UT) 1975	Time(UT)	Subsatellite Point W. Long.	Subsatellite Point N. Lat.	Polarization Angle Measured	Polarization Angle Predicted	Polarization Angle Difference
6 Feb.	2110	93.93°	1.15°	-21.4°	-17.55°	-3.85°
7 Feb.	1900	93.96	1.06	-21.1°	-17.55°	-3.55
20 Feb.	2200	94.05	0.92	-20.5°	-17.61°	-2.89
28 Feb.	2230	94.02	0.69	-21.6°	-17.50°	-4.10
4 March	1917	94.02	1.10	-21.6°	-17.64°	-3.96
10 March	1800	93.99	1.09	-21.7°	-17.60°	-4.10
20 March	2005	93.93	0.88	-18.9°	-17.46°	-1.44
25 March	1909	93.98	0.98	-21.7°	-17.55°	-4.15
21 April	1800	94.06	0.84	-22.1°	-17.59°	-4.51
22 April	1313	94.12	0.89	-21.0°	-17.68°	-3.32
25 April	1400	94.09	0.97	-21.0°	-17.68°	-3.32
28 April	1056	94.09	0.34	-20.8°	-17.46°	-3.34
28 April	1215	94.08	0.72	-21.1°	-17.58°	-3.52
29 April	1433	94.05	1.01	-21.6°	-17.65°	-3.95
30 April	1420	94.04	1.01	-21.5°	-17.64°	-3.86

d. Satellite yaw variations

e. Day-to-day variations in the satellite antenna pointing

f. An overlooked propagation effect

These will be discussed in the sections which follow.

3.2.3.2 Validity of the Measurement Technique

3.2.3.2.1 Introduction

The clear weather polarization angle measurement technique employed in this experiment was based on two generally accepted premises about front-fed parabolic reflector antennas. These are (a) along the antenna boresight axis the cross-polarized pattern has a sharp null and the co-polarized pattern has a broad peak, and (b) along the boresight axis the measured CPR is a minimum when the antenna polarization (defined as the polarization of the co-polarized feed) is aligned with an incoming linearly polarized signal. Hence, when we find the co-polar peak and adjust the antenna position for minimum CPR, we were aligning the antenna with the incident signal.

3.2.3.2.2 Antenna Pattern Assymetry

The inability of our receiving system to measure the CPR at the bottom of the null introduced a further complication. We estimated the null position by finding the midpoint of the V-shaped CPR versus polarization angle plot. This assumes that the null is symmetric about its deepest point.

Suppose that the null is <u>not</u> symmetric. This would certainly affect the numerical value of the apparent polarization angle because the true null would not fall halfway between the two sides of the curve. Now the CPR response curve does seem to be slightly assymetric. Generally, the side west of the clear weather incident polarization (antenna polarization angle of -21.5° to -25° under normal conditions) is more linear and fits a $20 \log_{10} (\tan |\omega - \omega_o|)$

ORIGINAL PAGE IS
OF POOR QUALITY

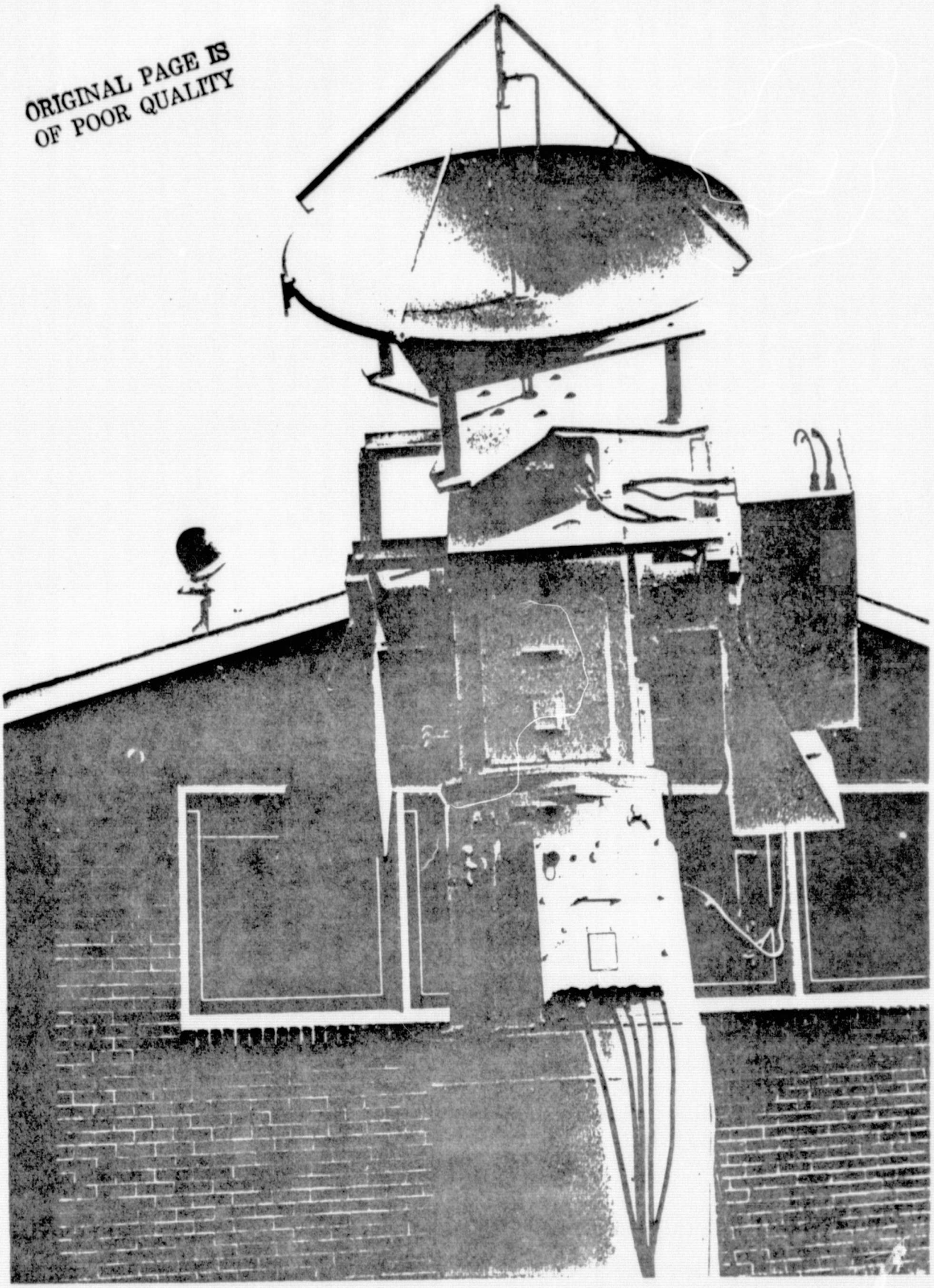

Figure 3.2. The VPI&SU antenna.

curve (where ω is the antenna polarization angle) better than the east side (-15° to -21.5°). This is consistent with the structure of the antenna (see Figure 3.2) since the waveguide from the co-polarized feed port (the side arm) is unsymmetrically mounted to the east of the boresight axis of the dish. The unsymmetric response thus may be due to scattering by this waveguide.

Granted that this lack of symmetry may cause a slight error in determining the exact value of ω_o, could it be responsible for the observed fluctuations in the polarization angle? We feel that it could not. The assymmetry is slight and it has shown no tendency to change with time. It could be and almost certainly is different for different angular distances from boresight (see the discussion on off-axis reception which follows), but before each measurement we carefully peaked the co-polarized signal level through fine adjustment of the antenna azimuth and elevation. It would have been better to null the cross polarized signal level instead, but this was beyond the capability of our receiver. Hence, the assymmetry each time should have been the same and should not have caused the observed pointing angle variations.

3.2.3.3 Off-axis reception

3.2.3.3.1 Introduction

Off-axis reception as a cause of depolarization in ground paths has been investigated extensively by Ghobrial and Watson (1973). It occurs on long ground paths when changes in the atmospheric refractive index change the direction of arrival of the received signal and bring it out of the null in the receiving antenna's cross-polarized response. Satellite paths offer the potential for off-axis reception through refraction as well as through improper pointing of the earth station antenna.

Off-axis reception offers two potential problems. One is purely geometrical.

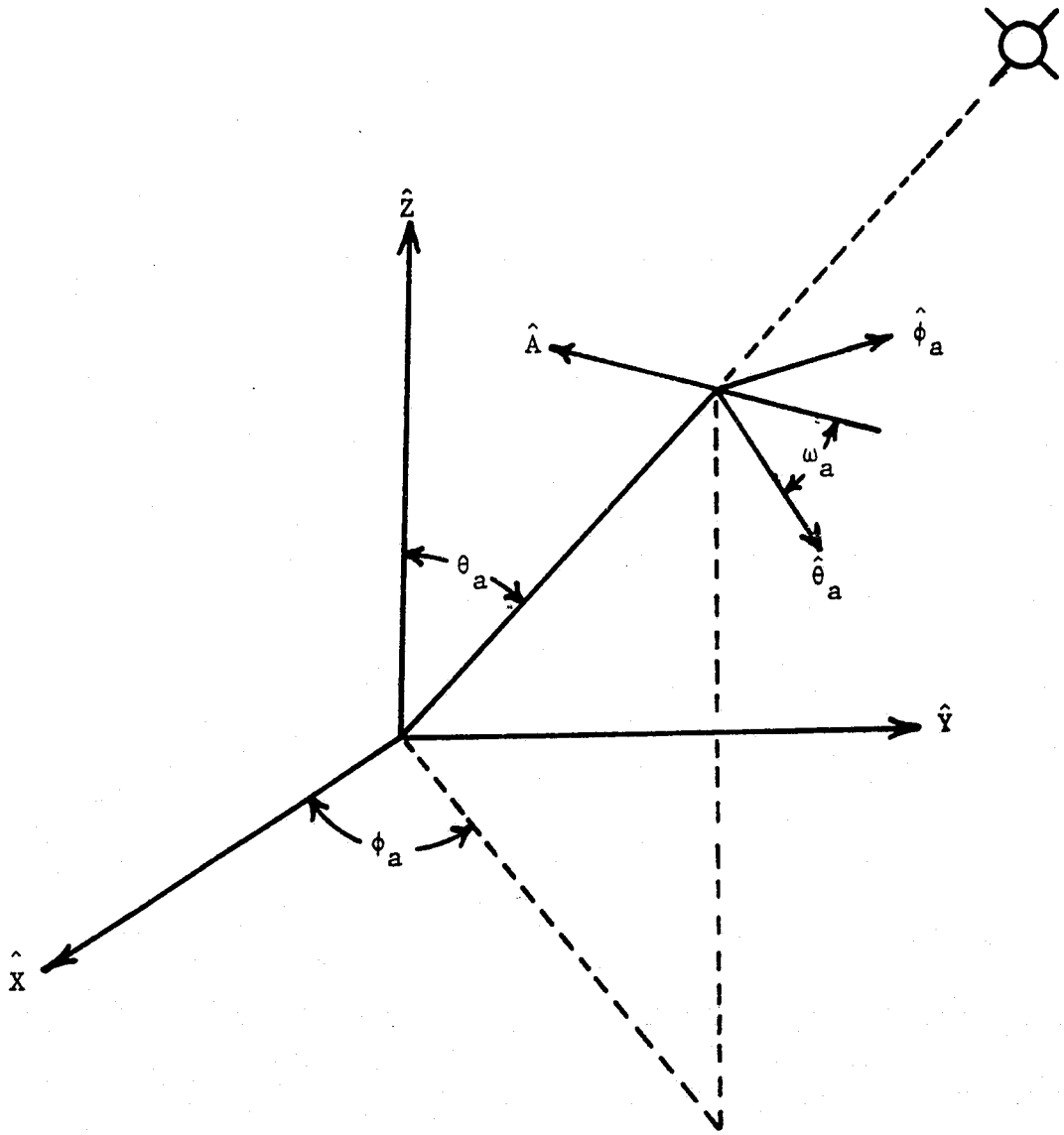

Figure 3.3. Coordinate system used to orient the ground antenna.

With our Scientific Atlanta polarization/elevation/azimuth antenna pedestal arrangement, the polarization angle of our antenna measured from the projection of local vertical onto the antenna varies with the antenna azimuth and elevation. Put another way, assuming that our antenna is perfectly linearly polarized in all directions and planes, the polarization that we measure for the satellite signal in clear weather will be incorrect if our azimuth and elevation settings are incorrect. The important question is how great is the polarization angle error likely to be?

A geometric analysis may be conducted by examing the angle between the received signal and the antenna feed as a function of the antenna and satellite coordinates. The coordinate system used to define the antenna pointing is shown in Figure 3.3. Here ϕ_a is azimuth, $(\pi/2 - \theta_a)$ is the elevation, and ω_a is the polarization angle.

$\hat{A}$ is a unit vector in the direction of the antenna polarization. Seen from the satellite the vectors look like this:

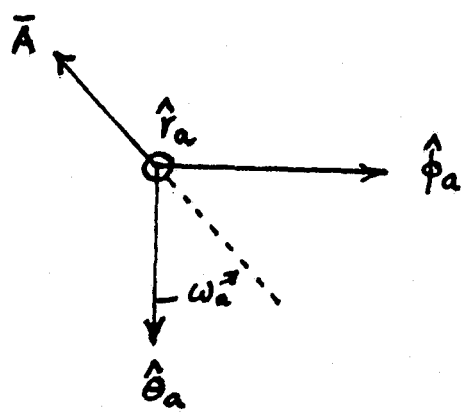

Geometrically $\hat{A} = -\omega_a \hat{\phi}_a \sin - \omega_a \hat{\theta}_a \cos.$ (1)

Let an incident plane wave from a satellite be traveling toward the

antenna and be polarized in the $\hat{S}$ direction. $\hat{P}$ is the unit vector in the direction of propagation.

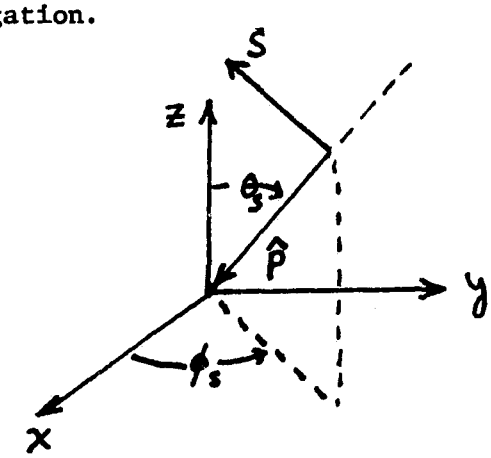

P is oriented by the direction angles ϕ_s and θ_s. These are the azimuth and co-elevation of the satellite. (Co-elevation = $\frac{\pi}{2}$ - elevation).

Since the incident wave is plane and linearly polarized, $\hat{S}$ is fixed in space

$$\hat{S} = S_x \hat{x} + S_y \hat{y} + S_z \hat{z} \tag{2}$$

where S_x, X_y, S_z are constant.

Along the line drawn from the satellite to the origin the situation (viewed from the satellite) is like this:

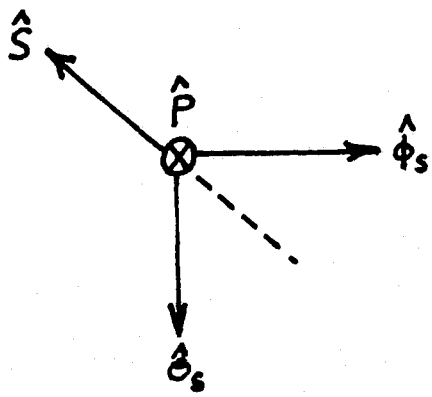

Here $\hat{\phi}_s$ and $\hat{\theta}_s$ are the unit vectors of the spherical coordinate system evaluated at θ_s, ϕ_s.

The angle measured between $\hat{S}$ and the unit vector $\hat{\theta}_s$ is ω_s.

Geometrically

$$\hat{S} = -\omega_s \hat{\theta}_s \sin - \omega_s \hat{\theta}_s \cos . \tag{3}$$

Hence,

$$S_x = \hat{S} \cdot \hat{x} = -\sin \omega_s \hat{\phi}_s \cdot \hat{x} - \cos \omega_s \hat{\theta}_s \cdot \hat{x}$$

$$= + \sin \omega_s \sin \phi_s - \cos \omega_s \cos \theta_s \cos \phi_s \tag{4}$$

$$S_y = \hat{S} \cdot \hat{y} = -\sin \omega_s \cos \phi_s - \cos \omega_s \cos \theta_s \sin \phi_s \tag{5}$$

$$S_z = \hat{S} \cdot \hat{z} = \cos \omega_s \sin \theta_s \tag{6}$$

Hence $\hat{S} = [\sin \omega_s \sin \phi_s - \cos \omega_s \cos \theta_s \cos \phi_s]\ \hat{x}$

$$+ [-\sin \omega_s \cos \phi_s - \cos \omega_s \cos \theta_s \sin \phi_s]\ \hat{y}$$

$$+ \cos \omega_s \sin \theta_s\ \hat{z} \tag{7}$$

In determining the CPR we are concerned with the angle Ω between $\hat{A}$ and $\hat{S}$ where

$$\cos \Omega = \hat{A} \cdot \hat{S} \tag{8}$$

This requires that we find A_x, A_y, A_z

$$A_x = \hat{A} \cdot \hat{x} = \sin \omega_a \sin \phi_a - \cos \omega_a \cos \theta_a \cos \phi_a \tag{9}$$

$$A_y = \hat{A} \cdot \hat{y} = -\sin \omega_a \cos \phi_a - \cos \omega_a \cos \theta_a \sin \phi_a \tag{10}$$

$$A_z = \hat{A} \cdot \hat{z} = \cos \omega_a \sin \theta_a . \tag{11}$$

Then

$$\cos \Omega = A_x S_x + A_y S_y + A_z S_z \tag{12}$$

and

$$\cos \Omega = [\sin \omega_s \sin \phi_s - \cos \omega_s \cos \theta_s \cos \phi_s] .$$

$$[\sin \omega_a \sin \phi_a - \cos \omega_a \cos \theta_a \cos \phi_a]$$

$$+ [\sin \omega_s \cos \phi_s + \cos \omega_s \cos \theta_s \sin \phi_s] .$$

$$[\sin \omega_a \cos \phi_a + \cos \omega_a \cos \theta_a \sin \phi_a]$$

$$+ \cos \omega_s \sin \theta_s \cos \omega_a \sin \theta_a \tag{13}$$

Physically Ω is the angle between the antenna polarization direction and the electric field vector of the satellite signal. In measuring the apparent clear-weather polarization angle ω_o one points the antenna so that $\theta_s = \theta_a$ and $\phi_s = \phi_a$. Then

$$\begin{aligned}
\cos\Omega = {} & [\sin\omega_s \sin\phi_a - \cos\omega_s \cos\theta_a \cos\phi_a]. \\
& [\sin\omega_a \sin\phi_a - \cos\omega_a \cos\theta_a \cos\phi_a] \\
& + [\sin\omega_s \cos\phi_a + \cos\omega_s \cos\theta_a \cos\phi_a]. \\
& [\sin\omega_a \cos\phi_a + \cos\omega_a \cos\theta_a \sin\phi_a] \\
& + \cos\omega_s \sin\theta_a \cos\omega_a \sin\theta_a \\
\cos\Omega = {} & \sin^2\phi_a (\sin\omega_s \sin\omega_a) \\
& + \cos^2\phi_a (\sin\omega_s \sin\omega_a) \\
& + (\cos^2\theta_a \cos^2\phi_a + \cos^2\theta_a \sin^2\phi_a + \sin^2\theta_a) \cos\omega_a \cos\omega_s \\
\cos\Omega = {} & \sin\omega_s \sin\omega_a + \cos\omega_a \cos\omega_s \\
\cos\Omega = {} & \cos(\omega_a - \omega_s) \qquad (14)
\end{aligned}$$

As expected, with proper antenna pointing Ω reduces to the difference of the two polarization angles.

To see what geometrical error is introduced by antenna misalignment, a computer program was written to evaluate (13) for various combinations of antenna and satellite coordinates. For misalignments of 0.2° in either or azimuth elevation these showed a shift of the polarization angle of 0.16° to 0.19° for nominal satellite coordinates near 45° elevation and 200° azimuth. For total misalignments of 0.3° [(total misalignment)^2 = (elevation misalignment)^2 + (azimuth misalignment)^2] the computed error in the measured polarization angle was less than 0.3°.

Whether or not a more exact analysis that included the effects of the antenna feed and reflector would show larger changes in the measured clear

weather polarization angle due to off-axis reception is unknown. Watson's detailed treatment of the off-axis problem yields the cross polarization isolation that would be measured for a given arrival angle off boresight. This is the problem of interest to a user with a fixed or preprogrammed antenna pointing, but it does not address the question of what value of polarization angle the receiving antenna would measure for the off-axis signal.

The problem can also be approached experimentally; a preferred way to do it would be to set up an antenna range with a transmitting antenna having precisely defined polarization characteristics and then measure the apparent received polarization angle as a function of angular distance from boresight. Unfortunately, this was impossible under the budget and equipment limitations of this experiment.

As a substitute on two occasions, we carefully adjusted our antenna pointing for maximum co-polarized response and then measured the apparent incoming polarization angle for various elevation and azimuth offsets. The first trial was conducted on March 4, 1975. Table 3.2 summarizes the results. These data indicate that an antenna misalignment of 0.2° could cause a polarization angle measurement error of as much as 0.5°.

In considering the matter further and remembering Watson's conclusion that the polarization characteristics of a front-fed parabola are worst ±45° from the principal planes of the pattern, we decide to repeat these measurements, this time introducing simultaneous azimuth and elevation offsets. This was done May 29, 1975, and the results are summarized in Table 3.3.

The values in Table 3.3 indicate that simultaneous +0.2° errors in azimuth and elevation can change the measured polarization angle by as much as 1.22°. However, this pointing error reduced the co-polarized signal level

Table 3.2. Polarization Angle Measurements on March 4, 1975

Time (UT)	Antenna Pointing	Apparent Polarization Angle	(Average Boresight)-(This Measurement)
1915	Boresight	-21.55°	-0.10°
	Boresight Azimuth $+0.2^{\circ}$ Elevation Offset	-22.15°	$+0.5^{\circ}$
	Boresight Elevation $+0.2^{\circ}$ Azimuth Offset	-22.10°	$+0.45^{\circ}$
1925 (est)	Boresight	-21.75°	$+0.10^{\circ}$

Table 3.3. Polarization Angle Measurements on May 29, 1975

Time (UT)*	Antenna Pointing	Apparent Polarization Angle	(Average Boresight)-(This Measurement)
1338	Boresight	+19.44°	+0.11°
1342	Boresight Elevation +0.3° Azimuth Offset	+19.69°	-0.14°
1348	Boresight Elevation -0.3° Azimuth Offset	+19.68°	-0.13°
1353	Boresight Azimuth +0.3° Elevation Offset	+18.65°	+0.90°
1400	Boresight Azimuth -0.3° Elevation Offset	+19.83°	-0.28°
1406	+0.21 Elevation Offset +0.21 Azimuth Offset	+18.51°	+1.04°
1412	-0.21 Elevation Offset +0.21 Azimuth Offset	+20.19°	-0.64°
1416	-.21 Elevation Offset -.21 Azimuth Offset	+19.43°	-0.12°
1420	+.21 Elevation Offset -.21 Azimuth Offset	+18.83°	+1.22°
1425	Boresight	+19.66°	-0.11°

* These are the nominal times to the nearest minute that the antenna rotated through the CPR null.

by better than 1 dB below boresight. This change in signal level would reduce the signal level meter reading by a noticeable amount. It is hoped that such a misalignment would not have gone unnoticed during a polarization angle measurement.

3.2.3.4 Mechanical Drift in the Ground Antenna Positioning System

If the ground beneath our antenna system was settling or if the zero reference of the polarization positioner varied, the apparent clear-weather polarization angle would change with time. To rule out these potential sources of error, we attached a level to our antenna and checked the physical position of the antenna at 180° azimuth, 0° elevation, and 0° polarization every day for a week. No changes were noted.

3.2.3.5 Satellite Yaw Variations

The geometry of the ATS-6 satellite is such that any changes in the spacecraft yaw would be accompanied by proportional changes in the polarization angle of the received signal. Hence, many people have strongly suspected yaw variations to be the cause of the clear weather changes we have reported. But so far as we can determine the spacecraft yaw has held its nominal value to within ±0.1° or better during all polarization angle measurement periods for the duration of this experiment. This has been checked both with the real-time displays at ATSOCC and by examination of the spacecraft telemetry data. Yaw variations would seem to be eliminated as a cause.

3.2.3.6 Variations in the Satellite Antenna Pointing

The clear weather received polarization at a ground station depends on

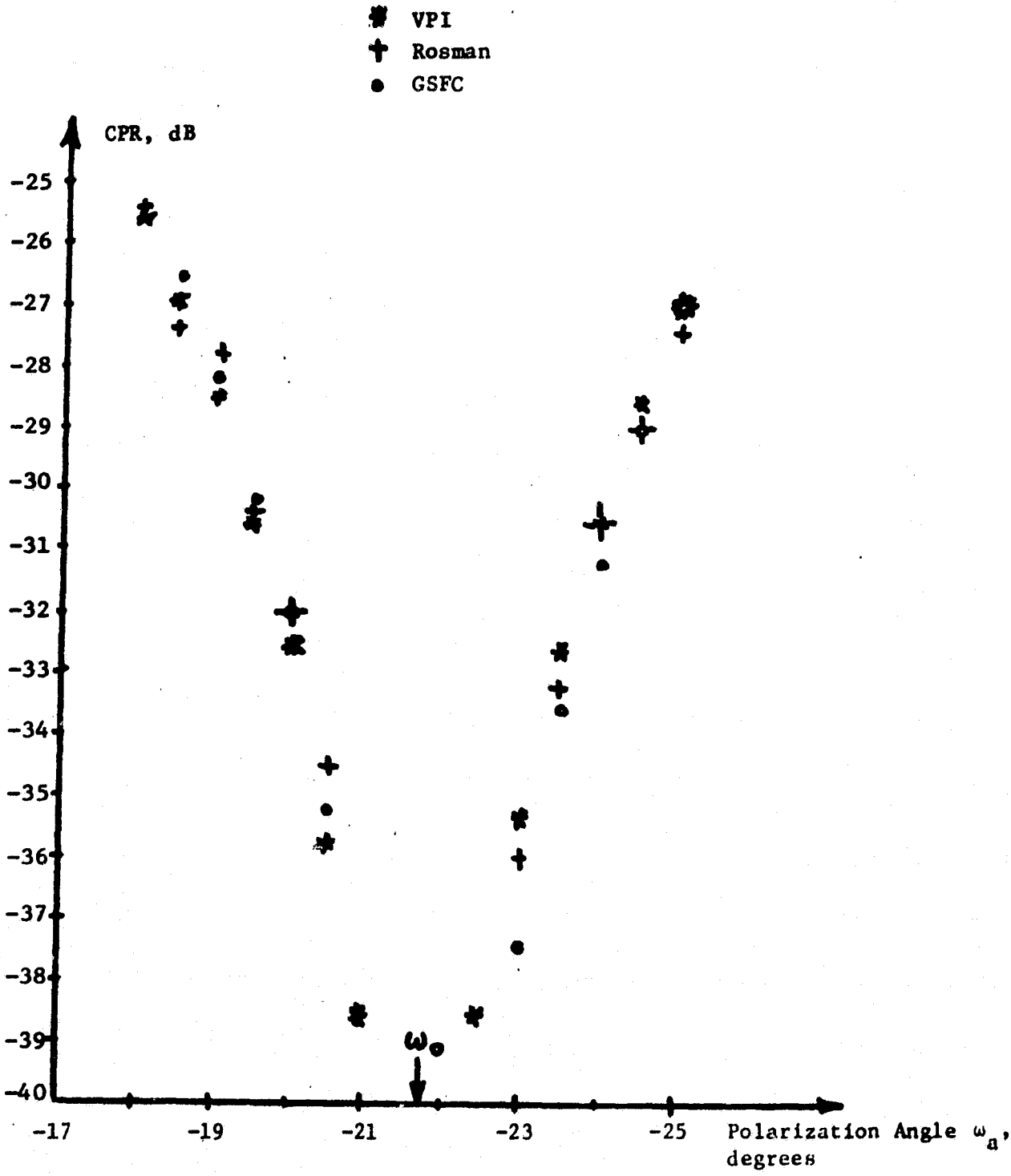

Figure 3.4. Plot of CPR versus ground antenna polarization angle for three spacecraft antenna pointings. These data were taken 1920-2005Z on 4 March, 1975.

the pointing of the satellite antenna. For this reason, we have excluded from this discussion all data taken when the spacecraft was not pointed at VPI&SU.

Was nominal VPI&SU pointing sufficiently repeatable that it would not have changed the received polarization? The answer would seem to be yes. On March 4, 1975, we made successive measurements with the spacecraft pointed at Rosman, at VPI&SU, and at GSFC. Figure 3.4 presents the data; note that the CPR null location did not change, indicating that small changes in the spacecraft antenna pointing were immaterial. (At the spacecraft the angle between VPI&SU and Rosman is 0.36 degrees.)

3.2.3.7 An Overlooked Propagation Effect

3.2.3.7.1 Experimental Data

In an effort to find an atmospheric explanation for the clear-weather polarization variations, ATSOCC arranged 20 hours of on-axis VPI&SU transmission for 2100Z on June 6, 1975 to 1700Z on June 7, 1975. Due to an equipment failure we were only able to take data until 0530Z on June 7. These appear in Table 3.4. The surprising thing about them is the sharp change in polarization angle observed at 0030Z on June 7. It occurred at local sunset and was not accompanied by any significant changes in signal level or antenna pointing. This indicates that a propagation effect might be at work.* We know of only two hypotheses: Faraday rotation and scattering by atmospheric stratifications.

3.2.3.7.2 Faraday Rotation

Faraday rotation is a well known depolarization mechanism at 4 and 6 GHz, but its inverse-square frequency dependence would seem to make it unimportant at 20 GHz. This was confirmed by a careful check of the literature (Vilar, 1974)

*Solar heating of the antenna is another hypothesis However, the satellite was setting in the east while the sun was setting in the west and the reflecting surface and feed were not in the sunlight during this series of measurements.

Table 3.4. Measured data for 6-7 June, 1975.

Time(UT)	Slap Elevation	Slap Azimuth	Actual Elevation	Actual Azimuth	Co-polarized Signal Level Measured	Polarization Angle
2100	21.85	117.51	22.45	117.10	-97.0 dBm	42.00
2130	21.81	117.42	22.41	117.02	-97.0 dBm	42.00
2200	21.78	117.32	22.38	116.92	-97.0 dBm	42.00
2230	21.76	117.20	22.36	116.80	-97.0 dBm	42.00
2300	21.76	117.07	22.36	116.67	-97.0 dBm	42.00
2330	21.76	116.94	22.36	116.54	-97.0 dBm	42.00
0000	21.77	116.79	22.36	116.29	-97.0 dBm	41.75
0030	21.79	116.64	22.19	116.29	-97.0 dBm	43.00
0100	21.81	116.48	22.21	116.18	-97.0 dBm	43.00
0130	21.84	116.31	22.24	115.91	-97.0 dBm	42.75
0200	21.87	116.15	22.40	115.71	-95.0 dBm	42.80
0230	21.91	115.98	22.40	115.61	-95.0 dBm	42.90
0300	21.94	115.81	22.40	115.35	-94.7 dBm	42.90
0330	21.97	115.64	22.40	115.20	-94.7 dBm	43.10
0400	21.99	115.48	22.50	115.10	-94.7 dBm	43.60
0430	22.01	115.32	22.50	115.00	-97.3 dBm	43.50
0500	22.02	115.17	22.50	114.70	-97.5 dBm	43.40
0530	22.02	115.03	22.50	114.60	-97.8 dBm	43.50

(Murakami and Wickizer, 1969) and a discussion with Dr. Rogert Taur of Comsat Laboratories, both of which indicated that the greatest Faraday rotation we could expect to see is on the order of 0.3°. This would seem to eliminate Faraday rotation from further consideration.

3.2.3.7.3 Scattering by Stratified Layers

Depolarization in scattering by a dielectric sheet has been investigated by Beckmann (1968). If the atmosphere can be modeled as a system of stacked horizontal layers with different refractive indices, then perhaps this type of scattering is responsible for the clear-weather polarization angle variations. Since the horizontal stratification might disappear as the atmosphere cooled, this hypothesis is attractive as a potential explanation for the sharp change we observed at sunset. Unfortunately, the numbers do not support it.

As a worst case, we will treat the atmosphere as a horizontal dielectric sheet with a refractive index n = 1.00045, a handbook value for the maximum refractive index at the ground (GTE Lenkurt Inc., 1972). Using the method and notation of Kraus and Carver (1973) for a worst-case analysis we will assume a left-handed elliptically polarized wave incident at a 40° angle (Kraus and Carver's θ_i) with a tilt angle of 15° and an axial ratio of 0.01. Inside the dielectric the wave propagates with a tile angle of 14.9999989°, representing a polarization rotation of 1.02×10^{-6} degrees which is negligible. Hence, there seems to be no plausible combination of stratified layers that could produce significant depolarization and no obvious propagation explanation for clear weather in the received polarization.

3.2.4 Conclusions

In the preceding paragraphs we have made cases for and against a number of explanations for clear-weather polarization angle variations. Since the largest changes in the apparent polarization angle result from elevation errors in pointing our receiving antenna, the evidence seems to favor this explanation even though we have attempted to get a boresight pointing of the ground antenna before each measurement. If true, this would place rather tight tracking requirements on a dual orthogonally polarized satellite communications system if crosstalk is to be minimized.

At the time we noticed the clear weather polarization angle variations on the ATS-6 downlink, the Bell Telephone Laboratories ATS-6 receiving station was out of operation and no other U.S. site was capable of making precise polarization angle measurements. Hence, there has been no independent confirmation or denial of our observations. We discussed the situation at great length with the British groups who took over the ATS-6 millimeter wave experiment, in May, 1975, and they intend to make polarization angle measurements at several locations. Hopefully, from their observations we will be able to identify the cause of the apparent polarization angle variations.

3.3 Depolarization by Snow

3.3.1 Introduction

Depolarization by snow is a somewhat controversial topic. When the subject was brought up at recent meetings of millimeter wave propagation researchers, opinions ranged from "snow never depolarizes" to snow "sometimes depolarizes." Our experience supports the "sometimes" faction, as we have observed five (5) snow storms and have seen significant depolarization and attenuation in only one of them. These are summarized in Table 3.5.

Table 3.5. Summary of Snow Depolarization Investigation

Storm No.	Date(Z)	Time of Observation(Z)	Offical Accumulation*	Official Median Temperature For Nearest EST Day, °F	Depolarization and Attenuation
1	30 Nov. 74	2134 - 2400		37	Yes
	1 Dec. 74	0000 - 0100		35	
		2227 - 2400			
	2 Dec. 74	0000 - 0024		35	
		1900 - 1950	10"		
2	4 Feb. 75	1302 - 1534	5"	27.5	No
3	1 Mar. 75	1906 - 1930, 2252 - 2333	None	40	No
4	2 Mar. 75	1650 - 1740	2"	28.5	No
5	10 Mar. 75	1745 - 2003	4"	33.5	No

* For the entire storm.

3.3.2 Data and Analysis

The only snow storm for which we saw depolarization began at approximately 2015Z on November 30, 1974, and continued until approximately 2000Z on December 2, 1974. Snow and occasional freezing rain fell during most of this time interval, but from time-to-time there was considerable variation in the ground precipitation rate. The net accumulation was measured as 10 inches by our local U.S. Weather Service observer. The snow drifted extensively and this behavior led us to conclude that it was dry. This is contradicted by the temperature observations of our local weather station which indicated an unusually high air temperature for a snow storm.

Spacecraft operational restrictions and an initial problem with our receiver prevented us from obtaining a continuous look at the signal from beginning to end of the storm. Instead we made a series of separate observations, each several hours in length. After the storm was over, we made clear sky calibration runs on December 3 and 6 to aid in data analysis.

In clear weather conditions at the time of measurement the incoming signal was polarized at an angle of -19.5°, but with this antenna polarization the cross-polarized signal component was below the receiver phaselock threshold. Since then we improved the receiver sensitivity to the point that it would maintain lock on the cross-polarized component for any antenna orientation. But at that time we normally operated the antenna at angle of -16.5°; this provided a clear weather isolation of -28 dB and enabled the receiver to work properly. However, on December 2, the snow depolarization was such that we were able to make measurements at -19.5°.

While the 3° antenna misalignment was necessary for us to collect data and seems to be a valid approach to modeling a real dual polarized communications system with a residual isolation in the -25 to -30 dB range, it is less than

optimum for a scientific study of rain and snow depolarization. This was brought to our attention by Mr. Erwin Hirschmann of NASA/GSFC with the following analysis.

Suppose that the clear weather polarization angle of the satellite signal is -21.5° and that to maintain phaselock the ground station antenna is set for -22.5°, a one-degree misalignment. Now suppose that precipitation rotates the satellite signal polarization from -21.5° through -22.5° to -23.5°. The received CPR will start at the clear weather value, go toward $-\infty$ as the angle reaches -22.5°, and then return to the clear weather value at -23.5°. The receiver would thus be indicating no depolarization (CPR = clear weather value) while in reality the precipitation would be causing a 2° rotation in the polarization of the satellite signal.

At very high rain rates the potential error introduced by antenna misalignment is less important than at low rain rates. For example, the CPR for an 8° rotation differs from the CPR for a 7° rotation by only 1.2 dB, while the CPR for a 2° rotation differs by 6 dB from the CPR for a 1° rotation. This is another reason why almost all measurements of rain depolarization show better agreement with the theory at high rain rates than at low rain rates. But the misalignment technique is intended for use a low rain rates, and potentially this is where it introduces the greatest error. Hence, we discarded it as soon as improvements to our receiver performance permitted, but most of the snow data were taken this way.

The data for this storm were taken on a chart recorder. In reducing the chart recorded output we attempted to obtain approximately one-minute-average values for the co-polarized and cross-polarized signal levels at ten-minute intervals. In almost all cases this was done immediately after we had updated our antenna pointing so as to minimize or eliminate the possibility of bad data due to improper tracking. The exceptions to this procedure were those

cases when the spacecraft antenna pointing was being changed or when the operator did not log an antenna update. In these cases, data were reduced for the closest time for which we know definitely that all antennas were pointed correctly.

From each average co-polarized signal level, we subtracted -66 dBm (the clear-weather reference) to get the excess attenuation. The cross polarization ratio was calculated as the cross-polarized signal level minus the co-polarized signal level plus 15 dB (at that time this was the fixed attenuator setting in the co-polarized channel at the receiver RF front end).

Figure 3.5 displays average measured values of attenuation and cross polarization ratio versus time for the data runs between November 30 and December 6, 1974. Breaks in the time axis emphasize that this figure is a collection of data from 5 different runs spread over 6 calendar days.

The onset of the storm on November 30, 1974, was preceded by at least 8 hours of heavy cloud cover. Precipitation in the form of light rain mixed with snow began at 2015Z, but an initial thermal problem in our RF front end prevented our acquiring the satellite signal until 2134Z.

At approximately 2400Z on November 30, 1974, the spacecraft antenna was redirected to Rosman from VPI&SU. No significant signal change resulted from this move. We continued taking data until the operator, concerned about his ability to get home in the drifting snow and anticipating a satellite shutdown (due to battery overheating) by 0200Z (December 1, 1974), turned the receiver off at 0100Z.

By local dawn on December 1, 1974, the heavy snow had subsided. When significant snow began again at approximately 2130Z we acquired the signal and monitored it until 0024Z (December 2, 1974). During this time interval the ground snowfall rate was never significant, but surprising attenuation and CPR

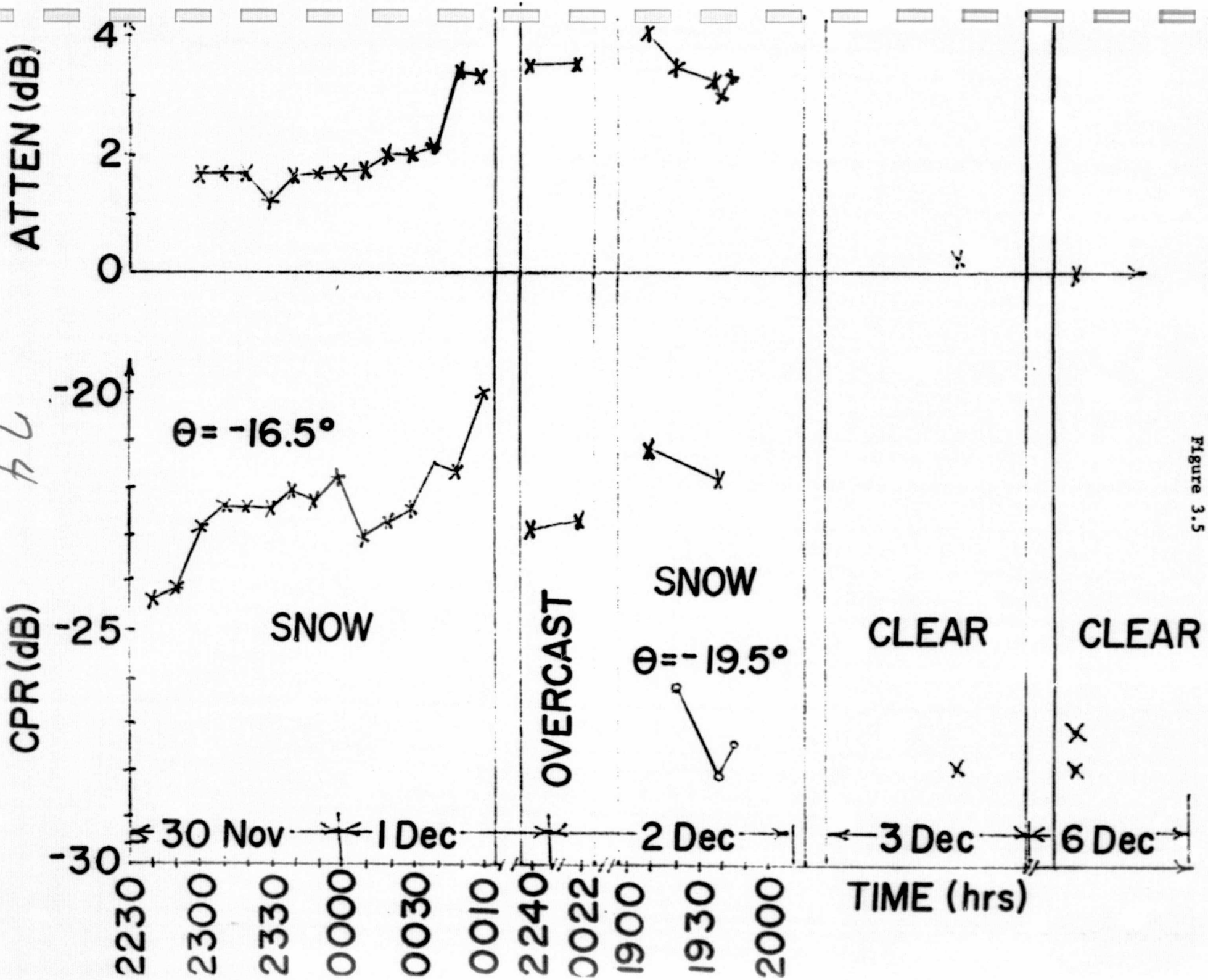
ATTEN (dB)
4
2
0
CPR (dB)
-20
-25
-30
θ= -16.5°
SNOW
OVERCAST
SNOW
θ=- 19.5°
CLEAR
CLEAR
30 Nov
1 Dec
2 Dec
3 Dec
6 Dec
2230
2300
2330
0000
0030
0010
2240
0022
1900
1930
2000
TIME (hrs)

Figure 3.5

levels were recorded. As we were monitoring the 20 GHz CW, satellite was slewed to Rosman for measurement of the spacecraft antenna patterns, thus we were unable to make a meaningful plot of attenuation and CPR versus time. However, the starting and ending values were measured when the spacecraft was known to be pointing at Rosman and these appear in Figure

At 1900Z on December 2, 1974, Mr. Cooper Chapman, the Experiment Engineer on duty at ATSOCC, notified us that the spacecraft would be available for one hour. This period coincided with the onset of a very intense snow shower and more data were acquired. For the first time in the course of the experiment the depolarization was sufficiently severe that we were able to make CPR measurements at -19.5°. (We had not thought to try -19.5° on the previous days.) These appear in Figure 3.5, along with some companion measurements made at -16.5°. As the hour progressed the snow rate began to decrease and we saw corresponding changes in the attenuation and CPR. Unfortuately, we lost use of the satellite at 1950Z, about 20 minutes before the snow ceased, and were unable to see what would have happened to the -19.5° CPR as ground snowfall stopped. During this data period the antenna feed was carefully checked to insure that no snow had collected in it.

On December 3, 1974, the snow clouds were gone and we made clear weather calibration measurements. These agreed with a subsequent set made on December 6; both appear in Figure 3.5.

We are somewhat limited in our ability to assess the data from this storm because no theoretical model exists for snow depolarization and because we have no means for measuring snowfall rate at our location. In addition, with our computer inoperative we were unable to record wind data. Some insight into the nature of snow depolarization may be gained by plotting snow attenuation versus CPR and and examining the result. This is done in Figure 3.6 for all of the data presented in Figure 3.5.

Theoretically, what should the data in Figure 3.6 look like? Without a propagation theory for snow, about all that one can do is to compare snow data with theoretical prediction for rain. These comparisons shown in Figure 3.7, which displays attenuation versus cross polarization isolation for a 19.3 GHz, 1 km, rain-filled path with 45° linear polarization and a variety of residual (clear weather) CPR values. This is not a theoretical model for our 20 GHz snow data for the satellite path; it is introduced to show the trend of these curves and the effect on them of the residual isolation. For details of how the curves are generated the reader should consult (Bostian, 1974) or (Bostian *et al*, 1974).

The effect of varying our antenna polarization angle is to change our residual CPR. At -19.5° it is no greater than -33 dB (our measurement threshold) and by the Bell Laboratories measurements it is more likely on the order of -50 dB. This means that the theoretical curve for -19.5° would intersect the horizontal axis of Figure 3.7 far to the left of the origin, and this is exactly what would happen to a straight line drawn through the three $\theta = -19.5°$ data points in Figure 3.6. Such a line would cross the CPR axis at a CPR of -46.4 dB, which is consistent with the -50 dB figure. At -16.5° the clear weather CPR is -28 dB; the measured data at -16.5° bear some resemblance to the -30 dB theoretical curve of Figure 3.7.

A question to be resolved about all of this is where did the depolarization and attenuation occur? Was it in the obvious snowflakes near the ground, or is it in the clouds, or do both play a part? Certainly our data of 2240Z on December 1 through December 2, 1974, implicate the clouds, because little or no ground precipitation occurred during this time. On the other hand, the attenuation and CPR levels noted during 1900-1950Z on December 2, 1974, were noticeably correlated with the snow intensity at ground level. When both clouds

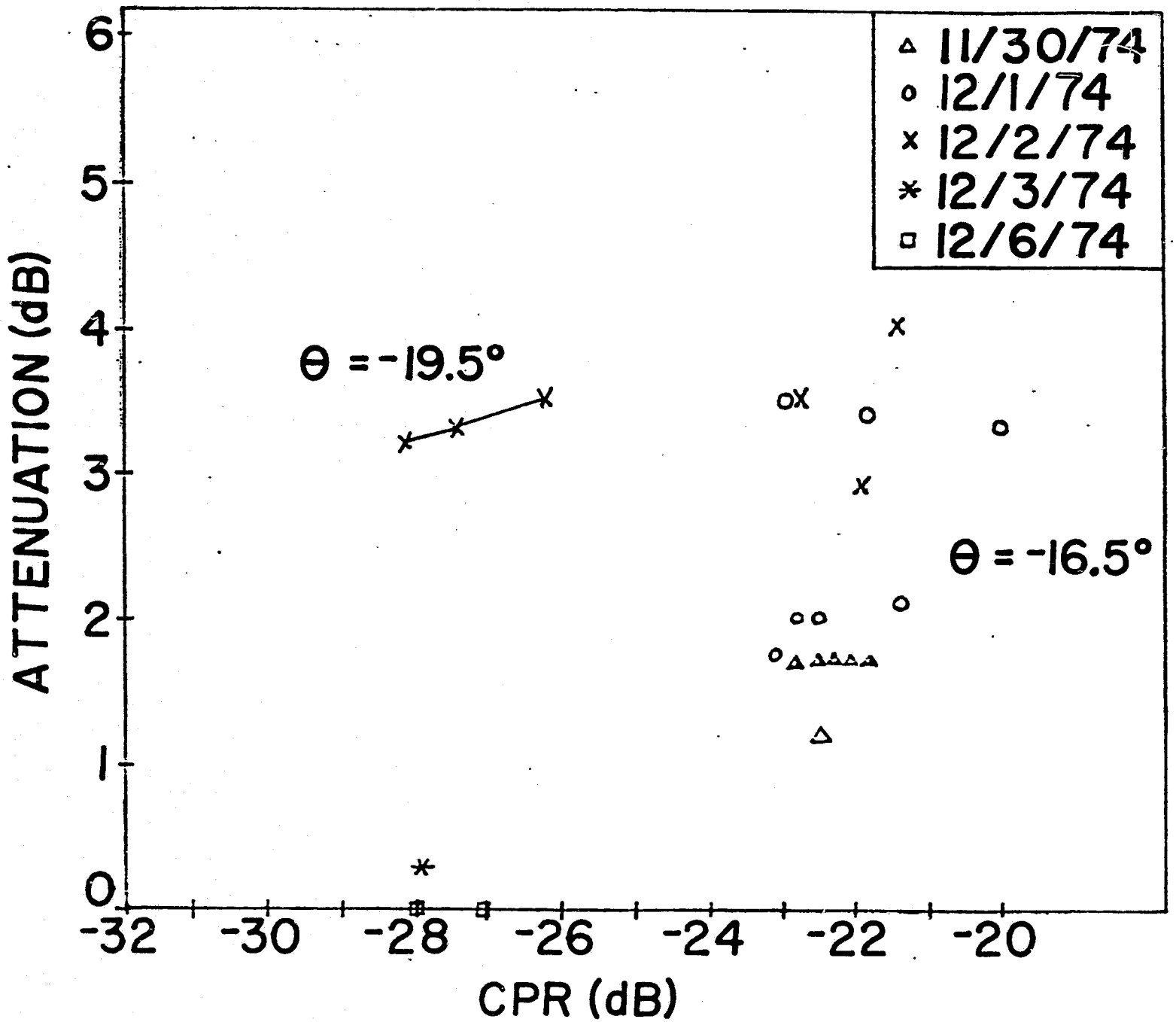

Figure 3.6 Cross polarization ratio versus attenuation for snow storm of November 30 - December 2, 1975 and period following storm.

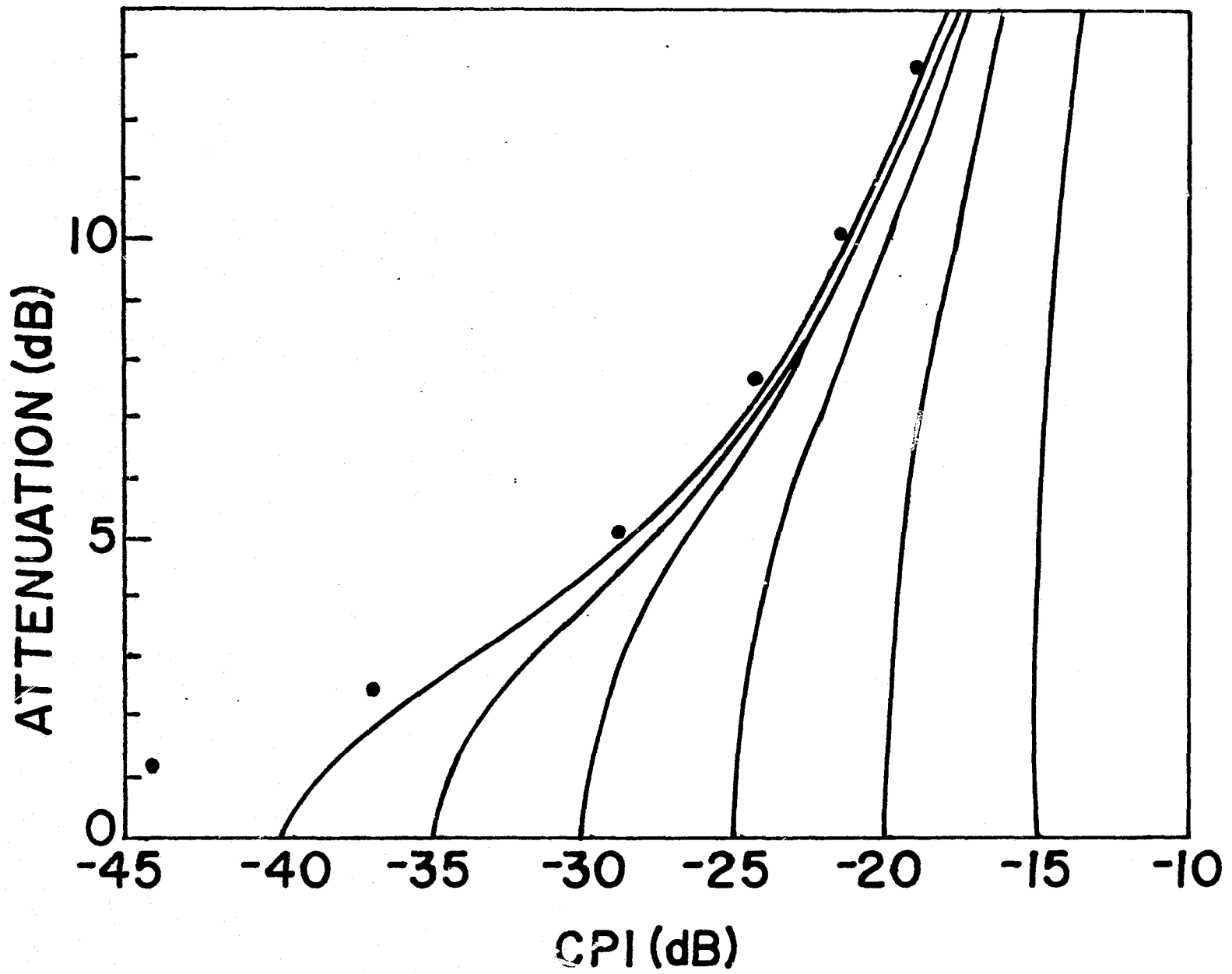

Figure 3.7: Rain induced fade versus cross polarization level (including antenna effects) at 19.3 GHz, a 1 Km path, and 45° linear polarization. The abscissa intercepts are the residual (clear weather) antenna isolations. Points indicate scattering model theory for no antenna effects.

and snow were gone, the clear weather signal returned to their normal values. The obvious conclusion is that ground precipitation and higher altitude phenomena both play a role; the only sure way to separate the two is to compare snow depolarization data measured simultaneously on terrestrial and satellite paths.

We have not seen attenuation and depolarization in any other snowstorm. But then no other snow storm was as warm and as intense.

3.3.3 Conclusions

We feel that our data from the November 30 - December 2, 1974, storm represent a true instance of depolarization by snow. This assertion could be challenged by the arguments that (1) we had snow or ice on the reflector and feed or (2) what we saw resulted from off-axis reception. To counter the first, we note that we carefully watched the antenna to be sure it remained clear, and in addition, the antenna was coated with snow during later storms when we saw no depolarization. Second, the antenna was carefully adjusted for maximum signal before the published data points were recorded.

A striking feature of snow depolarization compared to rain is the large CPR observed for a given attenuation. For example, to get a CPR of -28 dB the leftmost -19.5° point in Figure 3.6 with rain would require for a terrestrial link at least 7 dB attenuation and possibly as much as 20 or 30 dB, depending on path length and raindrop canting angle.

Some theoretical case may be made for associating small attenuation and severe depolarization with scattering by bodies which are relatively lossless but lack rotational symmetry. Certainly snowflakes and high altitude ice crystals fit this description, but the very fragmentary data available for snow do not necessarily support this conclusion. G. C. McCormick (1974) has reported snow depolarization in radar backscatter. Watson (1973) working at 11 GHz with a 13.7 km path reported a huge fade (24 dB) in wet snow accompanied by a CPR of

-22 dB. On the other hand, a rain fade of only 8 dB on the same path was associated with a -20 dB CPR. We had the reverse: less attenuation from snow and more depolarization than would be expected for rain.

From a practical point of view snow depolarization will not be a serious problem for commercial satellite communications systems operating in our area since in an entire winter we saw only one snow storm with significant depolarization. Whether this will be true at higher latitudes remains to be determined.

3.4 Data Collected During Rain

In order to successfully collect data, it is necessary that (1) the satellite be available with correct pointing and be operating nominally, (2) the ground station equipment be operating properly, and (3) a relatively intense rain event occur. During the ATS-6 project, these three requirements were seldom satisfied simultaneously. Thus, a large data base for satellite to ground propagation at 20 GHz does not yet exist. The amount of attenuation and depolarization data actually collected during rain events is summarized in Table 1.1. There are essentially only three storms which have data worthy of reporting; those of March 30, May 27, and June 12, 1975. In this section, we shall discuss the data obtained from the first two of these storms, and the June 12 storm will be discussed in the next section because it occurred during low elevation angle pointing.

Almost all of the rain data was collected during the last few months of the project. Typically, data reduction procedures are developed by processing a few storms by hand and then writing computer programs to replace the hand computations. With the short time frame for data reduction, the computer programs were not developed until very late in the project. Thus, for the sake of expediency all data presented in this section were obtained from chart recordings

and processed by hand. Another reason for this is that our PB440 on-line computer became very unreliable toward the end of the project and the digital data obtained from it are to be suspected.

On March 30, 1975, the first significant rain depolarization data was collected. In Figure 3.8 the rain rate, CPR, and the attenuation are plotted for the storm. The CPR and attenuation data points represent samples taken at one-minute intervals and the blank spaces are times when the receiver lost phaselock. The rain gauge data in Figure 3.0 are from three tipping bucket gauges. Gauge 1 (solid line) is directly beside the receiving antenna. Gauge 2 (dashed line) is 650 feet away and approximately 2500 feet away in the general direction of the satellite and about 2500 feet below the path. Since our 15 GHz radar indicated the rain was about 9 miles deep (in the direction of the satellite) and 3 miles high, we suspect that gauge 3 may have malfunctioned and reported only during the most intense rain.

A striking feature of these data is the strong correlation between the rain rate peaks and the CPR peaks. The CPR peaks occurred slightly earlier than the rain rate peaks because of the time required for the raindrops to fall from the path to the gauges.

Unlike what we have observed on terrestrial radio systems, the attenuation and CPR are not well correlated with each other. The plot of attenuation versus CPR from terrestrial path data follows a well-defined curve. Peaks of attenuation and peaks of CPR occur simultaneously (Bostian et al., 1972). Figure 3.9 shows average attenuation for each integer value of observed CPR. The attenuation does not continually increase with CPR. No explanation is offered for the lack of correlation between attenuation and CPR from satellite path data. More experimental observations are needed.

The storm of March 30, 1975 was the only hard rain for which we were able

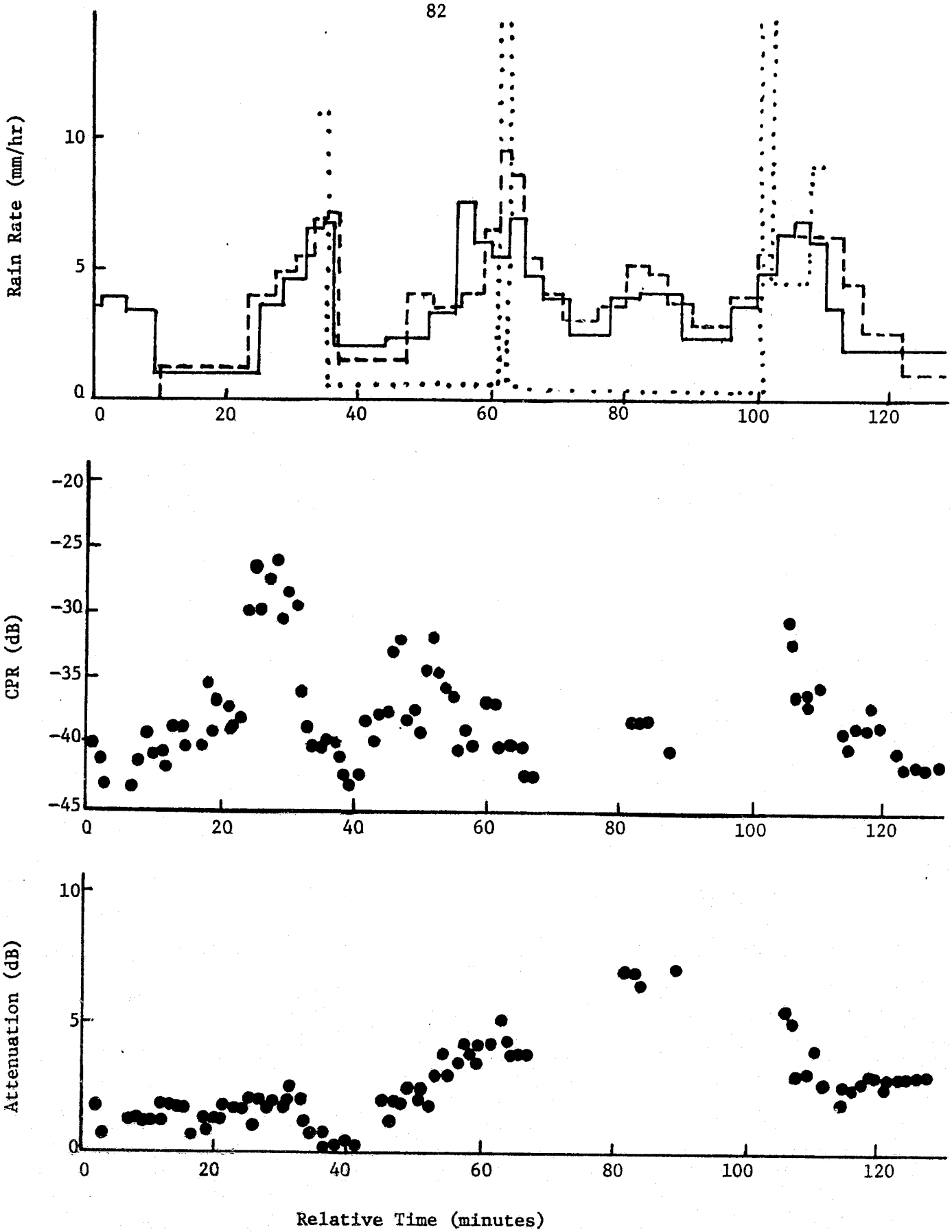

Figure 3.8 Data from rain storm of 30 March, 1975.

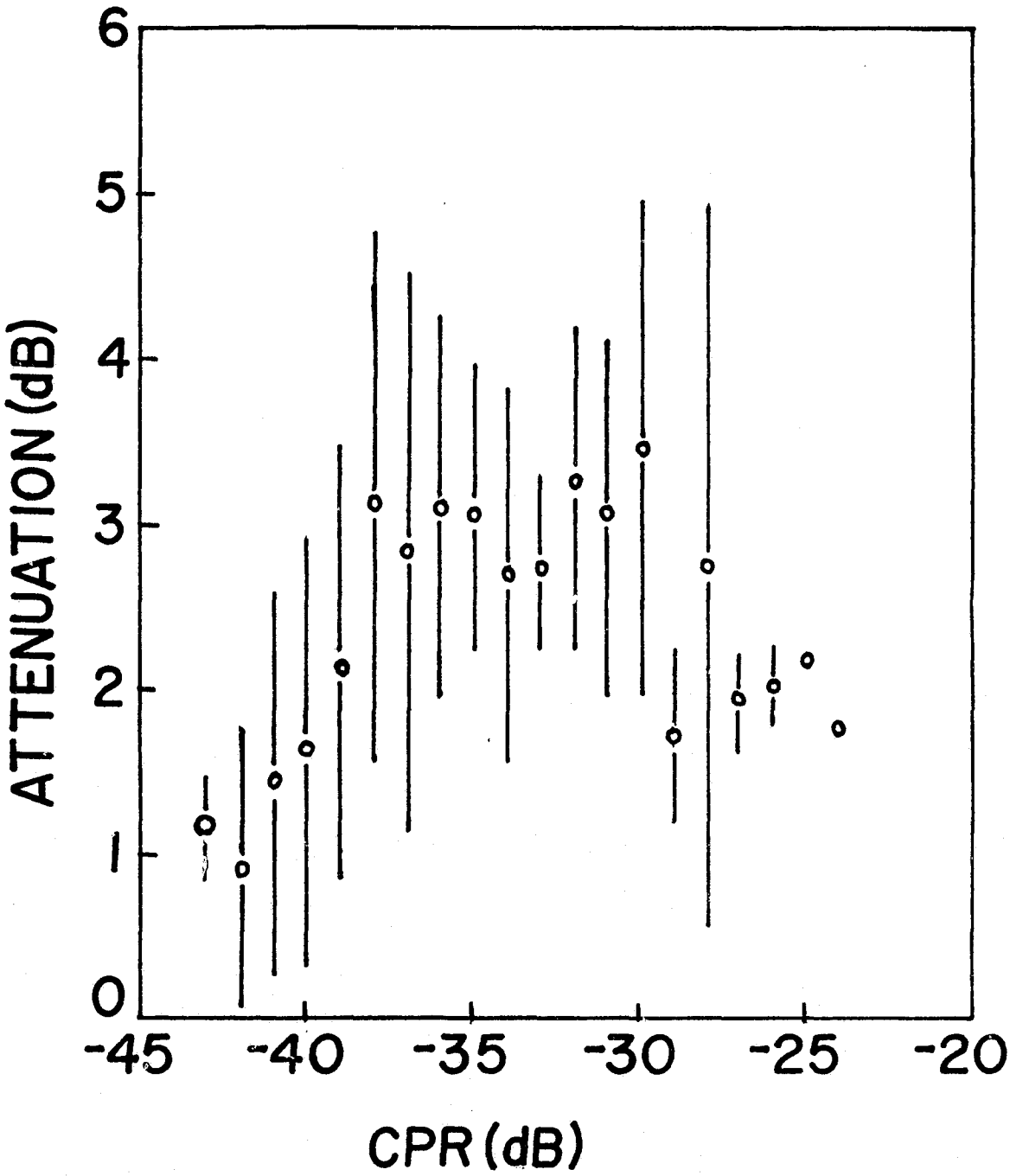

Figure 3.9 Attenuation versus CPR for the storm of March 30, 1975. Each point represents the average attenuation at each 1 dB interval of CPR. The vertical bars extend ± one standard deviation from the average.

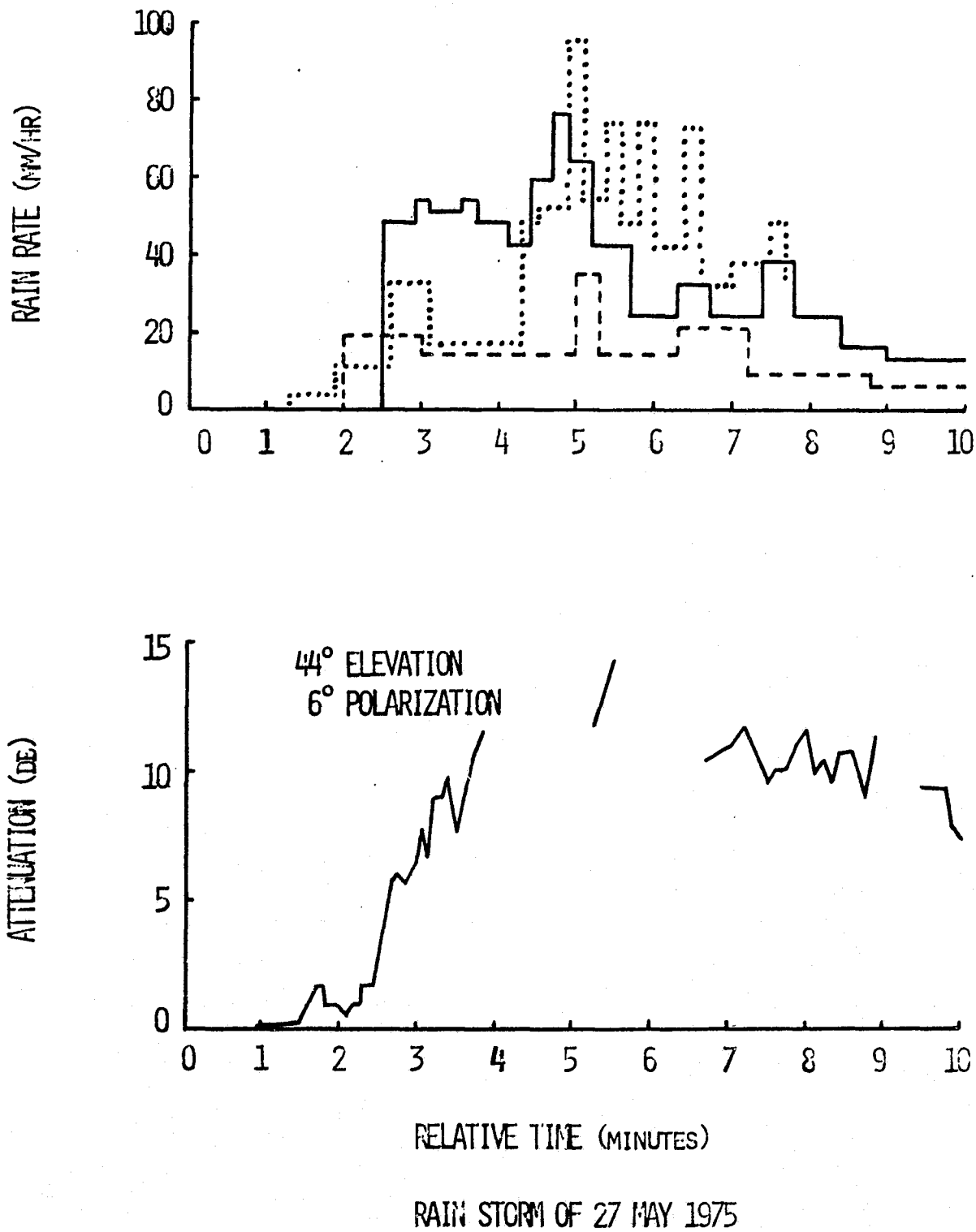

Figure 3.10 Data from storm of 27 May, 1975.
No CPR was observed.

to get data prior to the movement of the satellite toward 35° E. As the satellite moved east, the clear weather polarization angle that we observed at our station began to increase toward 0° from its nominal -21° value. It passed through 0° when the spacecraft was directly south of us and increased to about +50° when we lost signal on June 13, 1975.

On May 27, 1975, the polarization angle was +6°, and on that day we experience a severe thunderstorm with fading in excess of 14 dB. The data for this storm are presented in Figure 3.10. The blank portions in the attenuation data are when the receiver lost phaselock due to power failures. The interesting feature is that there was essentially no change in the CPR during this rain. One possible explanation for this is that the polarization angle was so close to vertical that the incident electric field was aligned with the raindrop minor axes and thus there was no depolarization.

3.5 Measurements at Low Elevation Angles

3.5.1 Introduction

At the conclusion of this experiment, we were able to monitor the satellite more or less continuously for elevation angles ranging from about 9° down to 1°. This gave our group and many of the other East Coast ATS-6 Millimeter Wave Experiment participants a unique opportunity to study 20 GHz propagation at extremely low angles.

During the observing periods the weather changed rapidly, alternating between sunshine, rain, and fog; at times all three seemed to be occurring simultaneously on different segments of the path. For this reason, it was frequently difficult to associate changes in the received signal with any particular weather condition.

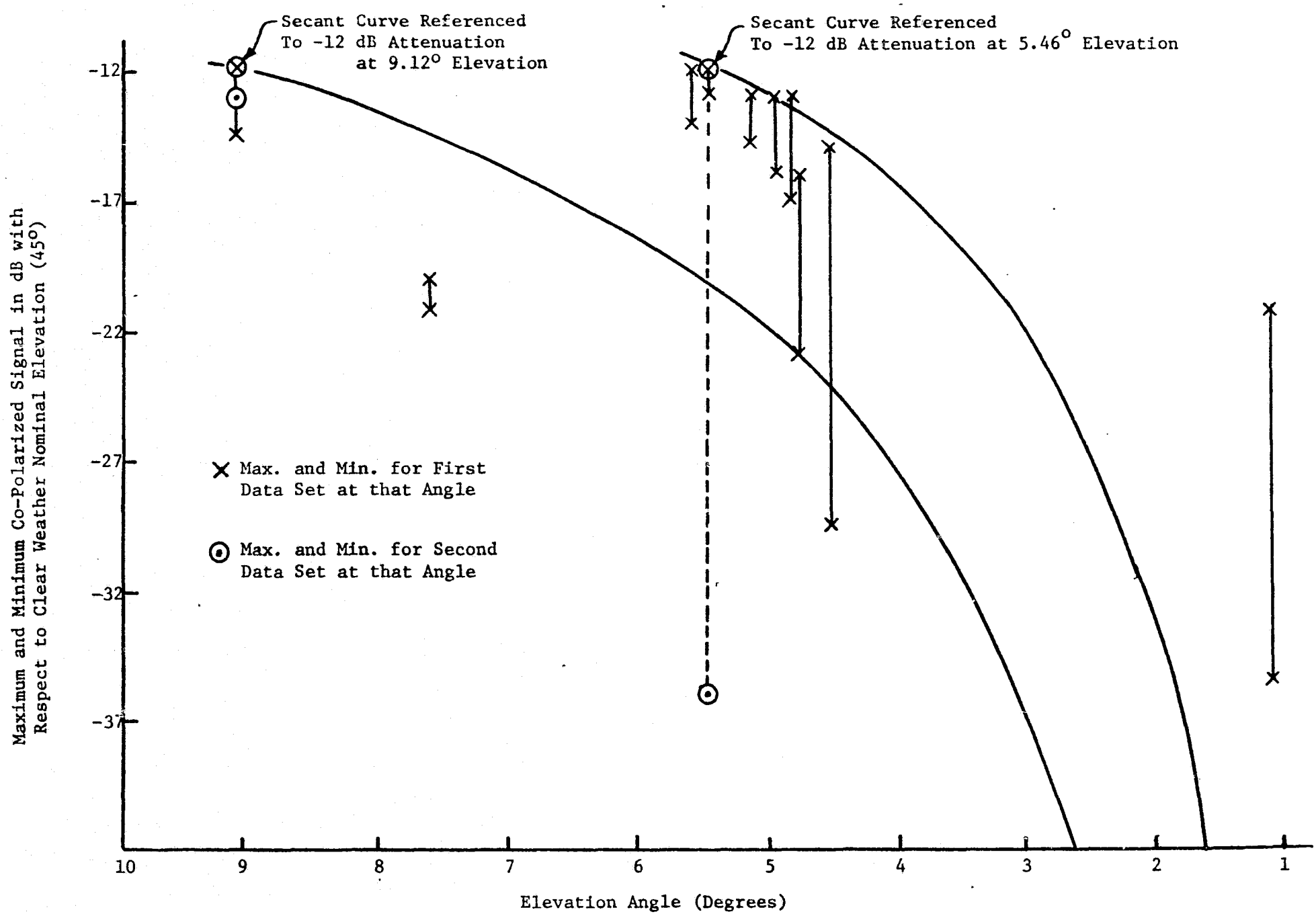

Figure 3.11 Attenuation at low elevation angles.

3.5.2 Narrative Discussion of the Data

As was stated earlier, our antenna pedestal went out of control and broke a number of cables when the satellite was at 22° elevation. We were able to repair the equipment and re-acquire the signal at 9.12° elevation, but our data have an unfortunate gap between these two angles.

At the time we re-acquired the satellite the clear weather signal was 12 dB below what it had been at 45° elevation. This measurement provided the first set of points in Figure 3.11 which shows the overall behavior of the co-polarized signal. The maximum and minimum signals occurred no more than four (4) minutes apart. These represent two sets of observations taken before and after a light rain.

The data measured at 7.61° elevation was taken after a storm that reached 30 mm/hr and before a 6 mm/hr sprinkle. Although the weather radar indicated no rain along the downlink, the sky was partly cloudy and there was light rain in the area. The time between the maximum and minimum signal strengths was no more than two (2) minutes. The clearest sky observed during tests below 10° elevation (excluding 1.1°) occurred at the elevation angle of 5.6°. The sky was hazy; however, the weather radar gave no indication of rain within 15 miles of the station. The scintillation frequency was approximately 1/6 Hz. As the elevation angle moved to 5.46°, rain began moving into the area. The 1 dB scintillation was observed before the rain entered the path. At one time rain extended nine (9) miles up that path. As the rain began to dissipate, the signal, as expected began to increase. Before the signal returned to the clear weather reference, it started down again even though the radar indicated that the rain had completely dissipated along the path. The receiver then lost and regained phase lock three (3) times in ten minutes although there was no radar indication of rain along the path. When the receiver did regain phase

lock on a strong signal, the co-polarized signal would fall about 0.5 dB/sec until the receiver again lost phase lock. After the receiver re-acquired the 20 GHz CW signal for the third time, the signal strength returned to the clear weather level with the same scintillations observed initially at 5.46° elevation. The data measured at 5.11° elevation were taken after a storm that reached 25 mm/hr. The data taken from 4.95° to 4.80° elevation were not interrupted by rain; however, the sky was hazy along the path. The scintillations tended to become larger and more frequent as the angle decreased. A 15 mm/hour drizzle preceded the measurements at 4.8° elevation; and although there was no radar indication of rain along the path, the signal level never came up to the clear weather reference. The scintillation patterns were composed of the higher frequency variations noted at 5.46° elevation but superimposed on sixty (60) second scintillations of the magnitude indicated in Figure 3.11. The large variation indicated at 4.54° elevation only occurred once. The remaining twelve (12) minutes of data taken at 4.54° elevation produced scintillations up to 8 dB of the type described at 5.46° elevation. The sky was partly cloudy at this time.

3.5.3 Antenna Pattern Broadening

After the satellite was re-acquired at 9.12°, we noticed a pronounced broadening of the antenna radiation pattern in the elevation plane. The signal remained quite sharp in azimuth but in elevation the 3 dB points were frequently separated by several degrees. The same effect was noted by our colleagues at Comsat Laboratories.

On the last day that we were able to receive the signal, the broadening disappeared and the elevation pattern returned to its former sharpness. At this time the peak co-polarized signal occurred at an elevation angle of 1.1°,

and the boresight telescope indicated that at this elevation the antenna was pointed below the crest of a nearby mountain! Presumably the propagation mechanism was knife-edge diffraction, but in that case the signal should have originated from the crest of the mountain.

We think that multipath propagation was responsible for the pattern broadening. Given the low elevation angle, and assuming horizontal stratification in the atmosphere, it is easy to hypothesize rays entering the receiving antenna from a statistical distribution of elevation angles. Certainly the scintillations, and the focusing and cross polarization effects (both described below) that we saw indicate the presence of multipath.

3.5.4 Clear Weather Attenuation at Low Angles

As the satellite elevation angle decreased, the tropospheric part of the propagation path lengthened. In a horizontally stratified atmosphere this would cause a decrease in signal strength proportional (in dB) to the secant of the elevation angle. Our intent was to measure the co-polarized signal clear-weather level at 45° elevation and look for this secant behavior. This effort was complicated by the lack of any data between 22° and 9.12°. Between 45° and 22° the secant law predicts a 1.2 dB increase in path loss. Taking the signal levels at 9.12° and 5.46° elevation as references, we have plotted two secant curves in Figure 3.11. These show fair agreement with the data in the 9° to 4° range. Of course at extremely low angles the horizontal stratification model breaks down.

3.5.5 Rain Attenuation at Low Angles

We were able to observe significant rain attenuation at 7.59°, 5.35°, and 4.70°. The results are displayed in Figures 3.12, 3.13, and 3.14. In each case these display attenuation (calculated from the clear-weather signal level immediately before or after the storm) and the rain rate at the rain

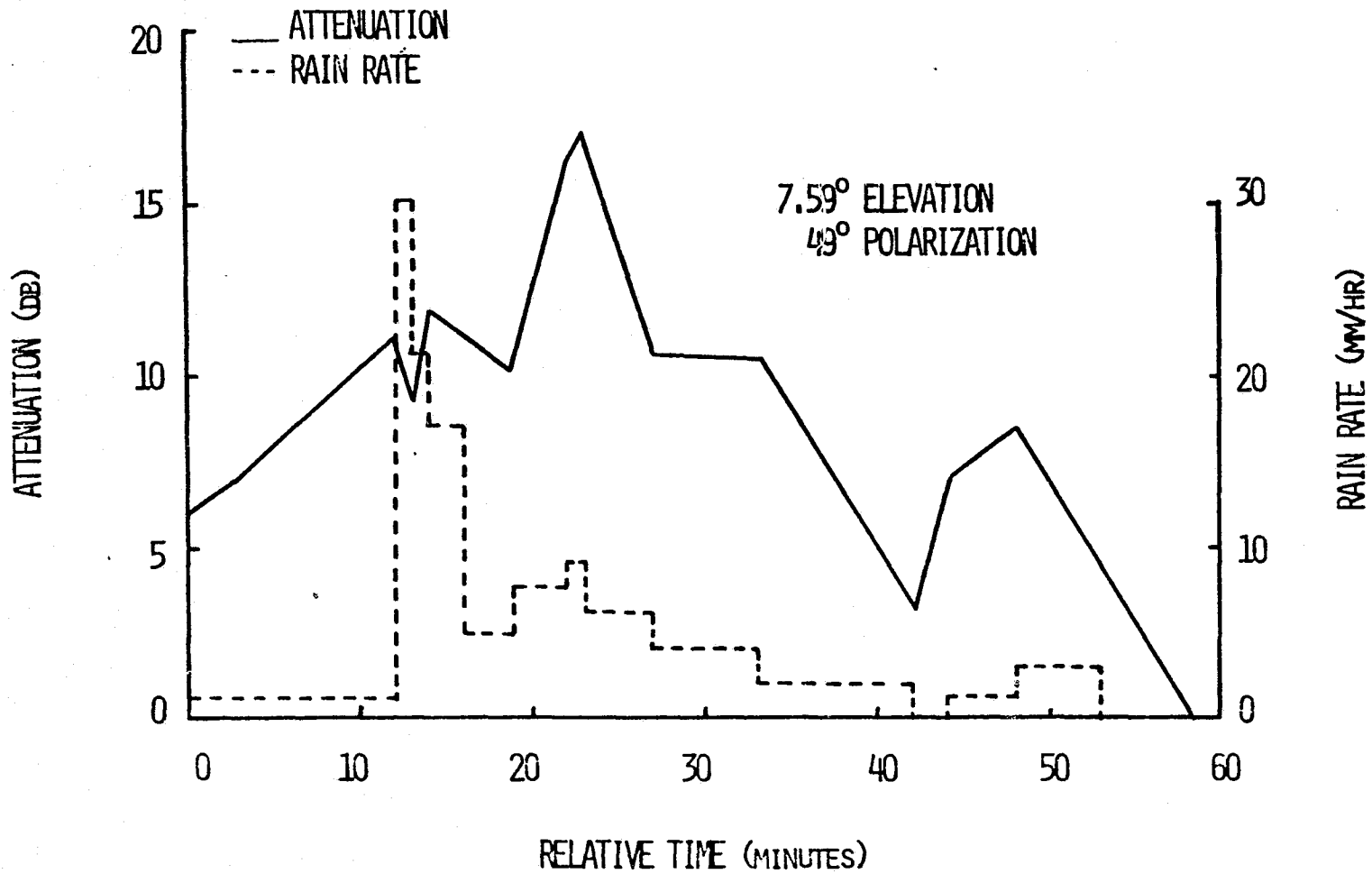

RAIN STORM OF 12 JUNE, 1975 (0359-0502)

Figure 3.12

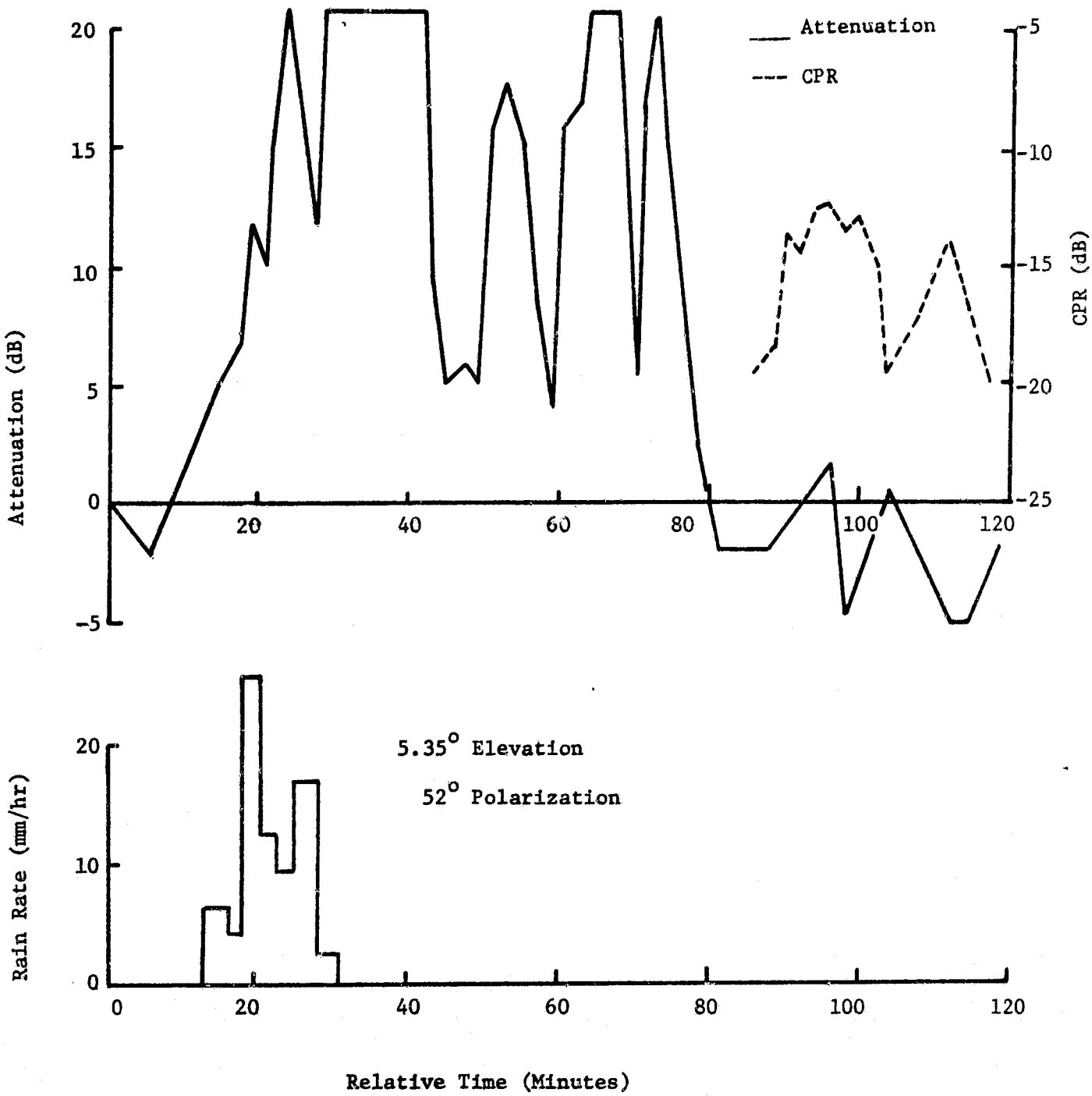

Figure 3.13. Storm data collected June 12, 1975
1615 - 1810 (UT).

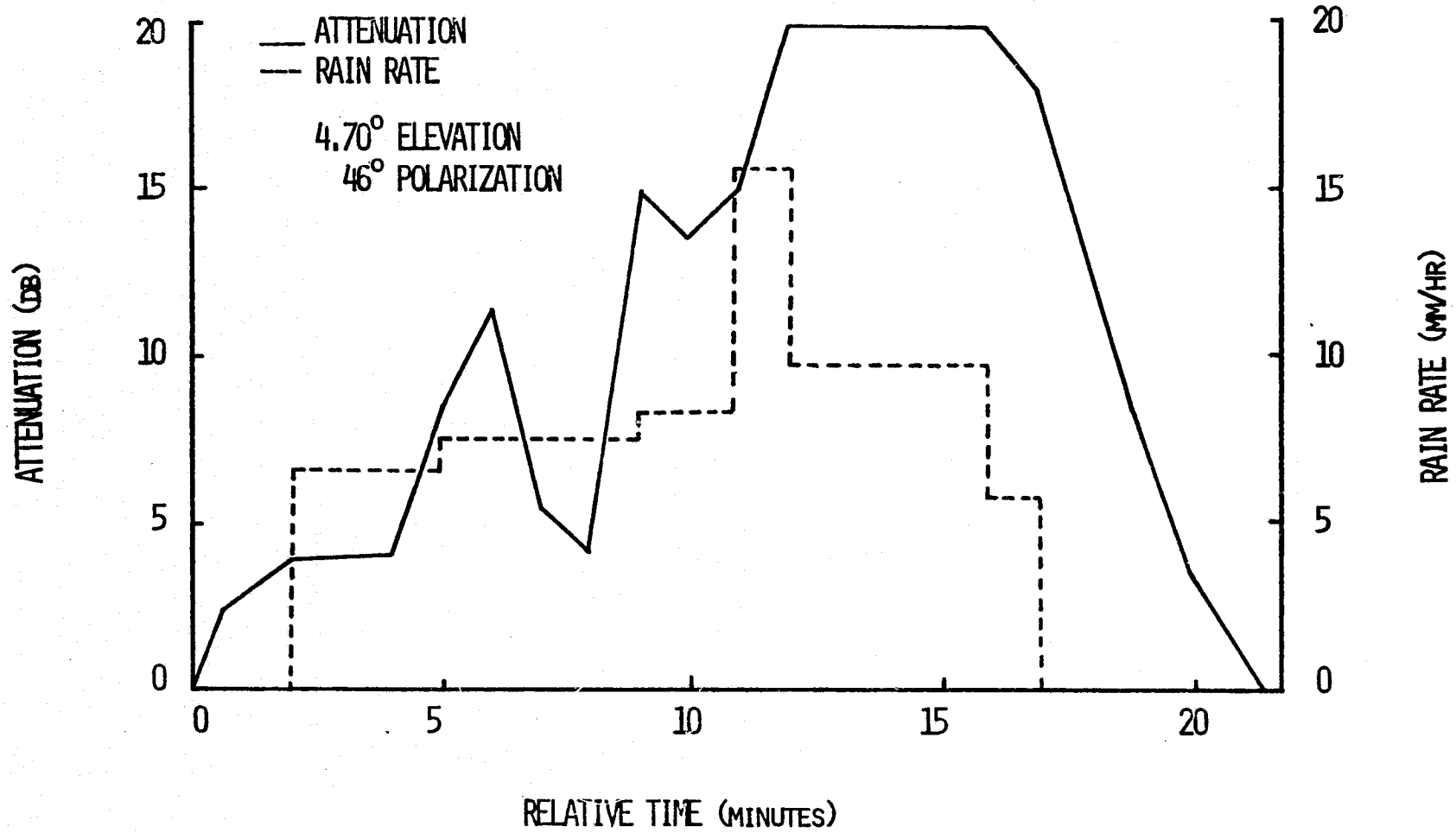

RAIN STORM OF 12 JUNE, 1975 (2053-2113)

Figure 3.14

gauge located beside the receiving antenna. The rain rate is shown for only one rain gauge because the other gauges were no longer under the propagation path. The correlation between the rain rate and attenuation in Figures 3.12 and 3.14 is outstanding. The high attenuation for a given rain rate is a result of the extremely long rain path.

3.5.6 Polarization Effects at Low Angles

3.5.6.1 Pattern Broadening

The polarization response of our antenna was a sharp "V" at 45° elevation (see Figure 3.1); below 9.12°, however, the polarization null became very wide and measuring the polarization angle with precision was more difficult. Nevertheless, finding the null location and finding average of the two polarization angles for which the co-polarized and cross-polarized signal levels were equal both gave similar results. Presumably the broadening was due to multipath.

3.5.6.2 Clear Weather Polarization Angle Variations

At first the measured polarization angles tracked the theoretical predictions. Thus, for measurements made at 9.12° elevation and 7.61° elevation the polarization angle was +49.0°. Data taken at 5.60° to 5.11° were recorded at a polarization angle of +52.0°. As expected the polarization angle moved to 52.5° for the data sets at 4.95° and 4.85° elevation; however, at 4.80° the polarization angle was measured to be +47.0° and it moved to +46.0 at 4.54° elevation.

We have no explanation for this reversal at 4.8°. Perhaps it is related to the clear weather polarization angle effects noted at higher elevation.

3.5.6.3 Depolarization

The 12 dB loss in signal level between 45° and 9.12° that was discussed

earlier forced us to remove the last 12 dB of front-end attenuation from the co-polarized channel. Given the limited dynamic range of the ATS receiver, this meant that we would only measure CPR values greater than -20 dB. Rain depolarization of this magnitude requires considerable harder rain than we experienced; hence, we observed no rain depolarization at extremely low angles. However, we did record one case of severe CPR increase due to multipath; this appears in Figure 3.13.

The event began at about 1730 on June 12 when the co-polarized signal level abruptly jumped from 20 dB below clear reference to as much as 5 dB above (an attenuation of -5 dB). Simultaneously, the CPR rose sharply and peaked at about -12 dB. Negative attenuation and high CPR continued for about 40 minutes. When he saw this happening, the operator carefully rechecked the antenna polarization angle and found it to be correct.

What was observed here appears to be a case of severe multipath. The 6 dB increase in co-polarized signal level over clear weather corresponds exactly to the arrival of equal-amplitude in-phase signals at the co-polarized channel. The situation for the cross-polarized signal is more complicated, but we feel that it can be explained as follows. The cross-polarized pattern of the antenna has a sharp null on axis. For the same incident polarization, a signal arriving off axis will be out of the null and the antenna will receive a larger cross-polarized component than it would if the signal came in on-axis. This is the central point of Watson's work on clear weather depolarization on ground paths. Since the phase response of the antenna also varies with angle of arrival, the CPR measured by an antenna for two signals with the same polarization but different arrival angles will be very simular to the CPR measured for two signals with slightly different polarizations and (perhaps greatly) different phases.

An analytical treatment of the second situation is relatively straight

forward. Consider the electric field vectors drawn in Figure 3.15, where $\overline{E}_{NI}$ represents the normal incident signal and $\overline{E}_{MP}$ is a multipath signal which differs in orientation from $\overline{E}_{NI}$ by θ "spatial" degrees and is out of phase with $\overline{E}_{NI}$ by ϕ "phase" degrees. The total received electric field $\overline{E}_T$ is given by

$$\overline{E}_T = \overline{E}_{NI} + \overline{E}_{MP}. \tag{15}$$

Its complex polarization factor (Beckmann, 1968), ρ, is

$$\rho = \mathrm{CSC}(\theta)e^{-j\phi} + \mathrm{COT}(\theta) \tag{16}$$

From ρ we may calculate the Stokes parameters (Kraus and Carver, 1973) of $\overline{E}_T$ and from there we may calculate the average power received by the co-polarized and cross-polarized antenna fields. The ratio of these quantities is the CPR. This is done and the results are presented in Figures 3.16, 3.17, and 3.18.

At first glance, these results are somewhat surprising since, for example, two signals differing in polarization by only 1° can produce a CPR of +40 dB if their relative phase difference is near 180°. This happens because for this particular combination of parameters the cross-polarized components add and the co-polarized components subtract. Hence, multipath depolarization is potentially a more serious problem at low elevation angles than is rain depolarization.

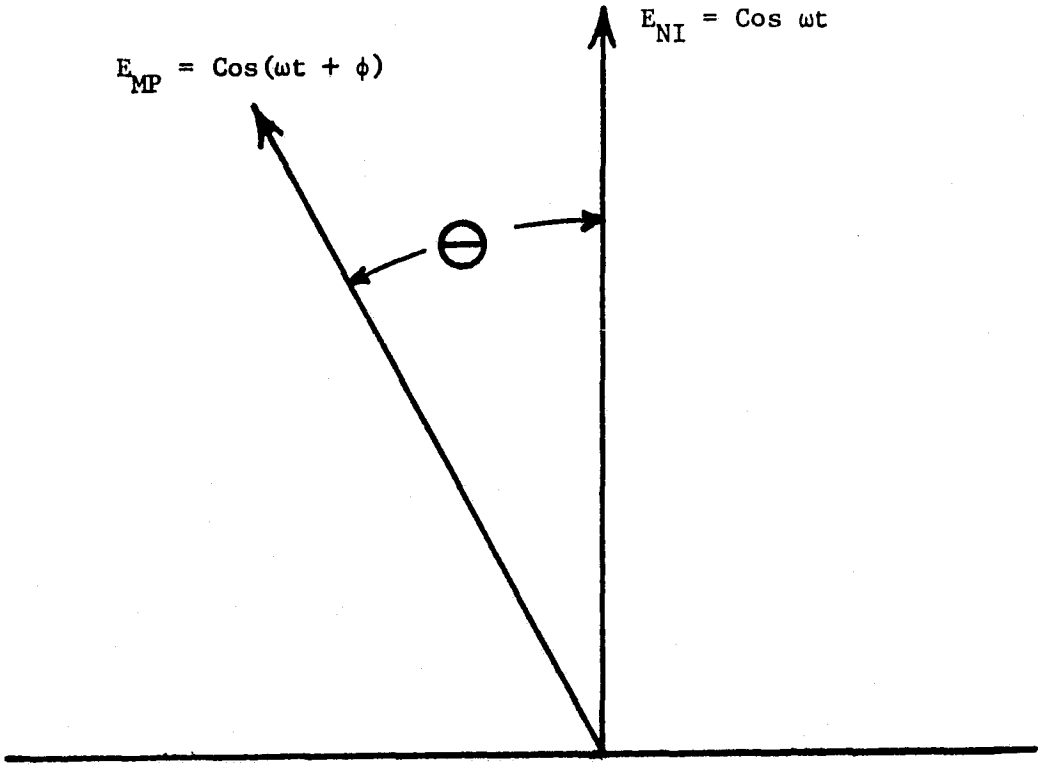

Figure 3.15 Relative spatial and temporal orientation of direct E_{NI} and multipath E_{MP} electric fields arriving at the receiver.

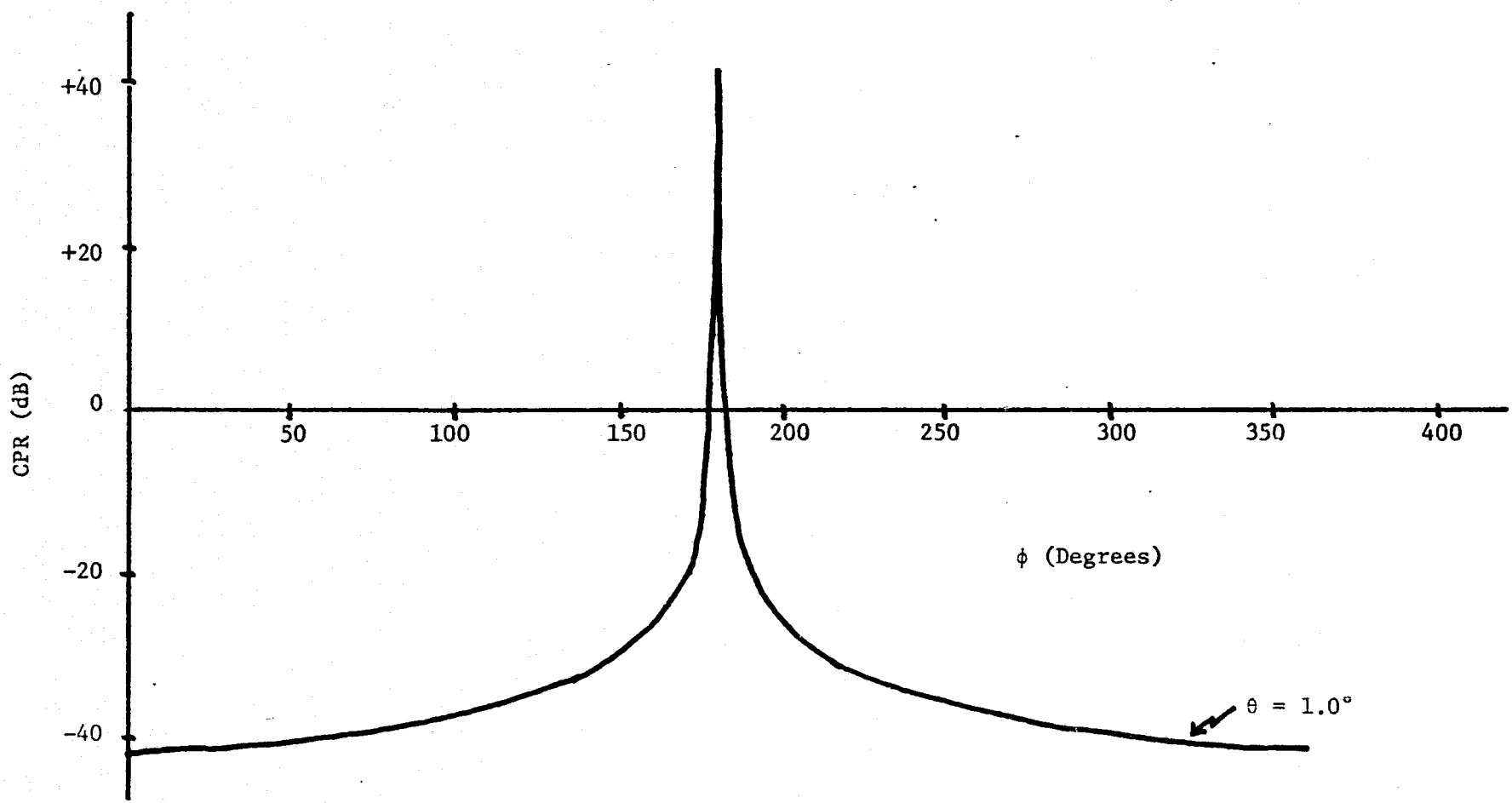

Figure 3.16 Cross Polarization Ratio Due To A Boresight Signal And An Equal Amplitude Multipath Signal Displaced θ Degrees From The Boresight Linear Polarization And Separated ϕ Degrees In Phase.

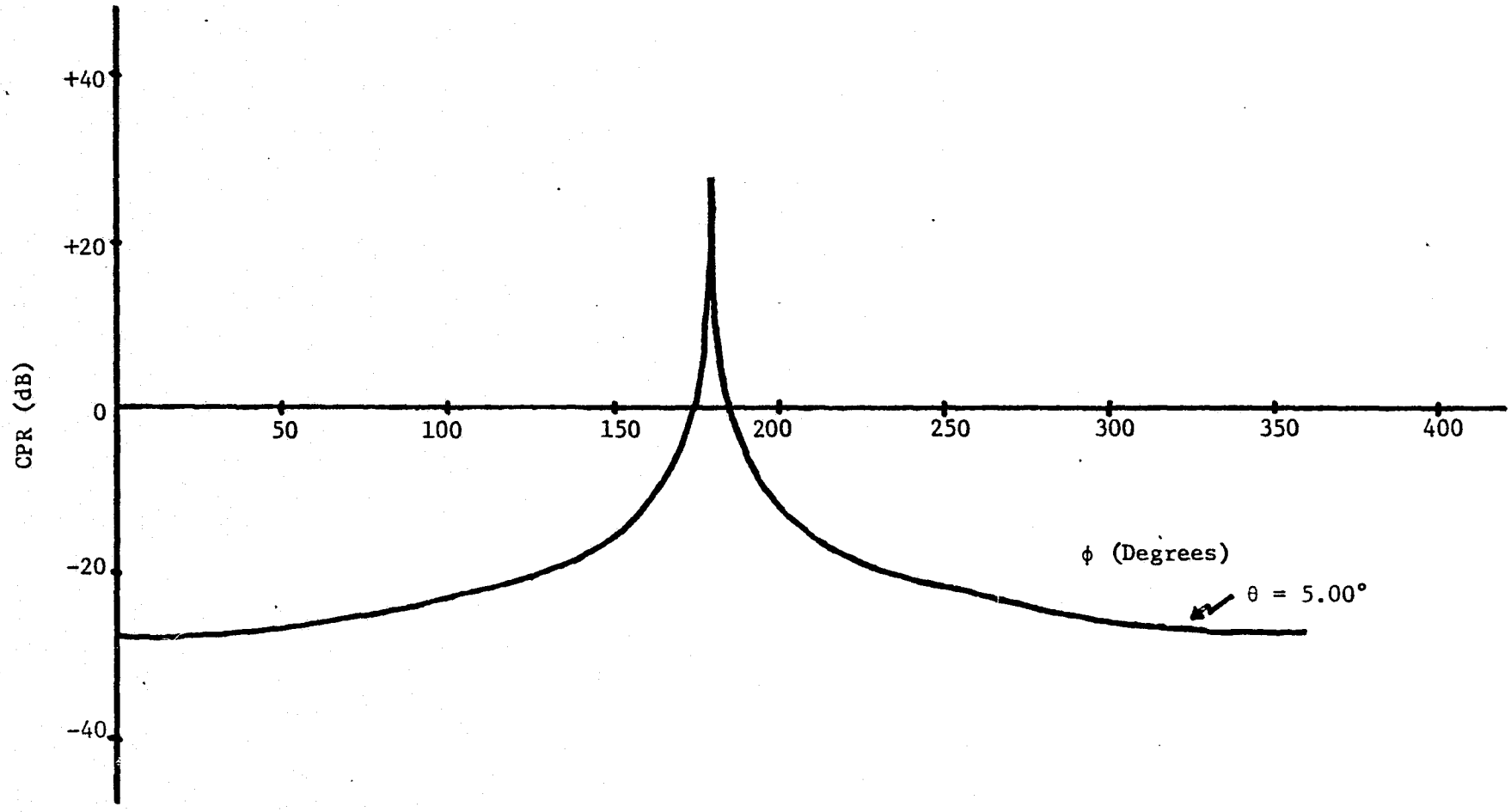

Figure 3.17 Cross Polarization Ratio Due To A Boresight Signal And An Equal Amplitude Multipath Signal Displaced θ Degrees From The Boresight Linear Polarization And Separated ϕ Degrees In Phase.

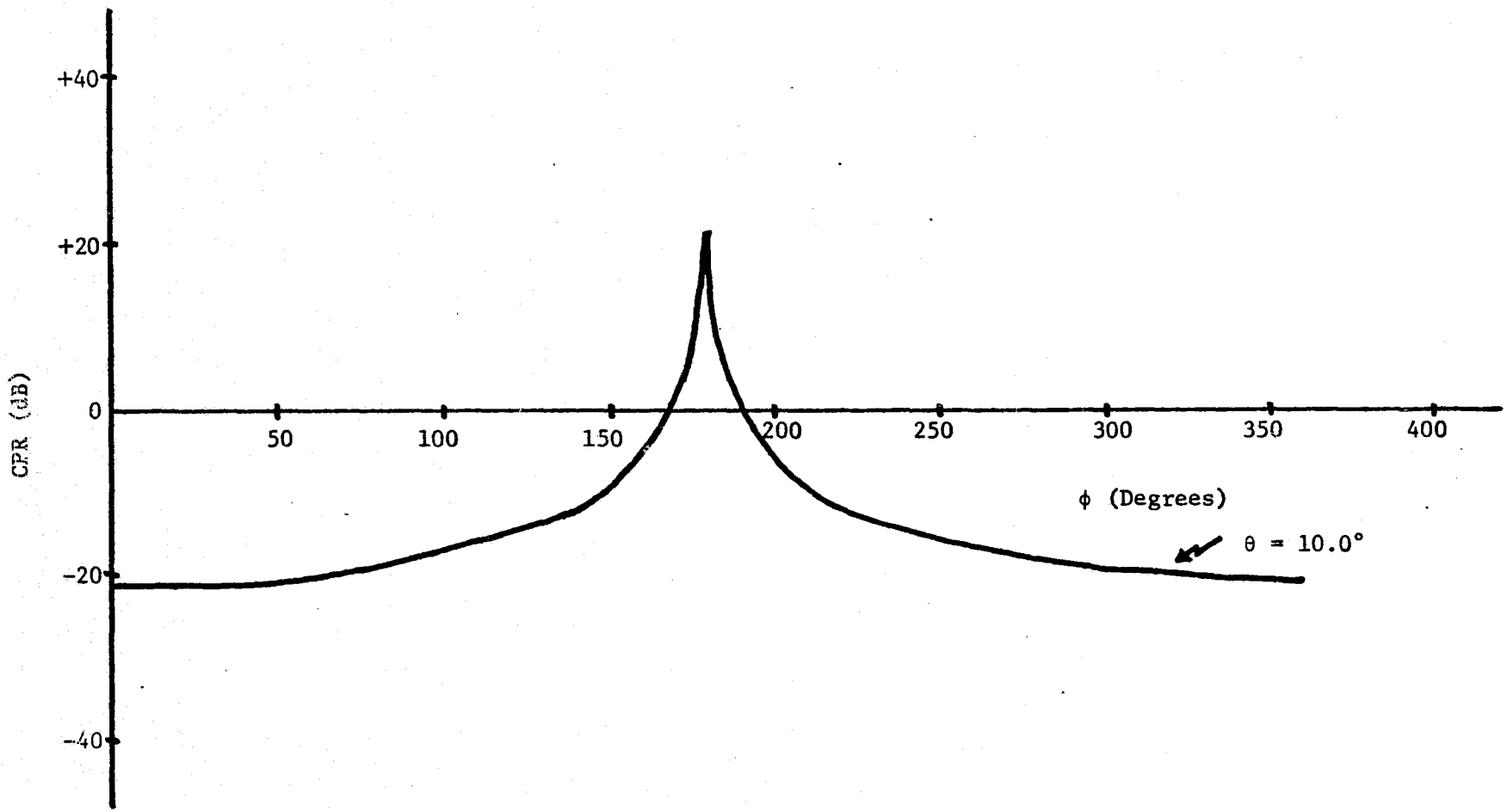

Figure 3.18 Cross Polarization Ratio Due To A Boresight Signal And An Equal Amplitude Multipath Signal Displaced θ Degrees From The Boresight Linear Polarization And Separated ϕ Degrees In Phase.

4. Conclusions

The main objective of this project was to collect data for depolarization of a 20 GHz signal along a satellite-to-ground path. Possible sources of depolarization are rain along the path, snow along the path, multipath effects at low elevation angles and clear air effects. The data base was not sufficiently large in any of these areas to form statistically meaningful conclusions. Also not enough is known to develop an accurate theoretical model. However, the experiment revealed several trends which in several cases are supported by simple theoretical explanations. We shall summarize these results below.

a) There was more depolarization due to rain (at -21.5° polarization angle) observed along the satellite path for a given ground rain rate than has been observed for a terrestrial link. (See Section 3.4).

b) From our measurements of one rain storm at a polarization angle near vertical, we tentatively conclude that depolarization may be significantly less for a dual polarized system whose polarizations are vertical and horizontal. (See Section 3.4).

c) From several measurements made during snow, we conclude that snow can introduce significant depolarization (and without high attenuation). As discussed in Section 3.3 higher altitude phenomena may contribute to this depolarization.

d) Observations at very low elevation angles (see Section 3.5) showed that attenuation can be introduced during clear weather by multipath effects. When rain is present additional significant attenuation is also present; furthermore, depolarization occurs.

e) The possibility of clear weather depolarization is discussed in depth in Section 3.3. The received signal polarization angle rotated

several times under clear weather conditions during the project. Many possible mechanisms for this rotation have been ruled out. We have concluded that it is due either to elevation pointing errors or it is, in fact, a real atmospheric effect.

In addition to the primary goal of collecting propagation data, a few secondary goals were accomplished. These fall under the general topic of satellite communication system design and are summarized below.

f) Rain water on a front fed dual polarized receiving antenna does not produce any degradation of the system performance.

g) A weather surveillance radar can be used to predict the motion of a rain cell which is of sufficient intensity to impare communication. The radar could be used with communications systems as a warning device and could initiate a rerouting of communication traffic off of one polarization temporarily.

h) Satellite ground station hardware should be designed carefully, particularly for frequencies of 20 GHz and above. The many hardware problems encountered during this project have led to several recommendations for the CTS project and are discussed in Chapter 6.

i) Operation of satellite links at 20 GHz and low elevation angles (on the order of 10° or less) probably should be avoided.

5. References

1. P. Beckmann (1968), The Depolarization of Electromagnetic Waves, Boulder, Colorado: The Golem Press.

2. C. W. Bostian, W. L. Stutzman, P. H. Wiley, and R. E. Marshall (1972), "Initial Results of an Experimental Study of 17.65 GHz Rain Attenuation and Depolarization," 1972 International IEEE G-AP Symposium Digest, pp. 250-253, December.

3. C. W. Bostian, W. L. Stutzman, P. H. Wiley, and R. E. Marshall (1974), "The Influence of Polarization on Millimeter Wave Propagation Through Rain," Final Report, NASA Grant NGR-47-004-091, NASA CR-143686, VPI&SU, Blacksburg, April.

4. C. W. Bostian (1974), "Antenna and Path Interaction in Rain Depolarization," 1974 IEEE-G-AP International Symposium Digest, pp. 392-394, June.

5. S. I. Ghobrial and P. A. Watson (1973, "Cross Polarization During Clear Weather Conditions," IEE Conference on Propagation of Radio Waves at Frequencies Above 10 GHz (IEE Conference Publication 98), pp. 179-182.

6. GTE Lenkurt, Inc. (1972), Engineering Considerations for Microwave Communications Systems, Second Edition.

7. D. Hodge (1973), Instructions for the Use of the Satellite Look Angle Program (SLAP), Electroscience Laboratory Technical Note #6, The Ohio State University.

8. J. D. Kraus and K. R. Carver (1973), Electromagnetics, Second Edition, New York: McGraw-Hill.

9. G. C. McCormick (1974), "Deterioriation of Circular-Polarization Clutter Cancellation in Anisotropic Precipitation Media," Electronics Letters, Vol. 10, No. 10, pp. 164-166, May 16.

10. T. Murakami and G. S. Wickizer (1969), "Ionspheric Phase Disturbances and Faraday Rotation of Radio Waves," RCA Review, Vol. 30, pp. 475-503, March.

11. E. Vilar (1974), "Faraday Effects at Microwave Frequencies," ITT Laboratories of Spain Report 73-TM.22.10-9.

12. P. A. Watson and M. Arbabi (1973), "Rainfall Cross Polarization at Microwave Frequencies," Proc. IEE (London), Vol. 120, pp. 413-418, April.

13. P. A. Watson (1973), "Cross Polarization Studies at 11 GHz," Final Report, European Space Research Organization Contract 1247/SL, University of Bradford, England, June.

14. P. H. Wiley, W. L. Stutzman, and C. W. Bostian (1974), "A New Model for Rain Depolarization," Journal de Recherches Atmospheriques (France), Vol. 8, pp. 147-153.

6. Appendix

6.1 Plans and Recommendation for CTS

6.1.1 Introduction

The authors will conduct a depolarization experiment with the CTS satellite that should overcome many of the difficulties encountered with ATS-6. The paragraphs which follow summarize our recommendations for the CTS project based on our experience with ATS-6.

6.1.2 Antenna

In the CTS system design a reflector antenna 12 feet in diameter was selected. This size will provide high gain with little noise. A reflector larger than 12 feet leads to excessive cost. The central question is whether to use a prime focus or Cassegrain feed. The Cassegrain system offers easy access to the feed horn with short waveguide runs (thereby reducing the noise). Also, spillover is into the sky rather than noisy ground as in the prime focus case. A disadvantage for the Cassegrain system is that the feed horn looks upward and may accumulate water. As discussed in Section 2.2, this can be disastrous. Therefore, a radome is required. The design of an innocuous radome may be a problem, but is one that can be solved.

The cross polarization isolation properties for prime focus and Cassegrain systems are not thoroughly understood. Generally speaking, for "small" antennas prime focus is superior; however, many factors are involved and if properly designed either a prime focus or Cassegrain system should be suitable for our application. Since the Cassegrain offers many advantages we would recommend it for use with a reflector 12 feet in diameter.

6.1.3 Tracking

A receiving antenna 12 feet in diameter at 11.7 GHz would have a half power beam width of about 0.5°. Our ATS-6 receiving antenna has a 0.9° beamwidth. Thus require tracking accuracy will be somewhat greater. If accurate orbital elements for the CTS spacecraft are supplied to us, the SLAP program should provide sufficiently accurate tracking data. See Section 2.3 for a discussion on tracking data accuracy with the ATS-6 project.

6.1.4 Receiver Recommendations for CTS

The main emphasis with the CTS RF front end will be on quietness and reliability. The fact that the receiver will operate in the X band will increase the reliability; however, every effort will be made to secure well tested "off the shelf" components. More attention will be paid to the noise figure of the receiver. This will be necessary because of the decreased satellite EIRP. The entire receiver system will be two channel in order to eliminate the noise-generating attenuator in the co-polarized channel.

A major problem with the ATS-6 receiving system was the loss of phase-lock while the receiver was switched to an undetectable cross-polarized signal. This will be eliminated by the use of two (2) ATS-E IF receivers. The cross-polarized receiver will be phase locked to the co-polarized receiver so that there will be no VCXO drift when the cross-polarized signal falls below the phase lock threshold. In addition the bandwidth of the filter detectors in the ATS-E IF receivers will be substantially reduced in order to increase the output signal-to-noise ratios.

6.1.5 Radar

The RD-110 radar will be used for the CTS project in the same manner as was planned for ATS-6. The main function of the radar will be to allow computer

analysis of rain rate versus radar backscatter. Eventually we hope to be able to calibrate the RD-110 radar with respect to rain rate from attenuation versus rain rate models developed from CTS data.

The RCA AVQ/46 X-band radar, operating at 9.5 GHz, may be of significant use in the CTS program, if the radar backscatter does not interfere with the downlink receiver operation. The receiver bandwidth should sufficiently attenuate the 9.5 GHz signal. The X-band radar may have enough power output to supply information about the existence of bright bands.

The backscatter characteristics of the AN/PPS-18 doppler radars will be studied to determine if raindrops canting angle information can be obtained. These homodyne doppler radars operate from 9.0 to 9.5 GHz.

The Bendix cable connectors on the RD-110 radar cables should be replaced with MS connectors for the CTS project. The modulator transformer for the AVQ/46 X-band radar should be replaced.

6.1.6 Weather Instrument for CTS

Insufficient data precludes making recommendations on the existing weather instruments at VPI&SU; however, the additions of a temperature sensor, a humidity sensor, and a barometer may increase the predictability of an approach precipitation event.

6.1.7 Data System for CTS

The CTS data system will be built around a new PDP-11 computer system. The PB-440 system has been scrapped.

6.2 Project Personnel

Many people at VPI&SU participated in the ATS-6 Depolarization Experiment. Here is a list of contributors; the authors apologize for any omissions.

Faculty

C. W. Bostian
E. A. Manus
R. E. Marshall
H. N. Pendrak
W. L. Stutzman
P. H. Wiley

Secretaries

Sherida Battrell
Mary Devens Donnally
Sandra Johnson
Cynthia Will

Graduate Assistants

B. S. Bong
W. W. Farley, Jr.
J. L. Hogler
C. W. Hupfeld
W. D. Jenison
S. R. Kauffman
R. P. Sherwin

Undergraduates

S. Cardwell
V. L. Dawson
W. George
D. L. Hausrath
L. E. Johnston
J. D. Landers
J. McCoy
R. J. Mele
K. E. Oliver
D. C. Patty
R. A. Strobel